KU Leuven
Group Biomedical Sciences
Department of Pharmaceutical and Pharmacological Sciences
Laboratory for Therapeutic and Diagnostic Antibodies

KU LEUVEN
DOCTORAL SCHOOL
BIOMEDICAL SCIENCES

Thrombin-Activatable Fibrinolysis Inhibitor

Serendipity in the Characterization of Inhibitory Nanobodies

Maarten HENDRICKX

October 15th, 2013
Doctoral thesis in Pharmaceutical Sciences

KU Leuven
Group Biomedical Sciences
Department of Pharmaceutical and Pharmacological Sciences
Laboratory for Therapeutic and Diagnostic Antibodies

Thrombin-Activatable Fibrinolysis Inhibitor

Serendipity in the Characterization of Inhibitory Nanobodies

Maarten HENDRICKX

Jury:
Supervisor: Prof. Dr. P. Declerck
Co-supervisor: Prof. Dr. A. Gils
Chair: Prof. Dr. M. Baes
Secretary: Prof. Dr. E. Lecrinier
Jury members: Prof. Dr. M. Hoylaerts
Dr. N. Mutch

October 15th, 2013
Doctoral thesis in Pharmaceutical Sciences

Tuesday October 15th 2013, 5 PM

Aula van de Tweede Hoofdwet
Thermotechnisch Instituut
Kasteelpark Arenberg 41
Leuven

Dankwoord

Na bijna vier jaar pipetteren, 'straf' nadenken en vervolgens mijn thesis schrijven mag ik mijn dankwoord uiten aan allen die me gesteund hebben. De voorbije vier jaar zijn voorbij gevlogen en ik heb enorm veel bijgeleerd zowel persoonlijk als professioneel mede dankzij volgende mensen die ik bij deze graag zou willen bedanken:

Paul, bedankt voor de voorbije vier jaar intensieve samenwerking, voor de steun die je me steeds gegeven hebt bij het aanvragen van beurzen en het volgen van conferenties en cursussen. Ik heb de vrijheid die je me gegeven hebt altijd erg kunnen appreciëren om 'eigenaardige' resultaten wat dieper te onderzoeken of om een 'side-projectje' te kunnen doen. Hoewel we vaak discussieerden over nieuwe conformationele veranderingen of nieuwe mechanismen van TAFI inactivate, zorgde je kritische ingesteldheid ervoor dat alles goed onderbouwd werd.

Ann, ook al loopt je onderzoeksfocus langzaam aan wat verder weg van TAFI, toch heb ik veel geleerd van je jarenlange ervaring. Je deur stond (bijna) altijd open voor het zoeken naar oplossingen of voor een wetenschappelijke (en andere) babbel zodat ook deze thesis (desondanks een vertraagd review proces ☺) toch op tijd klaar is.

Furthermore I would like to thank the members of my jury: Prof. Myriam Baes, Prof. Marc Hoylaerts, Prof. Eveline Lescrinier and Dr. Nicola Mutch for providing me with critical comments and good suggestions on my thesis manuscript.

Bedankt labcollega's: Els, Griet, Miet, Sophie voor de aangename sfeer in het labo en experimentele hulp; An, Chantal en Rita, voor de administratieve en logistieke organisatie. Britt, Ellen, Karlien, Niels, Niraj, Tine, Lize, Thomas, Gaelle, Xiao, Nick, Marlies en de collega's van het labo van Prof. P. De Witte voor de fijne momenten op congres, labo uitstappen, kerstfeestjes,… Verder zou ik ook nog graag de studenten willen bedanken die met glans een aantal projecten voor hun rekening hebben genomen: Anaïs De Winter, Else Balke, Ine Van Geneugden, Nils Mollekens, Monika Zatloukalova, Dawid Deneka, Tobias Kromann-Hansen en Alessandro Marturano.

Prof. Peter Andreasen, thanks for hosting me in your lab during my Erasmus-trip in Denmark, 2008. Together with Jeppe Madsen you guided me through my first lab experience (PAI-1 aptamer project) and ignited my passion for scientific research.

Prof. Serge Muyldermans bedankt voor de mogelijkheid om je in labo de nanobodies te genereren tegen de verschillende TAFI's en de kritische reviews van de manuscripten. Dr. Gholamreza Hassanzadeh-Ghassabeh and Jan Van Gompel thanks for the practical help during my two visits at the VUB.

An, Bart, Egon, 'collega' Jonathan en Ward voor de woensdagavond 'kotetentjes' die nadat we niet meer samen op kot zaten meer evolueerde naar 3-gangen diners op locatie! Ik neem aan dat we tevens de talrijke lezingen met receptie (of was het omgekeerd?) ook in de toekomst verder zullen afsluiten ;). Ook de rest van de Salco groep en medespelers van FC Dzjenghis Khan: merci voor de interesse in het onderzoek en occasionele bloeddonaties. Het 'hockeyteam': Alix, Gregory, Laura, Mathias en Margaux voor de ontspannende trainingen en etentjes (ook al wordt er nu niet veel meer getraind). Thanks to all co-organizers of the PhD Jobfair 2011 and 2012, especially Marlies and Yogesh, we are now all specialists in creating vzw's, book keeping and tax payments!

Als laatste een dankwoord aan mijn familie. Mama, Papa: bedankt voor de hulp in de zeer brede zin van het woord: gaande van gebruik maken van de 'faciliteiten' thuis, interesse in mijn projecten tot de hulp bij het fitten van data aangaande TAFIa conformationele veranderingen. Mede dankzij deze steun is alles zo vlot verlopen. Peter, ook al ben je niet direct thuis in de onderzoekswereld toch vond ik het fijn dat je interesse toonde door af en toe te vragen waar ik juist mee bezig was. Ik vergeet zeker en vast de vrijdagavonden op kot niet. Elke, jij bent iets meer thuis in de farmaceutische wereld, voor jou was het iets gemakkelijker om te volgen wat er juist gebeurde op gasthuisberg, bedankt voor je steun.

Ik kijk uit naar wat de toekomst brengt en hoop jullie paden nog vaak te mogen kruisen,

Maarten

PS: Diegene die de thesis volledig zullen lezen zullen 1842 keer het woord TAFI tegenkomen en weten nu ook direct waarover de thesis gaat!

Research funded by a Ph.D. grant of the Agency for Innovation by Science and Technology (IWT) to Maarten Hendrickx (SB 101179).

Table of contents

LIST OF ABBREVIATIONS

AA	amino acid
AUC	area under the curve
cDNA	complementary DNA
CDR	complementarity determining region
CPN	carboxypeptidase N
E. coli	*Escherichia coli*
ELISA	enzyme-linked immunosorbent assay
Fab	antigen-binding fragment
FbDP's	fibrin degradation products
Fc	fragment, crystallisable
GEMSA	guanidinoethylmercaptosuccinic acid
HcAb	Heavy chain Antibody
Hip-Arg	hippuryl-arginine
Ig	immunoglobulin
ka	association rate constant
KA	affinity constant
k_{cat}	catalytic rate constant
kd	dissociation rate constant
KD	dissociation constant
kDa	kilo Dalton
LCI	leech carboxypeptidase inhibitor
MA	monoclonal antibody
mTAFI	mouse thrombin-activatable fibrinolysis inhibitor
PAI-1	plasminogen activator inhibitor-1
PBS	phosphate buffered saline
PCR	polymerase chain reaction
PPACK	H-*D*-phenylalanyl-*L*-prolyl-*L*-arginine chloromethyl ketone
PTCI	potato tuber carboxypeptidase inhibitor
rTAFI	rat thrombin-activatable fibrinolysis inhibitor
rTAFI-CIYQ	rTAFI with mutations to Cys^{305} Ile^{329} Tyr^{333} Gln^{335}

SD	standard deviation
SEM	standard error of the mean
SDS-PAGE	sodium dodecyl sulfate - polyacrylamide gel electrophoresis
scFv	single-chain variable fragment
SPR	surface plasmon resonance
T	thrombin
T/TM	thrombin/thrombomodulin complex
TAFI	thrombin-activatable fibrinolysis inhibitor
TAFIa	activated TAFI
$TAFIa_i$	inactivated TAFIa
TAFI-TI	human TAFI harbouring the polymorphisms Thr^{147} and Ile^{325}
TAFI-CIIYQ	human TAFI with mutations to Cys^{305} Ile^{325}-Ile^{329}-Tyr^{333}-Gln^{335}
TF	tissue factor
TCI	tick carboxypeptidase inhibitor
TM	thrombomodulin
t-PA	tissue-type plasminogen activator
u-PA	urokinase-type plasminogen activator
VHH	variable domain of the heavy chain of a heavy chain antibody
VH	variable domain of the heavy chain
VL	variable domain of the light chain

List of Publications

Madsen JB, Dupont DM, Andersen TB, Nielsen AF, Sang L, Brix DM, Jensen JK, Broos T, **Hendrickx ML**, Christensen A, Kjems J, Andreasen PA. RNA aptamers as conformational probes and regulatory agents for plasminogen activator inhibitor-1. *Biochemistry*. 2010;49:4103-4115

Hendrickx ML, De Winter A, Buelens K, Compernolle G, Hassanzadeh-Ghassabeh G, Muyldermans S, Gils A, Declerck PJ. TAFIa inhibiting nanobodies as profibrinolytic tools and discovery of a new TAFIa conformation. *J Thromb Haemost*. 2011;9:2268-2277

Hendrickx ML, Zatloukalova M, Hassanzadeh-Ghassabeh G, Muyldermans S, Gils A, Declerck PJ. Identification of a novel, nanobody-induced, mechanism of TAFI inactivation and its *in vivo* application. *J Thromb Haemost, under review*

Hendrickx ML, Zatloukalova M, Hassanzadeh-Ghassabeh G, Muyldermans S, Gils A, Declerck PJ. *In vitro* and *in vivo* characterization of the profibrinolytic effect of an anti-rat TAFI nanobody. *Thromb Haemost, under review*

Hendrickx ML, Mollekens N, Verhamme P, Gils A, Declerck PJ. Development of a nanobody-based assay for activated thrombin-activatable fibrinolysis inhibitor (TAFIa). *Arterioscler Thromb Vasc Biol, submitted*

Chapter 1

General introduction

Haemostasis

The hemostatic system involves a tightly controlled interplay between the vasculature, circulating platelets, coagulation proteins and the fibrinolytic mechanism. The system comprises platelet aggregation, coagulation and fibrinolysis and its complexity is underscored by the enormous number of proteins involved. A delicate balance between forming an occlusive clot upon vessel injury (**coagulation**) and clot degradation (**fibrinolysis**) has to be maintained. Therefore, a disturbance of this delicate balance leads to unwanted intravascular thrombosis or extravasation of blood from the vasculature.

Coagulation

The coagulation is a complex cascade of enzymatic reactions with positive and negative feedback loops. The cascade involves consecutively activated serine proteases (coagulation factors) denominated with Roman numerals. The coagulation cascade can be described by three phases: the initiation, amplification and propagation phase.

The ***initiation phase*** is initiated by exposure of tissue factor (TF) by damage or activation of the endothelium. The catalytic complex between TF and factor VIIa activates factor IX and X. Activated factor X (FXa) generates small amounts of factor IIa (thrombin) which is able to activate factor VIII (generating FVIIIa) resulting in the complex FIXa:FVIIIa which is the start of the ***amplification phase***. The complex FIXa:FVIIIa is responsible for the amplification of the clotting process by stimulating the factor Xa (FXa) production which subsequent stimulates the thrombin generation. Furthermore, thrombin generation is enhanced by the FXa:FVa complex but also by itself through a positive feedback loop mechanism. This loop mechanism results in an increased thrombin generation to form a stable clot. Thrombin also activates platelets which results in an enhanced platelet aggregation. The recruitment of activated platelets initiates the ***propagation phase*** and is accompanied by a massive thrombin production. This burst of thrombin leads to generation of fibrin from fibrinogen and is responsible for a stable clot. Activation of factor XIII by thrombin leads to covalently cross-linked fibrin strands leading to a firm fibrin network. Furthermore, the generated thrombin also activates thrombin-activatable fibrinolysis inhibitor (TAFI) which protects the clot from plasmin-mediated fibrinolysis [1].

Fibrinolysis

Plasminogen, present in the blood as a zymogen, can be converted to plasmin by the plasminogen activators tissue-type plasminogen activator (t-PA) and urokinase-type plasminogen activator (u-PA). The catalytic efficiency of t-PA in the conversion of plasminogen to plasmin is rather low, however in the presence of fibrin, the generation of plasmin is enhanced. Plasmin can cleave fibrin and generates fibrin degradation products (FbDP's) thereby exposing C-terminal lysine residues at the fibrin surface. Both t-PA and plasminogen contain lysine-binding sites and upon binding to the C-terminal lysine residues an enhanced plasmin generation and subsequent fibrin degradation is observed. The C-terminal lysine residues can be removed by TAFI, thereby attenuating the formation of plasmin and leading to a stabilization of fibrin thrombi. Fibrinolysis can also be inhibited by plasminogen activator inhibitor-1 (PAI-1) and by direct plasmin inhibitors such as α_2-antiplasmin. However, plasmin bound to fibrin is protected from α_2-antiplasmin [2, 3] (Figure 1.1).

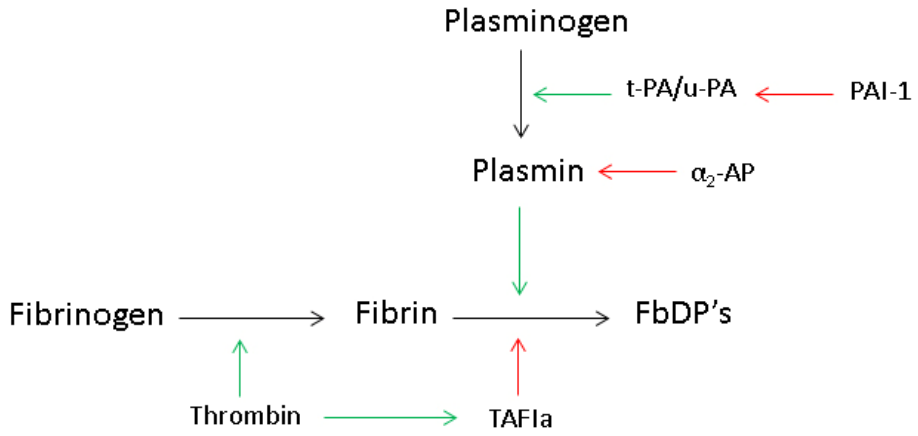

Figure 1.1: Overview of the fibrinolytic system. Plasminogen can be converted to plasmin by tissue-type plasminogen activator (t-PA) or urokinase-type plasminogen activator (u-PA). Both u-PA and t-PA can be inhibited by plasminogen activator inhibitor-1 (PAI-1) while plasmin is inhibited by α_2-antiplasmin (α_2-AP). Plasmin degrades fibrin to fibrin degradation products (FbDP's). Thrombin does not only converts fibrinogen to fibrin but also activates thrombin-activatable fibrinolysis inhibitor (TAFI) to TAFIa which in turn inhibits fibrinolysis by modifying the fibrin surface (black lines represent conversion, green lines represent stimulation and red lines represent inhibition).

Thrombin-Activatable Fibrinolysis inhibitor (TAFI)

Discovery and nomenclature

In 1989 a novel unstable basic carboxypeptidase in fresh human serum was reported distinct from the constitutively active carboxypeptidase N (CPN). The unstable enzyme, carboxypeptidase U (CPU, U stands for unstable), was suggested to originate from an inactive precursor circulating in the blood [4]. Independent research groups confirmed the discovery: Campbell *et al.* reported a carboxypeptidase protein with preference for arginine and named it arginine carboxypeptidase (CPR) [5] , Eaton *et al.* purified a new plasminogen-binding protein and named it, based on its sequence similarity with pancreatic carboxypeptidase B, plasma procarboxypeptidase B (plasma pro CPB) [6]. Bajzar *et al.* reported a zymogen that is activatable by thrombin and upon activation it attenuates clot lysis, therefore it was called thrombin-activatable fibrinolysis inhibitor (TAFI) [7]. Later it was demonstrated that proCPU, proCPR, plasma proCPB and TAFI are identical. Throughout this thesis TAFI and TAFIa are used for the zymogen and the activated form, respectively.

TAFI synthesis and distribution

The TAFI gene is located on chromosome 13 (13q14.11), it comprises 11 exons and spans approximately 48 kb of genomic DNA [8, 9]. A total of 19 single nucleotide polymorphisms have been identified of which only 6 are in the encoding region [10]. Only 2 result in an amino acid substitution (+505G/A : 147Ala/Thr and +1040 C/T: 325Thr/Ile) leading to four TAFI isoforms: TAFI-Ala^{147}Thr^{325}, TAFI-Ala^{147}Ile^{325}, TAFI-Thr^{147}Thr^{325} and TAFI-Thr^{147}Ile^{325} [11].

TAFI is synthesized in the liver as a 423 amino acids long peptide. The signal peptide is removed upon secretion in plasma where TAFI circulates at a concentration around 10 µg/ml [12, 13]. TAFI is also present in platelets, however the glycosylation pattern is different compared to TAFI that is synthesized in the liver. This suggests that TAFI is also synthesized in megakaryocytes [14]. The total amount of platelet TAFI is only 0.1% of the amount found in plasma. The low concentration of platelet TAFI does not suggests that there is no physiological role since the release of TAFI from platelets concentrated at the site of a thrombus may result in a local boost of TAFI [14].
TAFI harbors five possible glycosylation sites: four in the activation peptide (Asn^{22}, Asn^{51}, Asn^{63} Asn^{86}) and one in the active moiety (Asn^{219}). Glycosylation only occurs at the activation peptide and is responsible for ca. 9 kDa of the total molecular weight [15].

TAFI activation and TAFIa instability

TAFI can be activated to TAFIa by trypsin-like enzymes such as thrombin and plasmin. These enzymes proteolytically cleave TAFI, resulting in the generation of the TAFIa moiety (Ala^{96} - Val^{401}; 36kDa) and the release of the activation peptide (Phe^{1}-Arg^{92}; 20kDa) (Figure 1.2).

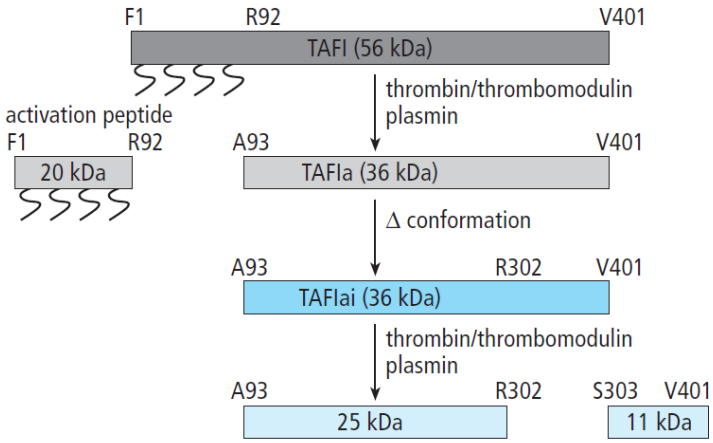

Figure 1.2: Schematic overview of TAFI activation and TAFIa inactivation [16]. TAFI (56 kDa) can be activated by thrombin, the complex thrombin/thrombomodulin or by plasmin. The activation comprises proteolytic cleavage at Arg^{92} which releases the activation peptide (20 kDa) from the TAFIa moiety (36 kDa). TAFIa is thermally unstable and inactivated through conformational changes to $TAFIa_i$. $TAFIa_i$ is subsequently degraded by thrombin/thrombomodulin and plasmin resulting in the formation of 25 and 11 kDa products.

Thrombin is a weak activator of TAFI, however in complex with thrombomodulin (TM) the activation of TAFI is accelerated 1250-fold. Due to this significant increase, the complex thrombin-thrombomodulin (T/TM) has been suggested to be the main physiological activator of TAFI [17]. At low concentrations of TM (< 5 nM), the T/TM complex mainly activates TAFI. At higher concentrations (ca 10 nM), the complex is also responsible for the conversion of protein C to activated protein C which has anticoagulant properties [18]. Therefore, depending on the concentration, TM contributes to the downregulation of the coagulation or the fibrinolytic cascade. The key enzyme of fibrinolytic cascade, plasmin, is also capable of activating TAFI, even more efficient than thrombin alone. In complex with heparin, plasmin-mediated TAFI activation is increased almost 20-fold [19] but the catalytic efficiency is still 10-fold lower compared to that of the complex T/TM [20].

TAFIa is a very unstable enzyme with a half-life of 8 to 15 min (at 37°C) depending on the amino acid (T or I) at position 325 [21, 22]. A more stable TAFIa variant (TAFIa A^{147}-C^{305}-I^{325}-I^{329}-Y^{333}-Q^{335}, TAFI-ACIIYQ) with a 180-fold increased stability has been described [23], all mutations within this variant are within the dynamic flap region, a region important for the stability [24]. Boffa *et al.* [25] reported that inactivation of TAFIa is associated with two consecutive conformational transitions

characterized by k_1 (0.5 min^{-1}) and k_2 (0.064 min^{-1}) (scheme 1). The second, rate limiting, step results in inactivation [25].

$$\mathbf{TAFIa_1} \xrightarrow{k_1} \mathbf{TAFIa_2} \xrightarrow{k_2} \mathbf{TAFIa_i} \qquad \text{(scheme 1)}$$

$TAFIa_i$ can be degraded by thrombin or plasmin into an 11 and 25 kDa fragment. Furthermore, plasmin is also able to cleave TAFI at position Lys^{327} and Arg^{330} resulting in a truncated TAFI-form of 45 kDa. This truncated form can still be cleaved at Arg^{92} but this does not result in an active fragment due to the absence of Tyr^{341} and Asp^{349} which are involved in substrate binding [26].

Since half-maximal inhibition of clot lysis time is achieved by 1 nM of TAFIa even a minimal activation of TAFI (concentration in the blood between 75-275 nM) will lead to a substantial attenuation of fibrinolysis [17].

Inhibition of TAFIa or prevention of TAFI activation

No endogenous TAFIa inhibitors were identified so far, however the *in vivo* TAFIa activity is regulated through its thermal instability. Since TAFI(a) is a very powerful antifibrinolytic drug, much research is performed to identify TAFI(a) inhibitors.

Due to the presence of a zinc ion in the active site, TAFIa is sensitive to inhibition by chelating agents such as EDTA and *o*-phenantroline. Reducing agents such as 2-mercaptoethanol and dithiotreitol disrupt disulfide bridges and interfere with the TAFIa activity [4, 6, 27]. Several small synthetic inhibitors have been developed such as arginine analogs MERGETPA (*DL*-2-mercaptomethyl-3-guanidinoethyl-thiopropanoic acid) and GEMSA (guanidinoethyl-mercaptosuccinic acid) and the lysine analog ε-ACA (ε-aminocaproic acid) [28]. Due to their inhibitory properties for other plasma carboxypeptidases such as carboxypeptidase N (CPN) the use of these non-selective compounds is not recommended [29]. Multiple attempts to develop TAFI(a) inhibitors with higher potency, less reactivity towards CPN and more favorable pharmacokinetic properties have been performed but the selectivity of these compounds remains an issue due cross-reactivity with pancreatic carboxypeptidase (CPB) [29]. Three naturally occurring inhibitors have been described with a higher selectivity for TAFIa; potato tuber carboxypeptidase inhibitor (PTCI), leech carboxypeptidase inhibitor (LCI) and tick carboxypeptidase inhibitor (TCI) [30-32].

Reversible active site-inhibitors such as PTCI and GEMSA exhibit a biphasic pattern in *in vitro* clot lysis assays: a strong enhancement of lysis at high concentrations and a prolongation of clot lysis time at lower concentrations [33]. The prolongation of clot lysis time was attributed to the

stabilizing effect that these compounds have on TAFIa, most likely by stabilization of the dynamic flap region [24]. The prolonged clot lysis time observed at low concentrations of inhibitor can be explained by an equilibrium between free and inhibitor-bound TAFIa. Free TAFIa is rapidly and irreversibly inactivated while inhibitor-bound TAFIa is protected from inactivation and forms a pool to 'replenish' free TAFIa [33, 34].

To overcome the problem of specificity, monoclonal antibodies (MAs) or nanobodies directed towards TAFI have been generated. The antibodies can hamper the activation of TAFI to TAFIa or directly interfere with the TAFIa activity. Two studies report antibodies (MA-T12D11 [35] and mAbTAFI/TM#16 [36]) selectively inhibiting the T/TM-mediated activation of human TAFI while another study reported an antibody that selectively inhibits the plasmin-mediated activation of human TAFI (MA-TCK11A9 [37]). In the latter study, an antibody inhibiting T-, T/TM- and plasmin-mediated activation of human TAFI was described (MA-TCK27A4 [37]). Unlike the previous antibodies MA-TCK26D6 cross-reacts with human, mouse and rat TAFI and inhibits the plasmin-mediated activation of TAFI, furthermore it exerts strong profibrinolytic effects in an *in vivo* mouse thromboembolism model [38]. Direct inhibition with the TAFIa activity was reported for two antibodies towards human and rat TAFI, MA-T9H11 and MA-RT30D8 respectively [35, 39]. However, antibodies of mouse origin show immunogenicity upon administration to humans. Therefore, single-chain variable fragments (scFvs) derived from MAs towards TAFI were generated and most of them show similar properties towards their target [40] however, low production yields and stability problems hamper their applicability. To solve these problems, nanobodies (single-domain fragments derived from heavy chain-only antibodies, such as e.g. VHH-TAFI-a204) interfering with the TAFI activation was generated by Buelens *et al.* [41].

Physiological and pathophysiological role of TAFI

Role of TAFI in fibrinolysis

During fibrinolysis, fibrin is converted to fibrin degradation products by plasmin. Plasmin is generated by conversion of plasminogen by t-PA. This conversion is enhanced by C-terminal lysine residues. The C-terminal lysine residues are important regulators of fibrinolysis through multiple mechanisms: (a) the affinity of plasminogen for partially degraded fibrin is increased, leading to an accelerated conversion of plasminogen to plasmin by t-PA [42] (b) plasmin bound to partially degraded fibrin is protected from inactivation by α_2-antiplasmin, (c) partially degraded fibrin also acts as a co-factor in the plasmin mediated conversion of Glu-plasminogen to Lys-plasminogen which is a better substrate for t-PA [43]. TAFIa inhibits fibrinolysis by removing C-

terminal lysine residues from partially degraded fibrin resulting in a down-regulation of the t-PA-mediated conversion of plasminogen to plasmin.

The antifibrinolytic function of TAFIa is mediated through a threshold-dependent mechanism [44, 45]. As long as the TAFIa concentration remains above a certain threshold, fibrinolysis is inhibited. When the concentration of TAFIa drops below the threshold value, the C-terminal lysine residues on fibrin drastically augment and enhance the conversion of plasminogen to plasmin. The increased plasmin production boosts fibrinolysis. The threshold value depends on the concentration of t-PA, a high concentration leads to a higher threshold level. The time that the TAFIa activity remains above the threshold value depends on the extend of activation (e.g. by T/TM) and its stability. Therefore a slow and sustained rate of TAFI activation leads to a more efficient regulation of fibrinolysis than an extensive short TAFIa burst [45].

It has been suggested that the bleeding tendency in **hemophilia** is not only due to an impaired coagulation but also an aberrant fibrinolysis [46], with a prominent role for TAFI [47-49]. A reduced activation of TAFI is partially responsible for the aberrant fibrinolysis [50] and on-demand treatment of hemophiliacs with FVIII leads to an increased TAFI activation [51]. Foley *et al.* demonstrate that addition of TM, thereby activating TAFI, to FVIII deficient plasma corrects the premature lysis [52]. However, TM is also a cofactor for the activation of activated protein C, an anticoagulant enzyme that inhibits thrombin formation, and thus TM is not considered a viable approach for the treatment of bleeding complications in hemophilia.

Other roles of TAFI(a)

Several pro-inflammatory mediators such as anaphylatoxins C3a and C5a, thrombin-cleaved osteopontin and bradykinin were identified as TAFIa substrates [5, 53, 54]. Several *in vivo* studies have been performed indicating that TAFI may have a role in **inflammation** [55-57].

Since bradykinin has also vasodilating properties, TAFIa might also have a role in the regulation of **blood pressure** [53]. Furthermore, plasmin is involved in the extracellular matrix degradation which has a role in **wound healing**, since TAFIa attenuates the formation of plasmin, also a contribution in the wound healing might be expected and was observed in a study of te Velde *et al.* [58].

Zymogen activity of TAFI

Until 2006, it was generally believed that in order to obtain carboxypeptidase activity of TAFI, TAFI had to be activated to TAFIa. Willemse *et al.* reported for the first time the existence of intrinsic carboxypeptidase activity of TAFI (= zymogen activity) as interference in a CPN assay [59]. Valnickova *et al.* demonstrated that TAFI exhibits zymogen activity not only towards small synthetic substrates (as been reported by Willemse *et al.*) but also towards large peptide substrates (synthetic fibrinogen derived peptides). These data suggested that the zymogen activity is able to down-regulate fibrinolysis *in vivo* [60]. However, by using a highly sensitive HPLC-based assay for the TAFIa activity determination, Willemse *et al.* provided evidence that the clot lysis experiments of Valnickova *et al.* were compromised by an *in vitro* activation of TAFI. Furthermore, clot lysis experiments in the presence of batroxobin (a thrombin like enzyme unable to activate TAFI [61]) revealed no prolongation of clot lysis time upon addition of TAFI [62]. Valnickova replied by pointing out that the assay used for the determination of the TAFIa activity might also cross-react with TAFI or even other metallocarboxypeptidases. Furthermore, by western blotting no TAFIa formation or released activation peptide could be observed. Also the clot lysis experiment in the presence of batroxobin might not be the optimal setup for the effect of TAFI zymogen activity since the clot composition and protein content is different [63]. Foley *et al.* confirmed that the TAFI zymogen activity is capable of cleaving small substrates but that it does not play a role in the attenuation of fibrinolysis due to its inability to cleave plasmin-modified fibrin degradation products. The conclusion was mainly based on the fact that addition of PTCI (an inhibitor of TAFIa but not TAFI) abolished the prolongation of clot lysis time in TAFI depleted plasma (TDP) plasma spiked with TAFI [64].

Mishra *et al.* reported two nanobodies stimulating the zymogen activity of TAFI. Addition of these nanobodies to TDP reconstituted with TAFI-R92A (a non-activatable TAFI mutant) resulted in a prolongation of clot lysis time [65]. It was suggested that binding of nanobodies induces a translocation of the activation peptide thereby making the catalytic cleft more accessible for larger substrates (such as C-terminal lysine residues on partial degraded fibrin) [65].

TAFI crystal structure

Attempts to crystallize TAFI were severely hampered by the heterogeneous appearance of the protein due to the glycosylation. However, using a special cell line, lacking the N-acetylglucosaminetransferase, Marx *et al.* were the first to publish the crystal structure of recombinant TAFI (Figure 1.3) [24].

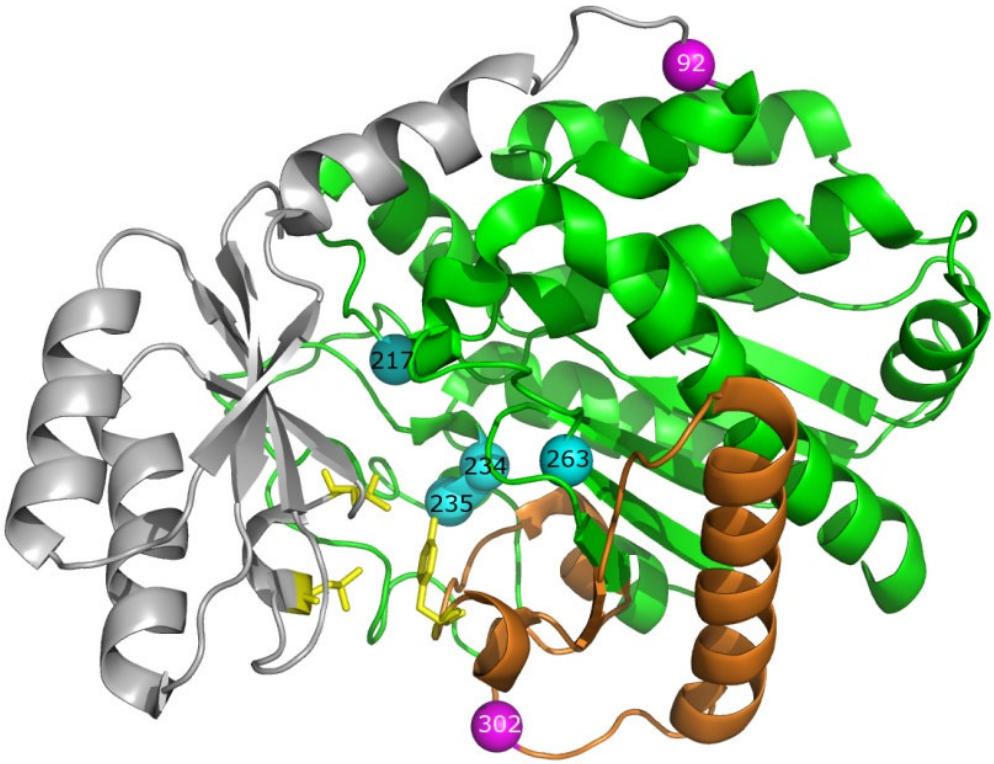

Figure 1.3: Ribbon drawing of the TAFI structure with the activation peptide and catalytic domain in grey and green respectively. Within the catalytic domain the dynamic flap region (amino acids 296-350) is colored in dark orange and the thrombin cleavage sites are depicted as purple spheres. Amino acids involved in substrate binding and hydrolysis are shown in blue and the amino acids important for the interaction between the activation peptide (Val^{35} and Leu^{39}) and catalytic domain (Tyr^{341}) are colored in yellow.

The TAFI structure consists of 2 domains; the activation peptide and the catalytic domain. The activation peptide is divided in two parts; the first 76-amino acids form 4 β-strands and 2 α-helices while the linker region (amino acids 77-92) is partially α-helical and connected to the catalytic domain. The catalytic domain (amino acids 93-401) consists of a central 8 stranded mixed β-sheet flanked by 9 α-helices. The activation peptide covers the catalytic pocket, which comprises the amino acids important for substrate catalysis (Arg^{217} and Glu^{363}) and for substrate specificity (Asn^{234}, Arg^{235} and Tyr^{341}) (see figure 1.3) [24].

Further studies on the TAFI structure revealed the presence of a dynamic flap region between amino acids 296 and 350. The dynamic flap region interacts with the activation peptide through hydrophobic interactions between Val^{35} and Leu^{39} located in the activation peptide and Tyr^{341} located in the dynamic flap region. Proteolytic cleavage at Arg^{92} leads to the release of the activation peptide and thereby compromises the interactions between the activation peptide and the TAFIa moiety. This leads to an increased mobility of the dynamic flap region and subsequently to the loss of enzymatic activity through conformational changes. This auto-regulatory mechanism explains the short half-life of the TAFIa activity. Furthermore, the induced conformational changes lead to exposure of Arg^{302}, a cryptic cleavage site for thrombin and plasmin resulting further degradation [24].

TAFIa inhibitors such as GEMSA are known TAFIa stabilizers and the crystal structure of the complex TAFIa-GEMSA confirms stabilizing interactions between GEMSA and the dynamic flap region. Furthermore, the existence of a region important for the stability of TAFIa was further supported by the fact that the majority of the stabilizing mutations are located within this dynamic flap region [24].

Measurement of TAFI/TAFIa

Elevated TAFI levels have been associated with an increased risk of angina pectoris [66], venous thrombosis [67], coronary artery disease [68], ischaemic stroke [69] and myocardial infarction [70]. Due to its critical role in different cardiovascular pathologies it is of interest to quantify TAFI(a) which can be determined by **antigen-** or **activity-based assays**.

Antigen-based assays: detection of TAFI

Different research groups have in-house developed ELISAs for the detection of TAFI [12, 13, 71], some ELISAs are commercially available. The ELISAs require no activation of TAFI and do not show any cross-reactivity with CPN. The commercial available ELISAs (e.g. VisuLize™ (Affinity Biologicals), Zymotest® (Hyphen Biomed) and Imuclone® (American Diagnostica)) were developed to measure TAFI, however some show partial cross-reactivity with TAFIa or have different reactivity towards different TAFI isoforms [71]. Due to the difference in reactivity of these assays for the different TAFI isoforms, conclusions in different studies are biased.

Antigen-based assays: detection of TAFIa/TAFIa$_i$

Even though different ELISAs were developed for the detection of TAFIa, they also recognize TAFIa$_i$. Ceresa *et al.* developed an ELISA to measure the extent of TAFI activation, based on two monoclonal antibodies. The ELISA was used in a study to compare TAFIa/TAFIa$_i$ levels between normolipidemic subjects and subjects with hyperlipidemia and showed a 10% increase in the latter [72]. The ELISA of Hulme *et al.* [73] is based on PTCI as capture agent and a mouse monoclonal antibody towards TAFI. A concentration of 500 pM TAFIa/TAFIa$_i$ was detected in pooled normal plasma. The ELISA was also used for the detection of TAFIa/TAFIa$_i$ in plasma of hemophiliacs and sepsis patients and demonstrated a 5-fold increased concentration in both pathologies [73, 74]. A commercial ELISA for the detection of TAFIa/TAFIa$_i$ (Asserachrom® Stago Diagnostica) reports TAFIa/TAFIa$_i$ values of 2.3 nM in healthy individuals and increased values in moderate and severe trauma patients; 4.3 and 8.4 nM respectively [75]. Since all the ELISAs cross-react with TAFIa$_i$ there is a need for a specific TAFIa ELISA.

Activity-based assays

The activity based assays are based on the ability of TAFIa to cleave arginine and lysine residues from small synthetic substrates. The quantification is then performed by different analytical methods such as HPLC, a spectrophotometric endpoint assay or a kinetic spectrophotometric assay.

All activity-based assays are based on the conversion of the substrate hippuryl-L-arginine to hippuric acid by TAFIa. The hippuric acid can be detected and quantified in the **HPLC-assisted assay** [76]. In the **spectrophotometric endpoint assay** hippuric acid can be detected by absorbance measurement at 254 nm [21] or 382 nm after reaction with cyanuric chloride [77]. A commercial kit based on this principle is available (Actichrome® TAFIa, American Diagnostica). **Kinetic spectrophotometric assays**, continuously monitor the absorbance increase as a result of substrate cleavage by TAFIa. These assays are mainly used for the determination of the kinetics of the TAFIa enzyme [78]. Due to the cross-reactivity of the substrates with CPN, Heylen *et al.* developed a new substrate with minimal enzymatic activity towards CPN [79].

Neill *et al.* described an alternative assay using larger substrates, better resembling the physiological C-terminal lysine residues on partially degraded fibrin [80]. The assay is based on the ability of TAFIa to decrease the co-factor activity of high-molecular-weight fibrin in the stimulation of plasminogen cleavage. The plasminogen in the assay is fluorescein labeled and an

increased TAFIa activity leads to a reduction of fluorescence. TAFIa concentrations as low as 10 pM can be detected.

Conventional antibodies, heavy-chain antibodies and nanobodies

The vertebrate immune system generates billions of antibody molecules, consisting of two heavy and two light chains. Their high diversity and selectivity make them attractive tools for research and therapeutics. A new antibody type was identified more than 20 years ago, first in the sera of dromedaries later in all members of the *Camelidae* family [81]. This new antibody type, called heavy-chain only antibody, does not contain a light chain and lacks the first constant heavy domain (CH1).

Conventional antibodies and derivatives

Conventional antibodies are glycoproteins and comprise four polypeptide chains: two light chains and two heavy chains. The light chains (Mr 25 kDa) are composed of one constant domain (CL) and one variable domain (VL). There are two types of light chains: lambda (λ) and kappa (κ) but a single antibody molecule can only contain either λ or κ light chains. The heavy chains (Mr 50 kDa) consist of constant and variable regions. The constant region consists of three or four constant domains (CH1, CH2, CH3 and CH4) and one variable domain (VH). The CH3 and CH2 domains situated at the carboxy-terminal site (Fc, crystallisable fragment) are responsible for the binding of the antibody to different immune-components. The Fab fragment, the amino-terminal site of the antibody, consists of the CH1 and VH domain of the heavy chain and the CL and VL part of the light chain. There are five antibody classes, IgG, IgA, IgM, IgE and IgD based on their heavy chains γ, α, μ, ε and δ respectively.

Antibody fragments such as the antigen-binding fragments (Fabs) and single chain variable fragments (scFvs) were generated (Figure 1.4). However, these smaller fragments have a strong tendency to aggregate and their production levels are quite low [82].

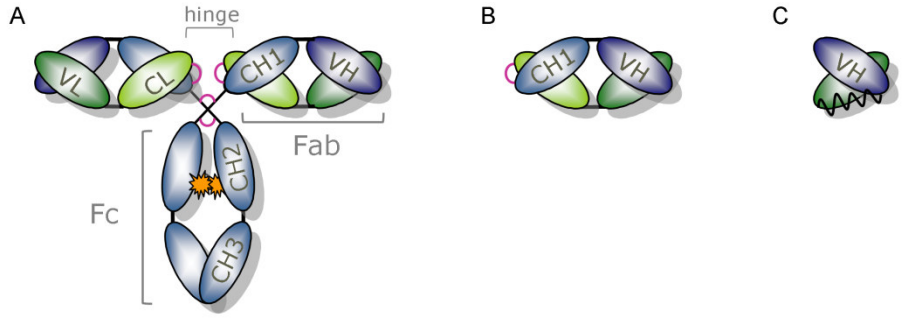

Figure 1.4: Schematic representation of a conventional antibody (A), the antigen-binding fragment, Fab (B) and single chain variable fragment, scFv (C). Conventional antibodies (A) consist of two heavy (blue) and two light (green) chains. Three constant domains (CH1-3, light blue) and one variable domain (VH, dark blue) form the heavy chain while the light chain contains one constant domain (CL, light green) and one variable domain (VL, dark green). Disulfide bridges between the two heavy chains and the heavy chains and the light chains are depicted as purple lines. The glycosylation site is depicted in orange. The antigen-binding fragment, Fab (B) contains the light chain linked by a disulfide bound to the variable and first constant domain of the heavy chain. The single chain variable fragment, scFv (C) is composed of only the variable domains of the light and heavy chain linked by a flexible linker (curved line). Adapted from [83].

Heavy-chain only antibodies

Besides conventional antibodies, Camelids (alpaca's, camels, dromedaries and lama's) also produce so called heavy chain-only antibodies (HcAbs). These HcAbs define 25 up to 75% of the serum antibodies and despite their abundance it is still unclear what the evolutionary advantage of such HcAbs could be. The more dense architecture could be better adapted to access hidden epitopes but the shorter distance between the two paratopes within one HCAbs might compromise simultaneous binding to two antigens. Due to the lack of light chains and the CH1 domain, HcAbs have a molecular weight of around 100 kDa [81] (Figure 1.5).

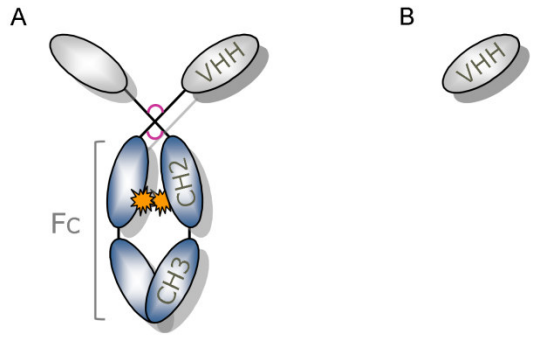

Figure 1.5: Schematic representation of a heavy-chain only antibody (A) and nanobody, VHH (B). The heavy-chain only antibody (A) contains only two heavy chains. The heavy chains consists of two constant domains (CH2-3, dark blue) and a variable domain (VHH, light blue). Disulfide bridges between the heavy chains are depicted in purple and the glycosylation site in orange. A nanobody, VHH (B), is only the variable domain of the heavy-chain only antibody. Adapted from [83].

Comparison between VH and VHH

Comparison of VH (from conventional antibodies) and VHH (from HcAbs) give some remarkable differences. The length of the CDR 1 and 3 in VHH's is considerably longer compared to those of a VH (Figure 1.6). This is most pronounced for the CDR3 region: from 9-17 AA in VH to 13-27 in VHH. The longer CDR 1 and 3 regions are responsible for a larger surface for interaction with the antigen and might compensate for the loss of three CDR regions in the VL domain. The long CDR3 region could give a higher flexibility of the CDR3-loop hampering antigen recognition, however often stabilizing disulfide bridges (Figure 1.6) are observed between CDR1 and CDR3. The disulfide bridges reduce the conformational flexibility and lead to an enhanced antigen recognition. Alignment of VH and VHH also reveals some amino acid differences in the framework 2 region (FR2). In VHH, amino acids Phe^{37} or Tyr^{37}, Glu^{44}, Arg^{45} or Cys^{45} and Gly^{47} are observed while in VH mainly Val^{37}, Gly^{44}, Leu^{45} and Trp^{47}. In conventional antibodies the FR2 region contributes to the interaction between VH and VL favoring the presence of more hydrophobic amino acids for correct VH-VL orientation [84].

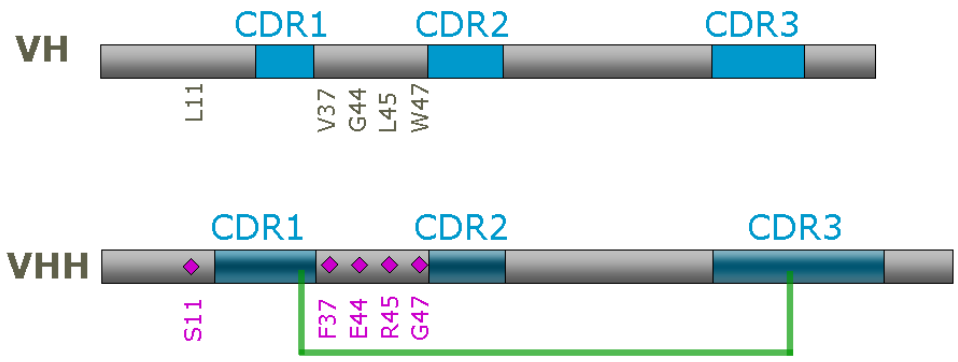

Figure 1.6: Comparison between VH and VHH [83]. Complementarity determining regions (CDR's) are colored in blue and illustrate that both CDR1 and CDR3 are generally longer in VHH compared to VH and are often connected by a disulfide bound (green line). Framework regions are colored in grey and 5 typical amino acids substitutions in VHH are depicted in purple.

Generation, production and purification of nanobodies

The variable part of the HcAbs, VHH, can be cloned and expressed recombinantly and is then called nanobody. This fragment retains its antigen-binding properties and is very soluble due to hydrophobic amino acids that are replaced by more hydrophilic amino acids (figure 1.6). Nanobodies can be considered as one of the smallest (15 kDa) antigen-binding fragments with intact antigen-binding capacity.

The nanobodies are easily produced after immunization of a member of the *Camildae* family. Therefore, lymphocytes are isolated and the mRNA is purified. After reverse transcription, the VHH repertoire is cloned into a phagemid vector which allows the VHH's to be expressed on the tip of phages. Two to three panning rounds are sufficient to enrich antigen-specific VHH's and allow individual clones to be screened in an ELISA [85]. Nanobodies can be expressed in bacteria using a secretion signal, transferring the nanobody to the periplasmic space. The purification is straightforward since the nanobodies are usually cloned in frame with a C-terminal 6-His-tag. By using immobilized metal affinity chromatography, yields of several mg per liter of medium are routinely obtained [86].

Properties of the nanobodies

Nanobodies are remarkably stable, they can be stored for months at 4°C and even longer at -20°C maintaining full antigen-binding capacity. Incubation for more than one week at 37°C seems to be tolerated as well [86]. Unlike conventional antibodies, nanobodies can successfully refold and bind to their antigen after incubation at 90 °C [87]. Furthermore, nanobodies are also very tolerant towards chemical denaturation [88].

Due to their long CDR3 region (Figure 1.7), nanobodies are often found to bind in cavities. Catalytic clefts of enzymes are frequently located in cavities and therefore it is not surprising that nanobodies are very potent enzyme inhibitors [85, 89, 90]. However, it should be noted that also nanobodies with a short CDR3 region were also found to exert strong inhibitory properties indicating that also other interactions between nanobody and antigen can be observed [91].

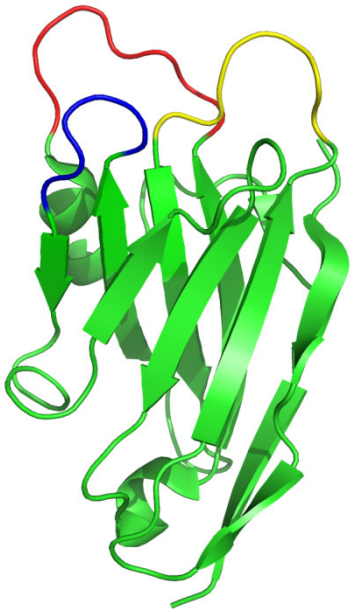

Figure 1.7: Ribbon diagram of the structure of a nanobody. Complementarity determining regions (CDR's) 1, 2 and 3 are colored in yellow, blue and red respectively. The framework regions are colored in green (PDB 1ZMY).

Due to the *in vivo* maturation, nanobodies are very strong binders; kinetic k_{on} and k_{off} rate constants of 10^5 M^{-1} s^{-1} to 10^6 M^{-1} s^{-1} and 10^{-2} s^{-1} to 10^{-4} s^{-1} respectively, are routinely observed, resulting in low nanomolar and even picomolar dissociation constants. Even though for most applications the affinity is sufficient, different *in vitro* affinity maturation approaches have been developed [92].

Due to the high degree of homology between VH and nanobodies, no immune response was observed in mice and humans after injection of nanobody-containing constructs [93, 94]. However a general strategy was developed to humanize nanobodies changing 12 out of 14 amino acids that differ between the camelid VHH and the human VH, maintaining the good solubility and expression yield without compromising the affinity and stability of the nanobody [95].

The monomeric behavior in combination with their small size make nanobodies ideal building blocks for the development of multidomain constructs [96]. Several dimeric nanobody constructs have been developed: (a) a bivalent, monospecific construct consisting out of two identical nanobodies thereby increasing the fuctional affinity for the target [97], (b) a biparatopic, monospecific construct obtained by combining two different nanobodies targeting the same antigen on different epitopes [98] and (c) a bispecific construct through combination of two nanobodies targeting different antigens [99].

Applications with nanobodies

The ease and economic production, small size, stable and soluble behavior, specific and high affinity make nanobodies ideal binders for various targets. Furthermore, it has been suggested that nanobodies recognize 'hidden' epitopes and many nanobodies modulate the function of the target. The unique properties stimulated research in many universities, pharmaceutical companies and biotech companies to develop nanobodies for therapeutic and diagnostic properties and as research tools [100]. The sections below focus on applications where nanobodies offer a special advantage.

Nanobodies as research tools

It has been proposed that nanobodies can assist in the crystallization process and structural determination of flexible or aggregating proteins. As crystallization chaperones, nanobodies may reduce conformational heterogeneity and mask counterproductive surfaces while extending surface predisposed to form crystal contacts [101]. Due to an increased availability of nanobodies rapid progress has been observed over the last couple of years. In this way multiple difficult targets due to poor crystallization [102] and unstable active-state conformations [103, 104] were crystallized. Nanobodies can also be used as imaging tools: fusion of a fluorescent protein with a nanobody and its intracellular expression allows visualization of a specific antigen in various cellular compartments [105, 106].

Nanobodies as diagnostic tools

Surprisingly, the use of nanobodies for the quantitative detection of targets has been very limited. Some ELISAs have been reported [107, 108] for the detection of *Taenia solium* and human papillomavirus. The existence of a limited amount of nanobody based ELISAs is most likely due to the fact that conventional antibodies are, due to their larger size, probably better suited for random coupling at solid surfaces [109].

Because of their small size (well below the renal clearance cutoff (ca. 50 kDa)) nanobodies are rapidly cleared from the blood and are therefore ideal for *in vivo* imaging, thereby reducing the radiation for the patient. Some nanobodies have been tested in mice for the detection of e.g. HER-2, a breast cancer antigen [110] and V-CAM1, an antigen used for the diagnosis of vulnerable atherosclerotic plaques [111].

Nanobodies as therapeutics

Several antibacterial toxins and antisnake venom nanobodies have been generated [112-114] and use of nanobodies for passive immunization of mice injected with scorpion toxin demonstrated a high neutralizing potency [115]. Nanobodies may also have an advantage in situations where functional domains on pathogenic substances as viruses and bacteria may be unaccesible ("hidden") for the much larger conventional antibodies [116, 117].

Ablynx, a Flemish biotech-company engaged in the discovery and development of nanobodies has several nanobody-derived therapeutics in their pipeline. These nanobodies target important acute and chronic diseases across a broad range of therapeutic areas including haematology (anti-von Willebrand factor nanobody used to treat people with thrombotic thrombocytopenic purpura), inflammation (anti-IL6R and anti-TNFα nanobody to treat rheumatoid arthritis) and oncology (anti-RANKL nanobody to treat bone loss associated with cancer, rheumatoid arthritis and post-menopausal osteoporosis) [109]. Some of these nanobody-derived therapeutics have passed phase I and are currently investigated in phase II tests, however there is a tough competition from other therapeutics. Due to the smaller size and remarkable stability of the nanobodies, the success of nanobody-based therapy could be found in alternative administration (i.e. topical, inhalation or oral) [118].

Objectives

One of the main disadvantages of current t-PA thrombolytic treatment is the increased bleeding risk. Upon activation, thrombin-activatable fibrinolysis inhibitor (TAFI) is a very powerful antifibrinolytic enzyme. Co-administration of a TAFI inhibitor during thrombolysis could reduce the t-PA dose required to obtain a comparable degree of lysis thereby decreasing bleeding risks without compromising the efficacy of the treatment.

Nanobodies interfering with the activation of TAFI to TAFIa through multiple mechanisms have been described [41]. Due to their long CDR3 region, nanobodies are ideal candidates for binding to cavities of enzymes such as activated TAFI (TAFIa). The *first objective* was the generation of inhibitory nanobodies towards human TAFIa and characterization of their profibrinolytic properties (**chapter 2**).

The previously described anti-TAFI(a) nanobodies towards human TAFI(a) lack cross-reactivity with mouse and rat TAFI and therefore could not be tested in an *in vivo* thromboembolism model. The *second objective* was the generation of inhibitory nanobodies towards mouse TAFI (**chapter 3**) and rat TAFI (**chapter 4**) and test their application in an *in vivo* mouse thromboembolism model.

Many ELISAs have been developed to measure TAFI antigen levels, mainly based on total antigen levels. However, not the total antigen levels but the amount of TAFIa represents the enzymatic activity essential for its biological function. The *third objective* was the development of an ELISA specifically detecting TAFIa (**chapter 5**).

Chapter 2

TAFIa inhibiting nanobodies as profibrinolytic tools and discovery of a new TAFIa conformation

M. L. V. HENDRICKX*, A. DE WINTER*, K. BUELENS*, G. COMPERNOLLE*, G. HASSANZADEH-GHASSABEH †, S. MUYLDERMANS †, A. GILS* and P. J. DECLERCK*

* Laboratory for Pharmaceutical Biology, Faculty of Pharmaceutical Sciences, Katholieke Universiteit Leuven, Leuven
† Laboratory of Cellular and Molecular Immunology, Faculty of Sciences, Vrije Universiteit Brussel, Brussels; and Department of Molecular and Cellular Interactions, NSF, VIB, Brussels, Belgium

J Thromb Haemost. 2011;9:2268-2277

SUMMARY

Background: Since activated thrombin activatable fibrinolysis inhibitor (TAFIa) has very powerful antifibrinolytic properties, co-administration of t-PA and a TAFIa inhibitor enhances t-PA treatment.

Objective: We aimed to generate nanobodies specifically inhibiting the human TAFIa activity and to test their effect in t-PA induced clot lysis.

Methods and results: Five nanobodies, raised towards an activated more stable TAFIa mutant (TAFIa A^{147}-C^{305}-I^{325}-I^{329}-Y^{333}-Q^{335}) are described. These nanobodies inhibit specifically TAFIa activity resulting in an inhibition up to 99 % at a 16-fold molar excess of nanobody over TAFIa, IC_{50}'s range between 0.38- and > 16-fold molar excess. *In vitro* clot lysis experiments in the absence of thrombomodulin (TM) demonstrate that the nanobodies exhibit profibrinolytic effects. However, in the presence of TM, one nanobody exhibits an antifibrinolytic effect whereas the other nanobodies show a slight antifibrinolytic effect at low concentrations and a pronounced profibrinolytic effect at higher concentrations. This biphasic pattern was highly dependent on TM and t-PA concentration. The nanobodies were found to bind in the active-site region of TAFIa and their time-dependent differential binding behavior during TAFIa inactivation revealed the occurrence of a yet unknown intermediate conformational transition.

Conclusion: These nanobodies are very potent TAFIa inhibitors and constitute useful tools to accelerate fibrinolysis. Our data also demonstrate that the profibrinolytic effect of TAFIa inhibition may be reversed by the presence of TM. The identification of a new conformational transition contributes to new insights on the conformational inactivation of the unstable TAFIa.

INTRODUCTION

Plasmin-mediated partial degradation of fibrin clots exposes terminal lysine residues. These residues enhance the cofactor activity of fibrin degradation products in the activation of plasminogen by t-PA [1]. The activated form of thrombin activatable fibrinolysis inhibitor (TAFIa), also known as carboxypeptidase U (CPU) [2] or plasma carboxypeptidase B [3], attenuates fibrinolysis by removing these lysine residues [4]. This results in decreased plasmin formation and prolongation of clot lysis time [5]. TAFI circulates in the blood as a 56 kDa zymogen. It can be activated into the active enzyme, TAFIa (Ala^{93}-Val^{401}; 36 kDa), by thrombin, thrombin/thrombomodulin complex and plasmin with release of the activation peptide (Phe^{1}-Arg^{92}; 19 kDa) [4, 6-8]. The TAFIa moiety is very unstable and is converted spontaneously into an inactive form ($TAFIa_i$) through a conformational change [7, 9].

An increased risk for angina pectoris, venous thrombosis and coronary artery disease has been reported to be associated with elevated TAFI levels. In different animal models for thrombosis, inhibition of TAFIa by a small molecule enhanced thrombolytic therapy without increasing the bleeding risk [10]. Therefore the development of a specific TAFIa inhibitor is of interest for use as an adjuvant in thrombolytic therapy and is an interesting tool to investigate the pathophysiological role of TAFIa *in vivo.*

So far, no endogenous TAFIa inhibitors are known. Inactivation of TAFIa mainly depends on its thermal instability [9] leading to a conformational change [7]. Two naturally occurring TAFIa isoforms show a temperature-dependent instability with a half life at 37 °C of 8 and 15 minutes for TAFIa isoforms $Thr^{325}$and Ile^{325}, respectively [11]. A more stable TAFIa mutant, TAFIa –A^{147}-C^{305}-I^{325}-I^{329}-Y^{333}-Q^{335} (TAFIa-ACIIYQ), with a 180-fold longer half life, compared to that of TAFI-wt, has been reported [12].

Many TAFI(a) inhibitors, inhibiting the TAFI(a) function through multiple mechanisms have been described. Even though some of these are potent TAFIa inhibitors, most of them lack specificity [13]. To circumvent the lack of specificity, monoclonal antibodies have been developed towards TAFI [14-16]. The reported monoclonal antibodies interfere with TAFI function either by inhibiting its conversion to TAFIa [15, 16] or by direct interference with the TAFIa activity or stability [14]. GEMSA and PTCI, both competitive inhibitors of TAFIa, show a biphasic *in vitro* effect: prolongation of clot lysis time at low concentrations and enhancing lysis at higher concentrations [17, 18]. The rationale behind this observation can be explained by an equilibrium between free and inhibitor bound TAFIa. While free TAFIa is rapidly and irreversibly inactivated, the bound form is protected

against conformational inactivation and refills the free pool by dissociating from its inhibitor in order to maintain the equilibrium [17, 18].

Besides conventional antibodies, the serum of *Camelidae* contains considerable amounts of unique antibodies, naturally devoid of the light chain and lacking the CH1-domain [19]. These functional antibodies, referred to as heavy-chain antibodies, bind their targets by a single domain, i.e. the variable domain of the heavy-chain antibodies (VHH) or Nanobody [20]. VHHs comprise 3 antigen-binding loops of which the first and third loop (i.e. the complementarity determining region-1 and 3 (CDR1 and CDR3)) are longer than the CDR1 and CDR3 of variable domains of classic antibodies. The potent enzyme inhibiting properties of VHHs are ascribed to their long CDR3 loop [21, 22].

Even though nanobodies towards TAFI have been reported recently, none of those showed a specific and exclusive inhibition of the enzymatic activity of TAFIa [23]. We hypothesized that immunization with a more stable, activated TAFI variant (TAFIa-A^{147}-C^{305}-I^{325}-I^{329}-Y^{333}-Q^{335}) might result in the generation of potent, TAFIa-specific inhibitory nanobodies binding in the active site.

MATERIALS AND METHODS

Materials

Wild-type recombinant TAFI-T^{147}-I^{325} (TAFI-TI), recombinant TAFI –A^{147}-C^{305}-I^{325}-I^{329}-Y^{333}-Q^{335} (TAFI-ACIIYQ), recombinant TAFI-A^{147}-C^{305}-I^{325} (TAFI-AI-Cys^{305}) and recombinant TAFI-A^{147}-C^{305}-I^{325}-I^{329} (TAFI-AI-$Cys^{305}Ile^{329}$) were prepared as described before [12, 15, 24]. All the experiments were performed with TAFI-TI unless indicated otherwise. Oligonucleotides used for cloning and sequencing were obtained from Sigma-Aldrich (St Louis, MO, USA), *Pfx*50 DNA polymerase was purchased from Invitrogen (Merelbeke, Belgium) and restriction enzymes were provided by New England Biolabs (Hertfordshire, UK). The polymerase chain reaction (PCR) was performed with the Mastercycler Gradient from Eppendorf (Hamburg, Germany). Plasmid DNA purification was performed with the Nucleobond^{TM} AX500 kit (Machery-Nagel, Düren, Germany). The DNA was sequenced by LGC genomics (Berlin, Germany).

Human thrombin and plasmin were purchased from Sigma-Aldrich and Enzyme Research Labs (South Bend, UK). Rabbit thrombomodulin (TM) was obtained from American Diagnostics (Greenwich, CT, USA). H-D-phenylalanine-L-propyl-L-arginine chloromethyl ketone (PPACK), aprotinin, hippuryl-L-arginine, guanidinoethyl-mercaptosuccinic acid (GEMSA) and potato tuber carboxypeptidase inhibitor (PTCI) were obtained from Biomol Research labs (Plymouth meeting, PA, USA), Fluka (Buchs, Switzerland), Bachem (Bubendorf, Switzerland), Calbiochem (La Jolla CA, USA) and Sigma-Aldrich respectively. Tissue-type plasminogen activator (t-PA) was a kind gift from Boehringer Ingelheim (Brussels, Belgium). Citrated plasma of 27 healthy individuals, collected with their written consent, was pooled for clot lysis experiments.

Nanobody library construction, expression and purification

The construction of the nanobody library was performed as described [23] using activated TAFI-ACIIYQ (TAFIa-ACIIYQ) as immunogen. Briefly, an alpaca (*Vicugna pacos*) was immunized by 7 weekly subcutaneous injections of 100 µg TAFIa-ACIIYQ mixed with Gerbu LQ#3000 (from Gerbu Biotechnik GmBH, Germany) adjuvant. Four days after the last injection blood samples were collected and lymphocytes were isolated. After isolation and purification of total RNA, the cDNA was obtained by reverse transcription and the VHH gene repertoire was amplified by PCR. Subsequently, the PCR products were digested with *Pst*I and *Not*I restriction enzymes and ligated into the phagemid vector pHEN4. After transformation in *E. coli* the VHH repertoire, was displayed on phage and the binders were selected via panning against TAFIa-ACIIYQ and TAFI-ACIIYQ, resulting in the a- and i-series, respectively. Identification of positive clones was

performed by ELISA and identical clones were detected via sequencing. For the positive clones the DNA encoding the VHH was recloned into the production vector pHEN6c using *Pst*I and *Bst*EII restriction enzymes. The constructs were transformed into *E. coli* WK6 cells, and nanobody expression was induced as described previously [22]. The periplasmic extract was isolated and dialyzed against 20 mmol/L Tris-HCl, 0.5 mol/L NaCl (pH 7.9) and filtered through a 0.45 µm filter prior to loading on a His-Trap HP column (GE Healthcare). Bound proteins were eluted using an imidazole gradient (0-350 mmol/L imidazole in 20 mmol/L Tris HCl, 0.5 mol/L NaCl; pH 7.9). Nanobody containing fractions were selected via SDS-polyacrylamide gel electrophoresis (PAGE) (Phast-Gel^{TM} gradient 10-15% gels) by coomassie staining. Finally the selected fractions were dialyzed against phosphate buffered saline (PBS; 140 mmol/L NaCl, 2.7 mmol/L KCl, 8 mmol/L Na_2HPO_4, 1.5 mmol/L KH_2PO_4; pH 7.4).

Evaluation of the overall inhibitory effect of the nanobodies on TAFI activation and TAFIa activity

The overall inhibitory effect of the nanobodies on TAFI was determined as described before [15] with minor modifications. TAFI (45 nmol/L, concentration during activation) was diluted in HEPES buffer (25 mmol/L HEPES, 137 mmol/L NaCl, 3.5 mmol/L KCl and 0.1% BSA; pH 7.4) and incubated for 10 min at 25 °C with either buffer or nanobody at concentrations ranging from 0.25- to 16-fold molar ratio of nanobody over TAFI. Subsequently, TAFI was activated by addition of thrombin, thrombomodulin and $CaCl_2$, at a concentration (during activation) of 20 nmol/L, 5 nmol/L and 5 mmol/L, respectively. After 10 min at 25 °C, activation was terminated by addition of PPACK (37.5 µmol/L, final concentration) and the substrate hippuryl-arginine (Hip-Arg, 4 mmol/L, concentration during substrate conversion) was added to the activation mixture and conversion was allowed to proceed for 15 min at 25 °C. The substrate conversion was stopped by addition of 20 µl HCl (1 mol/L) followed by neutralization with 20 µl NaOH (1 mol/L) and buffered with 25 µl Na_2HPO_4 (1 mol/L; pH 7.4). After addition of 30 µl 6% cyanuric chloride (in 1,4-dioxane), the mixture was vortexed (5 min) and centrifuged (Eppendorf centrifuge 5415D) at max speed for 2 min. Aliquots of 100 µl were transferred into a 96-well microtiterplate and the absorbance was measured at 405 nm. By comparison of the enzymatic activity generated upon activation of TAFI in the absence or presence of nanobody (Nb), the inhibiting capacity was calculated and expressed as percentage of inhibition (($[OD]^{no\ Nb}$- $[OD]^{with\ Nb}$)/($[OD]^{no\ Nb}$) x 100 = % inhibition). In this assay a reduced TAFIa activity could be due to either interference with the activation process or by a direct interference with TAFIa enzymatic activity.

Alternatively, the effect of the nanobodies on plasmin-mediated activation and thrombin mediated activation of TAFI was also investigated. For plasmin, the above procedure was followed except for i) the use of plasmin (500 nmol/L, during activation) instead of thrombin/thrombomodulin; ii) addition of aprotinin (1.25 µmol/L, final concentration instead of PPACK); iii) incubation with hippuryl-arginine for 30 min at 25 °C. For thrombin-mediated activation, thrombin was used at 100 nmol/L (during activation step) and the activation time was prolonged to 2 hours. Because of the thermal instability of TAFIa at 25 °C (resulting in too low TAFIa levels for reliable quantitative evaluation under these conditions) TAFI was replaced by TAFI-A^{147}-C^{305}-I^{325}-I^{329}-Y^{333}-Q^{335} (45 nmol/L, concentration during activation). The activation was stopped with PPACK (187.5 µmol/L, final concentration).

Evaluation of the effect of the nanobodies on the conversion of TAFI to TAFIa

TAFI (857 nmol/L, concentration during activation) was diluted in Tris buffer (20 mmol/L Tris, 0.1 mol/L NaCl; pH 7.4) and mixed with either buffer or nanobody (16-fold molar excess of nanobody over TAFI) for 10 min at 37 °C. Subsequently the mixture was activated by thrombin/thrombomodulin (20 nmol/L and 5 nmol/L, respectively) and $CaCl_2$ (5 mmol/L) at 37 °C for 10 min. The activation was stopped with 30 µmol/L PPACK. Addition of sodium dodecyl sulfate (SDS; 1% final concentration) was followed by heating for 30 seconds at 100 °C. The fragments separated by SDS-polyacrylamide gel electrophoresis (PAGE) (Phast-Gel™ gradient 10-15% gels) were visualized by silver staining [15]. As plasmin is also able to activate TAFI, a similar setup was designed for the evaluation of the effect of nanobodies on plasmin-mediated activation. The thrombin/thrombomodulin and PPACK however were replaced by plasmin (333 nmol/L) and aprotinin (960 nmol/L), respectively. Finalization of the experiment was performed as described above.

Evaluation of the direct inhibitory effect of the nanobodies on the TAFIa activity

For the determination of the direct inhibitory effect of nanobodies on the TAFIa activity, TAFI (45 nmol/L, concentration during activation) was diluted in HEPES and activated by addition of thrombin, thrombomodulin and $CaCl_2$ (20 nmol/L, 5 nmol/L and 5 mmol/L, respectively). After 10 min at 25 °C activation was terminated by addition of PPACK (37.5 µmol/L, final concentration). Subsequently an equal volume of either buffer or nanobody (resulting in a Nb:TAFI molar ratio ranging from 0.25 to 16) was added and the mixture was incubated at 25 °C for 10 min. Subsequently TAFIa activity was determined as described above and the percentage of inhibition of the TAFIa activity was calculated relative to the TAFIa activity in the absence of nanobody.

Evaluation of the effect of the nanobodies on fibrinolysis

Clot lysis was performed in microtiterplates as described before [25] with minor modifications. Plasma was pooled and mixed with either buffer or nanobodies diluted in Tris/Tween buffer (10 mmol/L Tris, 0.01% Tween 20, pH 7.5). The final concentrations of the nanobody resulted in a Nb:TAFI molar ratio ranging from 0.25 to 16, assuming a TAFI concentration of 179 nmol/L in plasma. A control nanobody, VHH-TAFI-a204, previously demonstrated to prevent TAFI activation and to exhibit profibrinolytic activity comparable to that of PTCI [23], was also included. After incubation for 10 min at 37 °C, t-PA was added. Subsequently, aliquots of 80 µl were transferred, in duplicate, to microtitre wells each containing 20 µl 53 mmol/L $CaCl_2$ resulting in the following final concentrations: 30% pooled plasma, 120 pmol/L t-PA, 10.6 mmol/L $CaCl_2$. The plate was incubated at 37 °C and read at 405 nm at 2 min intervals to determine the 50% clot lysis time, defined as the time needed from full clot formation (i.e. maximum turbidity) to the midpoint of the maximal turbid to clear transition. Under these conditions, clot lysis times (CLT) were 89.5 ± 12.1 min (inter-assay coefficient of variation 14%) and 134 ± 12 min (inter-assay coefficient of variation 9%) in the absence and presence of 1 nmol/L TM respectively. The reduction of clot lysis time was calculated relative to the clot lysis time in the absence of nanobody (CLT_{+Nb}/CLT_{-Nb}). Under these conditions the "positive" control VHH-TAFI-a204 [23] yielded a CLT_{+Nb}/CLT_{-Nb} value of 0.56 ± 0.07 and 0.36 ± 0.02 in the absence and presence of TM, respectively, reflecting a full inhibition of TAFI(a).

Alternatively, clot lysis experiments were performed with an increased amount of t-PA (final concentration: 360 pmol/L) and/or in the presence of various concentrations of added thrombomodulin (final exogenous concentration 0.5, 1, 5 nmol/L).

Evaluation of binding of the nanobodies to various TAFI forms

The affinity constants for binding of the nanobodies to TAFI(a) were determined by Surface Plasmon Resonance using a Biacore 3000 analytical system (Biacore, Uppsala, Sweden) equipped with the CM5 sensor chip as described before [23]. The nanobodies were covalently coupled up to 400 resonance units (using a concentration of 5 µg/ml in 10 mmol/L of acetate buffer pH 4.5). Purified TAFI variants (TAFI or TAFIa) (TAFI was activated as described below) were injected (180 µl) at concentrations between 5 and 200 nmol/L (in HBS-EP, Biacore, Uppsala, Sweden) at a flow rate of 30 µl/min, followed by a dissociation of 6 min. After each cycle the regeneration of the chip was performed by 10 µl of glycine-HCl (10 mmol/L pH 2.5, Biacore). Association and

dissociation rate constants were calculated with BIAcore 3000 evaluation software using the Langmuir binding model (Local fit).

For these experiments, activated TAFI (TAFIa) was generated by activation of TAFI variants (concentration during activation: 857 nM in Tris buffer; 20 mmol/L, 100 nmol/L NaCl, pH 7.4) with thrombin and thrombomodulin (20 and 5 nM, respectively) in the presence of $CaCl_2$ (5 mM) for 10 minutes at 37 °C. The reaction was arrested by addition of PPACK (30 µM). Subsequently, the samples were incubated at 37 °C. Fractions were taken after different incubation times at 37 °C for concomitant TAFIa activity determination and binding to the nanobodies (Biacore). The experiments were carried out with TAFI-TI for the five nanobodies and in addition with TAFI-AI-Cys^{305} and TAFI-AI-Cys305-Ile329 for VHH-TAFI-a428 and VHH-TAFI-i391.

Well-known TAFIa inhibitors like PTCI and GEMSA bind in the active site of TAFIa. We hypothesized that the nanobodies bind in the same region. Therefore competition experiments were designed in which TAFI is activated as described above followed by inhibition of TAFIa with either GEMSA (concentration ranging from 64000- to 250-fold molar ratio over TAFIa) or PTCI (concentration ranging from 100- to 0.1-fold molar ratio over TAFIa) (10 min incubation time at 25 °C). Four-fold serial dilutions of each inhibitor were tested in parallel using Surface Plasmon Resonance analysis to quantify residual binding of TAFIa to the nanobodies and using a chromogenic assay (as described above) to quantify residual TAFIa activity.

RESULTS

One hundred positive clones producing nanobodies towards TAFI(a) were identified. Evaluation of amino acid sequence identity, within the CDR3 region, revealed 16 clusters. Nanobodies of the same cluster are expected to target the same epitope on the antigen [26]. Subsequently 25 nanobodies (2 of each cluster or 1 for clusters with only one nanobody) were selected for production and purification. Evaluation of their inhibitory effects on TAFI activation and/or TAFIa activity revealed that the nanobodies from 5 clusters exclusively inhibit TAFIa activity, those of 3 clusters exhibit mainly inhibition of plasmin-mediated activation, nanobodies from 1 cluster exhibit mainly inhibition of T/TM-mediated activation and nanobodies from 7 clusters show no TAFI inhibitory effect. This paper focuses on the inhibitory features of the nanobodies exclusively interfering with the TAFIa activity. Therefore the strongest inhibitor out of each cluster was selected for further characterization (i.e. VHH-TAFI-a425, VHH-TAFI-a428, VHH-TAFI-i342, VHH-TAFI-i373 and VHH-TAFI-i391).

Characterization of the TAFI activation inhibitory properties of the nanobodies

Addition of VHH-TAFI-a425, VHH-TAFI-a428, VHH-TAFI-i342, VHH-TAFI-i373 and VHH-TAFI-i391 prior to TAFI activation revealed a reduction of TAFIa activity of 67.7 % ± 3.3, 47.9 % ± 3.9, 38.6 % ± 4.9, 73.8 % ± 3.7 and 99.2 % ± 0.5, (mean ± SD, n≥3) respectively, at a 16-fold molar excess of nanobody. Conversely, these five nanobodies did not affect activation of TAFI to TAFIa as evaluated by SDS-PAGE analysis of the fragmentation pattern after activation (data not shown). Taken together, these data are compatible with an exclusive effect on TAFIa activity.

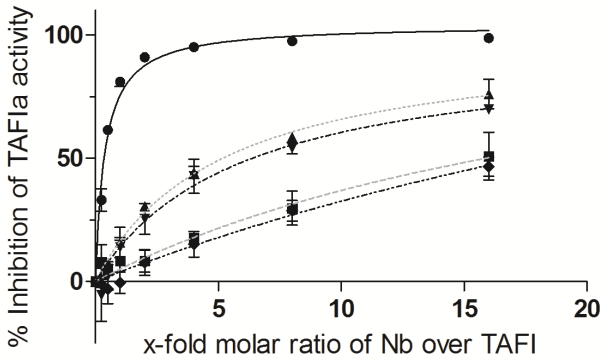

Figure 2.1: Concentration dependent inhibition of TAFIa by nanobodies: VHH-TAFI-i391 ; VHH-TAFI-a425 ; VHH-TAFI-i373 ; VHH-TAFI-a428 ; VHH-TAFI-i342 in a molar ratio ranging between 16- and 0.25-fold molar ratio of nanobody over TAFIa. TAFI (45 nM) was activated with T/TM at 25 °C for 10 min. Activation was stopped by addition of PPACK, nanobodies were added at the indicated ratio's and the residual TAFIa activity was measured. Mean ± SD, n ≥ 3.

Characterization of the direct inhibitory effect of the nanobodies on the TAFIa activity

At a 16-fold molar ratio over TAFI, VHH-TAFI-i391 completely inhibited TAFIa activity (98.8 % ± 0.5), the other four nanobodies showed a moderate inhibition between 46.6 % ± 3.9 and 76.1 % ± 6.0 (mean ± SD, n≥3 Table 2.1). Dose-response experiments revealed a maximum inhibition for VHH-TAFI-i391 at a 2- to 4-fold molar excess of nanobody over TAFI, whereas for the other nanobodies maximum TAFIa inhibition was not reached at the highest concentration tested (Figure 2.1). This resulted in an IC_{50} of 0.38 (molar ratio over TAFI) for VHH-TAFI-i391. For VHH-TAFI-a425 and VHH-TAFI-i373 an IC_{50} of 5.1 and 5.9, respectively, could be calculated based on the theoretical maximum, for VHH-TAFI-a428 and VHH-TAFI-i342 the IC_{50} exceeded 16 (Table 2.1).

Table 2.1: Evaluation of TAFIa inhibiting nanobodies

	% Inhibition of TAFIa activity[(1)]	IC_{50}-value[(2)]	CLT_{+Nb}/CLT_{-Nb} - TM[(1)]	CLT_{+Nb}/CLT_{-Nb} + TM[(1)]
- Nb	/	/	1	1
VHH-TAFI-a425	76.1 ± 6.0	5.1	0.61 ± 0.04**	0.71 ± 0.11$^{(NS)}$
VHH-TAFI-a428	50.9 ± 9.7	> 16	0.70 ± 0.01**	1.82 ± 0.24*
VHH-TAFI-i342	46.6 ± 3.9	> 16	0.56 ± 0.03*	0.68 ± 0.13$^{(NS)}$
VHH-TAFI-i373	69.8 ± 1.6	5.9	0.58 ± 0.02*	0.71 ± 0.11$^{(NS)}$
VHH-TAFI-i391	98.8 ± 0.5	0.38	0.53 ± 0.02**	0.42 ± 0.03**

[(1)] Molar ratio VHH:TAFI = 16; [(2)] Expressed as 'molar ratio VHH:TAFI'; Statistical significance (paired t-test) of difference compared to the data obtained in the absence of nanobody: [(**)] p<0.005; [(*)] p<0.05; [(NS)] not significant. CLT: clot lysis time. All data represent mean ± SD, n ≥ 3

Effect of the nanobodies in an *in vitro* clot lysis experiment

In absence of exogenous TM, the nanobodies, at a 16-fold molar excess over TAFI, reduced the clot lysis time yielding CLT_{+Nb}/CLT_{-Nb} values between 0.53 and 0.70 (Table 2.1). Dose-response curves (Figure 2.2) revealed that this effect on clot lysis was most pronounced for VHH-TAFI-i391 whereas VHH-TAFI-a428 only showed a minor dose-dependent effect. In the presence of 1 nmol/L TM, VHH-TAFI-a428 showed a dose-dependent increase of the clot lysis time (Figure 2.2B) whereas VHH-TAFI-a425, VHH-TAFI-i373, VHH-TAFI-i342 and VHH-TAFI-i391 showed a biphasic concentration effect with a transient increase in clot lysis time at lower concentrations of nanobody. The increase in clot lysis time was maximal around a 0.25-fold molar ratio of

nanobody VHH-TAFI-i391 over TAFI (Figure 2.2B) and at a 1- to 2-fold molar ratio of nanobody TAFI for VHH-TAFI-a425, VHH-TAFI-i373 and VHH-TAFI-i342 over TAFI (data not shown).

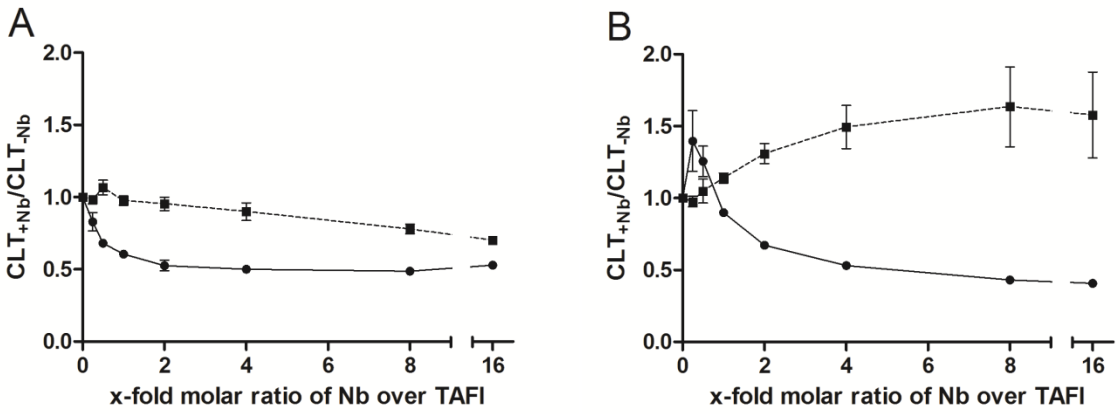

Figure 2.2: Concentration dependent effect of nanobodies on *in vitro* clot lysis time: Citrated plasma was incubated with VHH-TAFI-i391 (full line) and VHH-TAFI-a428 (dashed line), at different ratio's over TAFI, prior to clot formation and in the absence (panel A) and presence (panel B) of 1 nmol/L thrombomodulin, lysis was induced by addition of 120 pmol/L t-PA. CLT: Clot lysis time, Mean ± SD, n ≥ 3.

To evaluate the effect of TM on this biphasic pattern, experiments were designed with varying concentrations of TM (0, 0.5, 1, 5 nmol/L). As can be deduced from the data in figure 3, VHH-TAFI-a428 resulted in a prolongation of clot lysis time at all TM concentrations with the strongest increase observed at 5 nmol/L TM. For VHH-TAFI-i391 again this effect was transient in function of the nanobody concentration. In order to further explore the nature of the (transient) increase of clot lysis time by these TAFIa inhibiting nanobodies, the effect of a higher concentration of t-PA was also investigated. Under these conditions (360 pmol/L t-PA and 1 nmol/L TM) prolongation of clot lysis time was no longer observed at any of the nanobody concentrations (Figure 2.4).

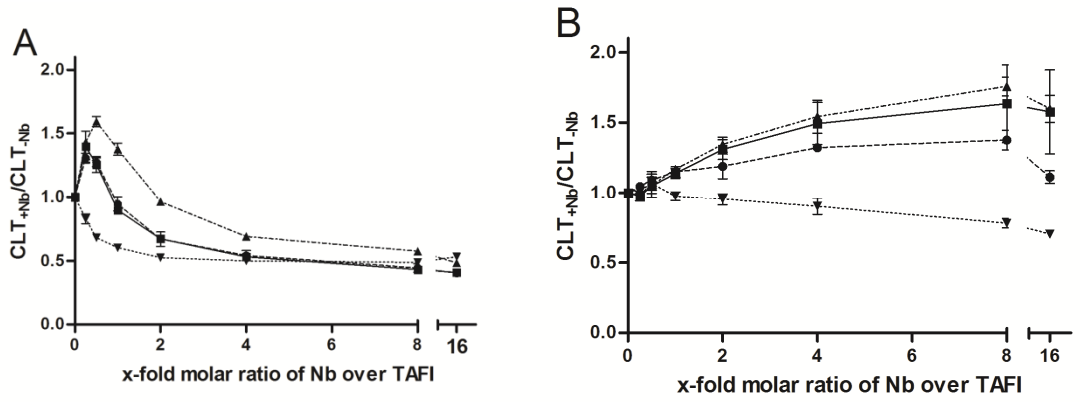

Figure 2.3: Concentration dependent effect of thrombomodulin on *in vitro* clot lysis time: Citrated plasma was incubated with different concentrations TM (5 nmol/L; 1 nmol/L; 0.5 nmol/L; 0 nmol/L) prior to clot formation. Clot lysis (t-PA, 120 pmol/L, induced) times were determined, in the presence of various ratio's of VHH-TAFI-i391 (panel A) and VHH-TAFI-a428 (panel B) over TAFI. CLT: Clot lysis time, Mean ± SD, n ≥ 3.

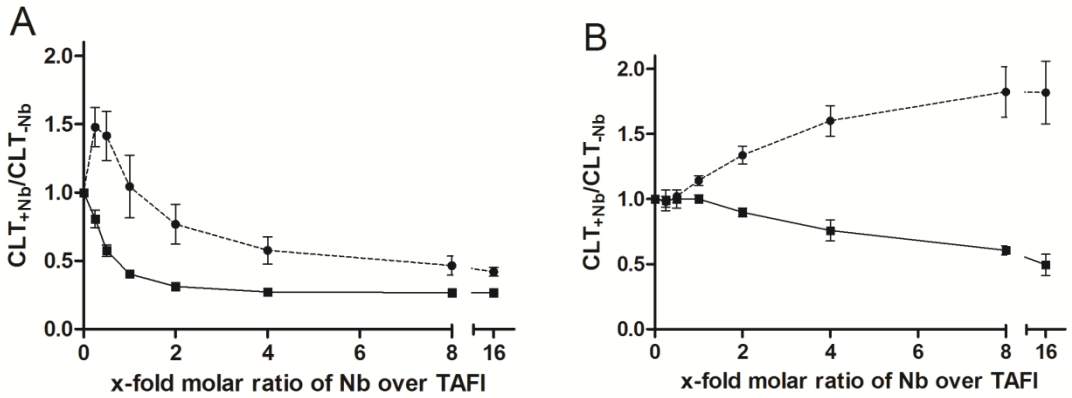

Figure 2.4: Concentration dependent effect of t-PA on *in vitro* clot lysis time: Citrated plasma was incubated with different concentrations of t-PA (120 pmol/L and 360 pmol/L) prior to clot formation, the effect on clot lysis time was determined in the presence of various ratio's of VHH-TAFI-i391 (panel A) and VHH-TAFI-a428 (panel B) over TAFI. CLT: Clot lysis time, Mean ± SD, n ≥ 3.

Role of the active site in the TAFIa-nanobody interaction

Affinities of the nanobodies towards the proenzyme TAFI and its activated form TAFIa were measured by Surface Plasmon Resonance analysis. The nanobodies bind only to TAFIa, and not the proenzyme TAFI (Table 2.2).

Table 2.2: Binding parameters for nanobodies towards TAFI(a)

	TAFI	TAFIa
	K_A (M^{-1})	K_A (M^{-1})
VHH-TAFI-a425	NB	$2.79 \pm 0.20 \times 10^8$
VHH-TAFI-a428	NB	$0.90 \pm 0.11 \times 10^8$
VHH-TAFI-i342	NB	$0.45 \pm 0.01 \times 10^8$
VHH-TAFI-i373	NB	$0.38 \pm 0.03 \times 10^8$
VHH-TAFI-i391	NB	$6.88 \pm 0.38 \times 10^8$

All data represent mean ± SD, n ≥ 3,
NB = no binding

To evaluate the role of the involvement of the active site in the interaction between nanobodies and TAFIa, the effect of temperature (37 °C) induced inactivation of TAFIa on the binding by nanobodies was investigated (Figure 2.5 A). As expected, TAFIa activity decreased upon heat inactivation with a half-life of 10.2 ± 0.5 min. Even though binding of nanobodies to TAFIa disappears upon inactivation of TAFIa, this loss of binding is significantly delayed relative to the loss of activity. A similar trend was observed for the other three nanobodies (data not shown). Temperature-dependent inactivation of TAFIa did not change the binding to the control nanobody VHH-TAFI-a360 (exhibiting equal binding to the proenzyme TAFI and its activated form TAFIa). Loss of binding due to proteolytic cleavage is excluded by determination of the TAFI fragmentation pattern by SDS-PAGE (data not shown).

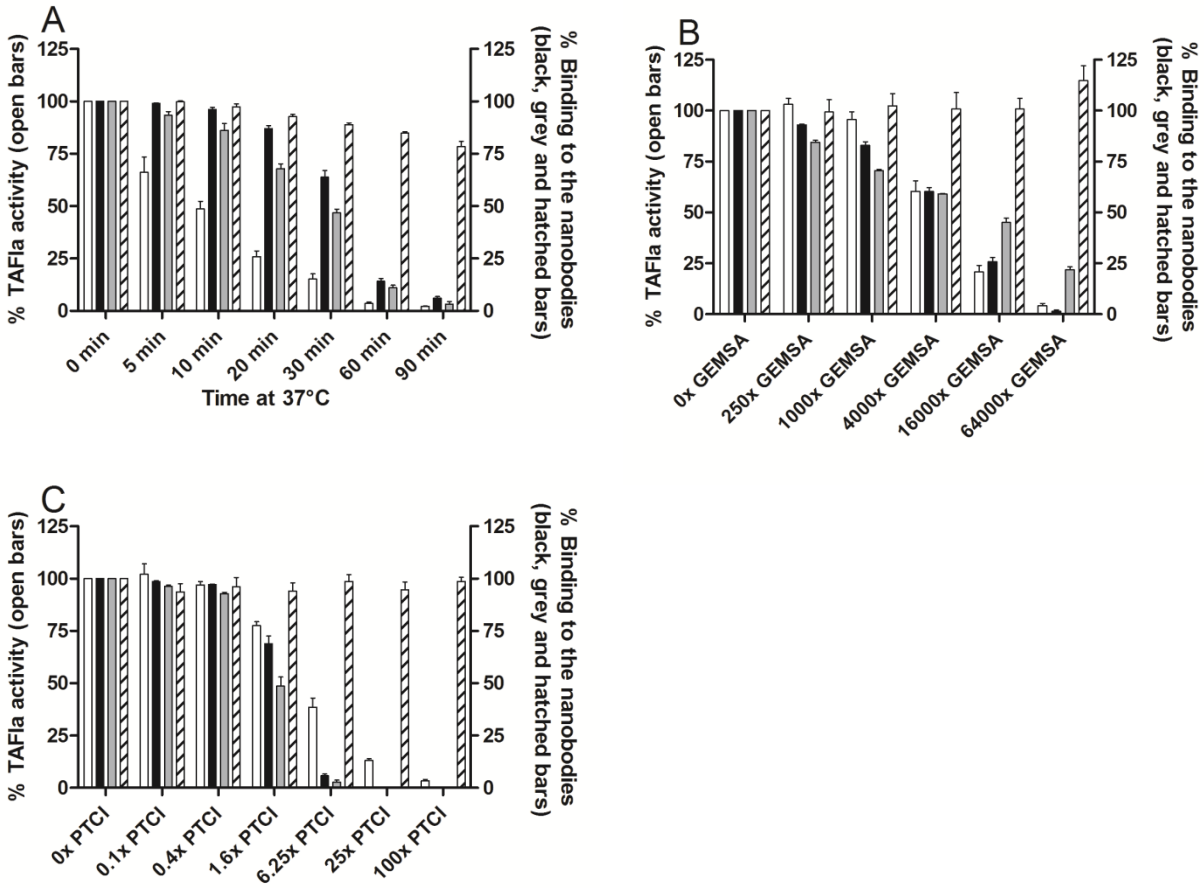

Figure 2.5: Effect of TAFIa inactivation or inhibition on nanobody binding. Activated TAFI was obtained by activation of TAFI by thrombin/thrombomodulin and subsequent addition of PPACK. Panel A: Activated TAFI was incubated for different time periods at 37 °C and at each time point residual TAFIa activity (open bars) and concomitant binding to the nanobodies (VHH-TAFI-i391, black bars; VHH-TAFI-a428, grey bars; VHH-TAFI-a360, hatched bars) was determined. Panel B and C: Activated TAFI was incubated with either GEMSA (panel B) or PTCI (panel C) at different molar ratio's over TAFIa and for each condition residual TAFIa activity (open bars) and concomitant binding to the nanobodies (VHH-TAFI-i391, black bars; VHH-TAFI-a428, grey bars; VHH-TAFI-a360, hatched bars) was determined. Data represent mean ± SD, n ≥ 3.

Subsequently, we evaluated the effect of well-known, small active-site inhibitors on the TAFIa/nanobody interaction. Incubation of TAFIa with increasing concentrations of GEMSA or PTCI resulted in reduction of TAFIa activity (Figure 2.5 B and 2.5 C). Under these conditions, a concomitant reduction of the TAFIa-GEMSA or TAFIa-PTCI complex binding to all nanobodies was observed. Addition of GEMSA at 64000-fold molar ratio over TAFIa resulted in a residual TAFIa activity of 4.2 % ± 1.1 (mean ± SD, n≥3 Figure 2.5 B). Accordingly, the residual binding to VHH-TAFI-i391 and VHH-TAFI-a428 was 1.4 % ± 0.7 and 21.9 % ± 1.5 (mean ± SD, n≥3), respectively. At lower concentrations of GEMSA, the effects on the binding were comparable to the effects on the activity. A similar effect was observed for other nanobodies (data not shown). The same trend was observed with PTCI for which a 100-fold molar ratio over TAFIa resulted in a residual

TAFIa activity of 3.1 % ± 0.7 (mean ± SD, n≥3) and a complete blocking of the binding to the nanobodies (Figure 2.5 C).

DISCUSSION

Activated thrombin activatable fibrinolysis inhibitor (TAFIa) removes C-terminal lysine residues from partially degraded fibrin. These C-terminal lysine residues accelerate the plasminogen to plasmin conversion by t-PA. Therefore TAFIa reduces plasmin formation, which results in a delayed clot lysis hampering fibrinolysis. Two different mechanisms of TAFI inhibition can be identified: inhibition of the conversion from TAFI to TAFIa or direct inhibition of TAFIa. Thrombolytic therapy based on t-PA or on new generation plasminogen activators all show similar bleeding complications [27]. Combination therapy with TAFI inhibitors might reduce these complications while enhancing the thrombolytic efficacy [28]. Many small synthetic TAFI inhibitors have been reported. However, most of these inhibitors lack specificity [13]. Antibody-based inhibitory approaches are highly specific but conventional monoclonal antibody-based inhibition encounters immunogenicity concerns. Nanobodies are the smallest naturally-occurring antigen binding antibody fragments with superior features such as high solubility, stability, low immunogenicity and high affinity towards their targets. Furthermore, nanobodies have been proven to be successful enzyme inhibitors [21]. We therefore aimed to develop nanobodies specifically inhibiting TAFIa activity.

Since TAFIa is very unstable, we hypothesized that immunization with a more stable variant could enhance our chances in retrieving a TAFIa inhibitor. Indeed, based on sequence identity of the CDR3 regions, a panel of 16 clusters was obtained of which 5 comprise nanobodies that specifically inhibited TAFIa activity. VHH-TAFI-i391 showed (at a 2-fold molar excess over TAFI) almost 100% inhibition of TAFIa activity and a strong reduction of clot lysis time comparable with the previously reported effects of VHH-TAFI-a204 (nanobody interfering with the activation of TAFI) and the well known TAFIa inhibitor PTCI [23].

Panning against activated and intact TAFI (resulting in the a-series and i-series, respectively) yielded a diverse set of nanobodies. Surprisingly, some nanobodies of the i-series showed specific binding to TAFIa, in spite of their selection towards intact TAFI. This apparent discrepancy could be explained by the possibility that TAFI, passively adsorbed to the microtiterplate, might undergo a conformational change (as observed for other antigens [29]) thereby displacing the activation peptide aside and making the catalytic cleft more accessible for nanobody interaction.

The nanobodies clearly have profibrinolytic properties but under certain conditions their presence leads to a prolongation of clot lysis time. Similar properties have been observed for

GEMSA and PTCI, both reversible inhibitors [18]. They interact with the enzymatic pocket and enhance clot lysis at higher concentrations while stabilizing fibrin clots at low concentrations due to their TAFIa stabilizing properties [18]. This biphasic pattern is also observed with the TAFIa inhibitory nanobodies and appears to be dependent on the concentration of the nanobody, TM and t-PA. Similarly Walker *et al.* [17] demonstrated that the effect of competitive inhibitors is dependent on inhibitor, TAFIa and t-PA concentrations. These observations are in line with the threshold dependent mechanism of TAFIa [30, 31]. As long as TAFIa activity remains above this threshold, lysis is prevented from proceeding into the propagation phase. By increasing the concentration of t-PA, the threshold value increases and TAFIa activity drops faster below this value leading to an enhanced fibrinolysis. Conversely, an increase of TM leads to higher TAFIa concentrations and consequently it takes longer to drop below the threshold, leading to a prolongation of clot lysis time. The observation that VHH-TAFI-a428 does not show a biphasic pattern but consistently prolongs lysis implies that under those particular conditions (i.e. the combined effect of the initial burst of TAFIa formation and the stabilization of TAFIa by the nanobody) TAFIa activity remains above the threshold at all concentrations. Our data demonstrate that any active-site inhibitor of TAFIa may under particular conditions, paradoxally, prolong fibrinolysis. It should be noted that the nanobodies described above are highly specific for human TAFIa and do not cross-react with mouse or rat TAFIa (data not shown), thereby excluding their evaluation in animal models.

Evaluation of the binding characteristics under various conditions, i.e. the proenzyme (TAFI), activated TAFI (TAFIa), temperature-inactivated TAFIa ($TAFIa_i$) and active-site blocked TAFIa (either by GEMSA or PTCI), strongly suggests that the nanobodies bind in the enzymatic pocket. However, other possibilities such as an association outside the catalytic site, but inducing a long-range conformational switch in the active site cannot be excluded. These properties also allowed us to use these nanobodies to monitor the accessibility of the active site and the conformational transitions associated with the temperature-dependent inactivation of TAFIa. The delayed loss of binding of the nanobodies upon inactivation of TAFIa compared to the loss of TAFIa activity suggests the existence of a transient inactive $TAFIa_i$-form which is still able to bind to the nanobodies and which is subsequently converted to another inactive but non-binding $TAFIa_i$-form. Boffa *et al.* [7] reported that inactivation of TAFIa is associated with two consecutive conformational transitions characterized by k_1 (0.5 min^{-1}) and k_2 (0.064 min^{-1}) (scheme 1). Only the second, rate limiting, step results in inactivation.

$$\mathbf{TAFIa_1} \xrightarrow{k_1} \mathbf{TAFIa_2} \xrightarrow{k_2} \mathbf{TAFIa_i} \qquad \text{(scheme 1)}$$

Our current observations suggest the presence of two inactive $TAFIa_i$ conformations, i.e. one in which the binding for the nanobodies is still available and one in which this binding site becomes inaccessible. Therefore, combined with the observations of Boffa *et al.* [7] the conformational changes occurring upon inactivation of TAFIa can be described as three consecutive conformational transitions, starting from $TAFIa_1$ and leading subsequently to the formation of $TAFIa_2$, $TAFIa_{i1}$ and $TAFIa_{i2}$ with corresponding k_1, k_2 and k_{i1} respectively (scheme 2).

$$\mathbf{TAFIa_1} \xrightarrow{k_1} \mathbf{TAFIa_2} \xrightarrow{k_2} \mathbf{TAFIa_{i1}} \xrightarrow{k_{i1}} \mathbf{TAFIa_{i2}} \qquad \text{(scheme 2)}$$

$TAFIa_1$, $TAFIa_2$ and $TAFIa_{i1}$ bind to the nanobodies, $TAFIa_{i2}$ represents the non-binding conformation. At the start of the reaction only $TAFIa_1$ is present and the concentration is set $[TAFIa_1]_0 = 1$. The concentration at each time for $TAFIa_1$, $TAFIa_2$ and $TAFIa_{i1}$ can therefore be calculated according to equation 1, 2 and 3, respectively (Eq.1-Eq.3).

$$\mathbf{[TAFIa_1] = \exp(-k_1 t)} \qquad \text{(Eq.1)}$$

$$\mathbf{[TAFIa_2]} = \frac{\mathbf{k_1}}{\mathbf{k_2 - k_1}} \mathbf{(\exp(-k_1 t) - \exp(-k_2 t))} \qquad \text{(Eq. 2)}$$

$$\mathbf{[TAFIa_{i1}]} = \frac{\mathbf{k_1 k_2}}{\mathbf{k_1 - k_2}} \mathbf{\exp(-(k_1 + k_2 - k_{i1})t - k_{i1}t)} \left(\frac{\exp(\mathbf{k_2 t})}{\mathbf{k_1 - k_{i1}}} + \frac{\exp(\mathbf{k_1 t})}{\mathbf{-k_2 + k_{i1}}} \right) + \frac{\mathbf{k_1 k_2} \left(\frac{1}{\mathbf{k_1 - k_{i1}}} + \frac{1}{\mathbf{-k_2 + k_{i1}}} \right) \exp(-\mathbf{k_{i1} t})}{\mathbf{k_2 - k_1}}$$

(Eq. 3)

Then, the total concentration of all the binding forms can be calculated as the sum of $TAFIa_1$, $TAFIa_2$ and $TAFIa_{i1}$. The experimental binding data (Figure 2.6, open circles), representing the binding of the total of $TAFIa_1$, $TAFIa_2$ and $TAFIa_{i1}$, were fitted using the combined equations 1, 2 and 3 using a value of 0.5 min^{-1} for k_1 as reported by Boffa *et al.* [7] and using an experimental k_2-value (for TAFI-TI) of 0.068 min^{-1}, derived from the half-life of 10.2 min ± 1.4 (mean ± SD, n=3), based upon loss of TAFIa activity. The latter value is very close to the one reported by Boffa *et al.* [7] i.e. 0.064 min^{-1} ± 0.001 corresponding to a half-life of 10.8 min. For TAFI-TI the fitting of the experimental binding data of VHH-TAFI-a428 and VHH-TAFI-i391 to the combined equations

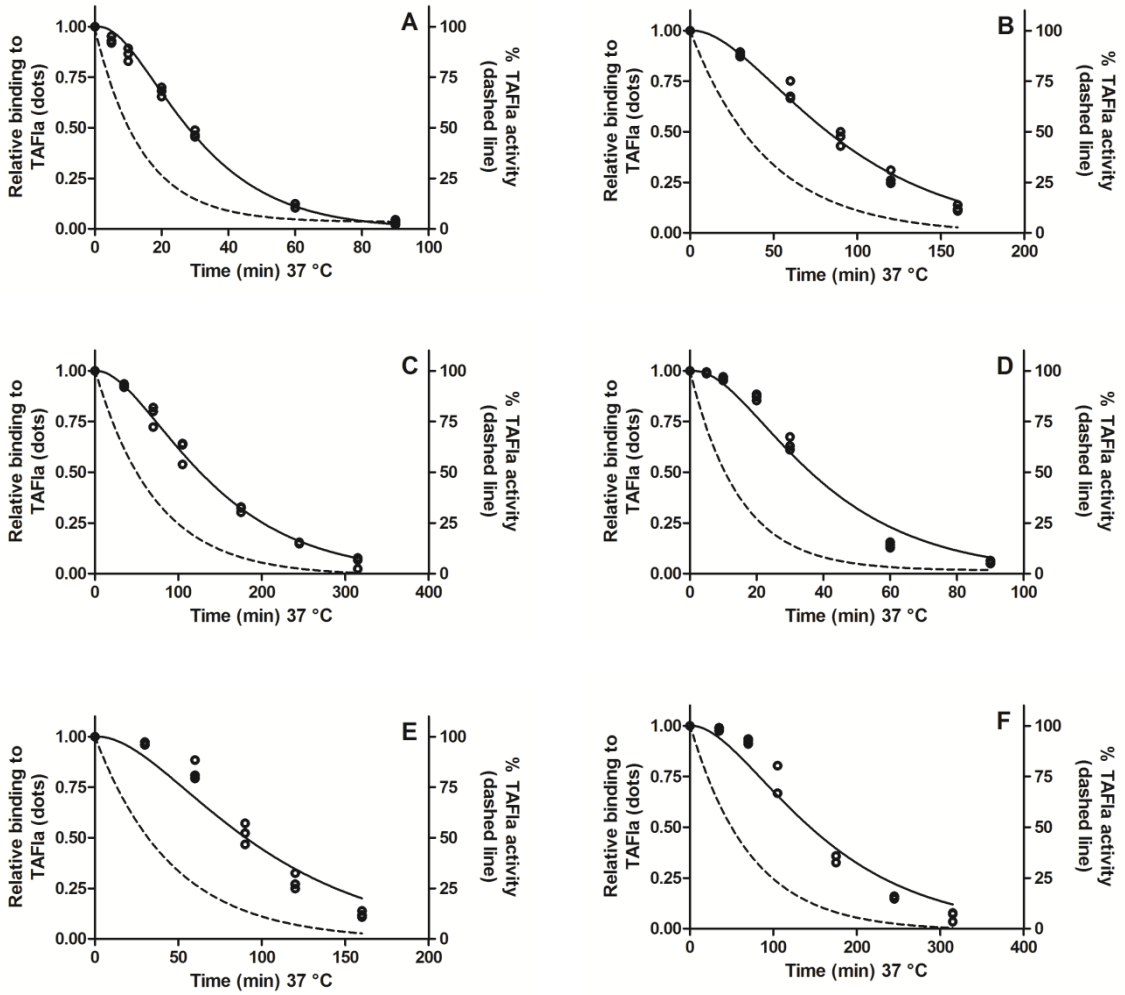

Figure 2.6: Activity of TAFIa (dashed line) and concomitant binding of $TAFIa_1$, $TAFIa_2$ and $TAFIa_{i1}$ (open circles) to the nanobodies at different incubation time periods and fitting of the data as described (full line). Activated TAFI variants, TAFI-TI (panel A and D), TAFI-AI-Cys^{305} (panel B and E) and TAFI-AI-Cys^{305}-Ile^{329} (panel C and F) were obtained by activation with thrombin/thrombomodulin and subsequent addition of PPACK. The activated TAFI variants were then incubated for different time periods at 37 °C and for each time point the residual TAFIa activity (dashed line, as determined by substrate conversion) and concomitant binding to the nanobodies (open circles, three data for each nanobody and TAFI variant) was determined. The binding data for VHH-TAFI-a428 (panel A, B and C) and VHH-TAFI-i391 (panel D, E and F) were fitted (full line) to the sum of equations 1-3 (see text).

(Figure 2.6 A and D, R^2 = 0.99 and 0.98 respectively) is compatible with the existence of a second $TAFIa_i$ formation and resulted in a k_{i1}-value of 0.0623 min^{-1} ± 0.0044 (mean ± SD, n=3) as determined by VHH-TAFI-a428 and 0.0377 min^{-1} ± 0.0021 (mean ± SD, n=3) as determined by VHH-TAFI-i391. The occurrence of a transient inactive $TAFIa_{i1}$ conformation was confirmed by further investigations on TAFI mutants with different half-lifes. For TAFI-AI-Cys^{305} an experimental k_2-value of 0.0217 was used, derived from the half-life of 32.2 min ± 2.8 (mean ± SD, n=3), based upon loss of TAFIa activity. Fitting of the experimental binding data of VHH-TAFI-a428 and VHH-TAFI-i391 to the combined equations (Figure 2.6 B and E, R^2 = 0.99 and 0.95

respectively) resulted in k_{i1}-values of 0.0203 ± 0.0018 and 0.0169 ± 0.0017 (mean ± SD, n=3). For TAFI-AI-Cys^{305}-Ile^{329} the experimental k_2-value of 0.0138 was used, derived from the half-life of 50.6 min ± 7.2 (mean ± SD, n=3), based upon loss of TAFIa activity. For this mutant, fitting the experimental binding data of VHH-TAFI-a428 and VHH-TAFI-i391 (Figure 2.6 C and F, R^2 = 0.99 and 0.96 respectively) resulted in k_{i1}-values of 0.0132 min^{-1} ± 0.0003 and 0.0102 min^{-1} ± 0.0005, respectively (mean ± SD, n=3). It is of interest to note that the k_{i1}-values appear to be related to the k_2-values. It is tempting to speculate that this might indicate that the molecular determinants involved in the stabilization of TAFIa activity also play a role in the newly identified conformational transition.

It has been reported that inactivated TAFIa has the tendency to aggregate into large non-soluble particles [32] and therefore our current findings could be linked to the formation of aggregates. We believe however that this is unlikely (since no irregular sensorgrams were observed and binding data with a control nanobody, VHH-TAFI-a360, also support a monomeric state for TAFIa). Overall the data confirm our hypothesis that after the conformational change resulting in a loss of activity, the nanobodies still bind and only after a subsequent conformational change, loss of nanobody binding occurs. The appropriate mathematical formula's describing these conformational transitions allowed the calculation of the respective k-values. The statistical parameters of the regression analysis provide evidence for the validity of the proposed model

Taken together, we have developed very potent and specific TAFIa inhibiting nanobodies and demonstrated their profibrinolytic properties. In addition, these unique nanobodies were shown to be excellent tools to investigate TAFIa conformational changes and allowed the discovery of a previously unknown $TAFIa_i$ form.

REFERENCES

1. Fleury V, Angles-Cano E. Characterization of the binding of plasminogen to fibrin surfaces: The role of carboxy-terminal lysines. *Biochemistry*. 1991;30:7630-7638
2. Hendriks D, Scharpe S, van Sande M, Lommaert MP. Characterisation of a carboxypeptidase in human serum distinct from carboxypeptidase n. *J Clin Chem Clin Biochem*. 1989;27:277-285
3. Eaton DL, Malloy BE, Tsai SP, Henzel W, Drayna D. Isolation, molecular cloning, and partial characterization of a novel carboxypeptidase b from human plasma. *J Biol Chem*. 1991;266:21833-21838
4. Bajzar L, Manuel R, Nesheim ME. Purification and characterization of tafi, a thrombin-activable fibrinolysis inhibitor. *J Biol Chem*. 1995;270:14477-14484
5. Wang W, Boffa MB, Bajzar L, Walker JB, Nesheim ME. A study of the mechanism of inhibition of fibrinolysis by activated thrombin-activable fibrinolysis inhibitor. *J Biol Chem*. 1998;273:27176-27181
6. Schatteman KA, Goossens FJ, Scharpe SS, Hendriks DF. Proteolytic activation of purified human procarboxypeptidase u. *Clin Chim Acta*. 2000;292:25-40
7. Boffa MB, Bell R, Stevens WK, Nesheim ME. Roles of thermal instability and proteolytic cleavage in regulation of activated thrombin-activable fibrinolysis inhibitor. *J Biol Chem*. 2000;275:12868-12878
8. Boffa MB, Wang W, Bajzar L, Nesheim ME. Plasma and recombinant thrombin-activable fibrinolysis inhibitor (tafi) and activated tafi compared with respect to glycosylation, thrombin/thrombomodulin-dependent activation, thermal stability, and enzymatic properties. *J Biol Chem*. 1998;273:2127-2135
9. Marx PF, Hackeng TM, Dawson PE, Griffin JH, Meijers JC, Bouma BN. Inactivation of active thrombin-activable fibrinolysis inhibitor takes place by a process that involves conformational instability rather than proteolytic cleavage. *J Biol Chem*. 2000;275:12410-12415
10. Wang YX, da Cunha V, Vincelette J, Zhao L, Nagashima M, Kawai K, Yuan S, Emayan K, Islam I, Hosoya J, Sullivan ME, Dole WP, Morser J, Buckman BO, Vergona R. A novel inhibitor of activated thrombin activatable fibrinolysis inhibitor (tafia) - part ii: Enhancement of both exogenous and endogenous fibrinolysis in animal models of thrombosis. *Thromb Haemost*. 2007;97:54-61
11. Schneider M, Boffa M, Stewart R, Rahman M, Koschinsky M, Nesheim M. Two naturally occurring variants of tafi (thr-325 and ile-325) differ substantially with respect to thermal stability and antifibrinolytic activity of the enzyme. *J Biol Chem*. 2002;277:1021-1030
12. Ceresa E, Peeters M, Declerck PJ, Gils A. Announcing a tafia mutant with a 180-fold increased half-life and concomitantly a strongly increased antifibrinolytic potential. *J Thromb Haemost*. 2007;5:418-420
13. Willemse JL, Heylen E, Nesheim ME, Hendriks DF. Carboxypeptidase u (tafia): A new drug target for fibrinolytic therapy? *J Thromb Haemost*. 2009;7:1962-1971
14. Hillmayer K, Vancraenenbroeck R, De Maeyer M, Compernolle G, Declerck PJ, Gils A. Discovery of novel mechanisms and molecular targets for the inhibition of activated thrombin activatable fibrinolysis inhibitor. *J Thromb Haemost*. 2008;6:1892-1899

15. Gils A, Ceresa E, Macovei AM, Marx PF, Peeters M, Compernolle G, Declerck PJ. Modulation of tafi function through different pathways--implications for the development of tafi inhibitors. *J Thromb Haemost*. 2005;3:2745-2753

16. Bajzar L, Nesheim ME, Tracy PB. The profibrinolytic effect of activated protein c in clots formed from plasma is tafi-dependent. *Blood*. 1996;88:2093-2100

17. Walker JB, Hughes B, James I, Haddock P, Kluft C, Bajzar L. Stabilization versus inhibition of tafia by competitive inhibitors in vitro. *J Biol Chem*. 2003;278:8913-8921

18. Schneider M, Nesheim M. Reversible inhibitors of tafia can both promote and inhibit fibrinolysis. *J Thromb Haemost*. 2003;1:147-154

19. Hamers-Casterman C, Atarhouch T, Muyldermans S, Robinson G, Hamers C, Songa EB, Bendahman N, Hamers R. Naturally occurring antibodies devoid of light chains. *Nature*. 1993;363:446-448

20. Muyldermans S, Atarhouch T, Saldanha J, Barbosa JA, Hamers R. Sequence and structure of vh domain from naturally occurring camel heavy chain immunoglobulins lacking light chains. *Protein Eng*. 1994;7:1129-1135

21. Lauwereys M, Arbabi Ghahroudi M, Desmyter A, Kinne J, Holzer W, De Genst E, Wyns L, Muyldermans S. Potent enzyme inhibitors derived from dromedary heavy-chain antibodies. *EMBO J*. 1998;17:3512-3520

22. Conrath KE, Lauwereys M, Galleni M, Matagne A, Frere JM, Kinne J, Wyns L, Muyldermans S. Beta-lactamase inhibitors derived from single-domain antibody fragments elicited in the camelidae. *Antimicrob Agents Chemother*. 2001;45:2807-2812

23. Buelens K, Hassanzadeh-Ghassabeh G, Muyldermans S, Gils A, Declerck PJ. Generation and characterization of inhibitory nanobodies towards thrombin activatable fibrinolysis inhibitor. *J Thromb Haemost*. 2010;8:1302-1312

24. Ceresa E, Van de Borne K, Peeters M, Lijnen HR, Declerck PJ, Gils A. Generation of a stable activated thrombin activable fibrinolysis inhibitor variant. *J Biol Chem*. 2006;281:15878-15883

25. Develter J, Booth NA, Declerck PJ, Gils A. Bispecific targeting of thrombin activatable fibrinolysis inhibitor and plasminogen activator inhibitor-1 by a heterodimer diabody. *J Thromb Haemost*. 2008;6:1884-1891

26. De Genst E, Silence K, Ghahroudi MA, Decanniere K, Loris R, Kinne J, Wyns L, Muyldermans S. Strong in vivo maturation compensates for structurally restricted h3 loops in antibody repertoires. *J Biol Chem*. 2005;280:14114-14121

27. Khan IA, Gowda RM. Clinical perspectives and therapeutics of thrombolysis. *Int J Cardiol*. 2003;91:115-127

28. Nagashima M, Werner M, Wang M, Zhao L, Light DR, Pagila R, Morser J, Verhallen P. An inhibitor of activated thrombin-activatable fibrinolysis inhibitor potentiates tissue-type plasminogen activator-induced thrombolysis in a rabbit jugular vein thrombolysis model. *Thromb Res*. 2000;98:333-342

29. Pereira Arias-Bouda LM, Kuijper S, van Deutekom H, van Gijlswijk R, Pekel I, Jansen HM, Kolk AH. Enzyme-linked immunosorbent assays using immune complexes for the diagnosis of tuberculosis. *J Immunol Methods*. 2003;283:115-124

30. Leurs J, Nerme V, Sim Y, Hendriks D. Carboxypeptidase u (tafia) prevents lysis from proceeding into the propagation phase through a threshold-dependent mechanism. *J Thromb Haemost*. 2004;2:416-423

31. Walker JB, Bajzar L. The intrinsic threshold of the fibrinolytic system is modulated by basic carboxypeptidases, but the magnitude of the antifibrinolytic effect of activated thrombin-activable fibrinolysis inhibitor is masked by its instability. *J Biol Chem*. 2004;279:27896-27904

32. Marx PF, Plug T, Havik SR, Morgelin M, Meijers JC. The activation peptide of thrombin-activatable fibrinolysis inhibitor: A role in activity and stability of the enzyme? *J Thromb Haemost*. 2009;7:445-452

Chapter 3

Identification of a novel, nanobody-induced, mechanism of TAFI inactivation and its *in vivo* application

M. L. V. HENDRICKX*, M. ZATLOUKALOVA*, G. HASSANZADEH-GHASSABEH †‡, S. MUYLDERMANS †§, A. GILS* and P. J. DECLERCK*

* Laboratory for Therapeutic and Diagnostic Antibodies, Department of Pharmaceutical and Pharmacological Sciences, KU Leuven, Belgium † Laboratory of Cellular and Molecular Immunology, Faculty of Sciences, Vrije Universiteit Brussel, Brussels; ‡ Nanobody Service facility (NSF), VIB, Brussels, Belgium and §VIB Department of Structural Biology, Brussels, Belgium

J Thromb Haemost. Under review

SUMMARY

Background: Downregulation of fibrinolysis due to cleavage of C-terminal lysine residues from partially degraded fibrin is mainly exerted by the carboxypeptidase activity of activated thrombin-activatable fibrinolysis inhibitor (TAFIa). Recently, some intrinsic carboxypeptidase activity (= zymogen activity) was reported for the proenzyme (TAFI), however, there is some discussion about its function and effect.

Objective: We aimed to identify and characterize nanobodies towards mouse TAFI that stimulate the zymogen activity and test their effect in an *in vitro* clot lysis assay and an *in vivo* mouse thromboembolism model.

Methods and results: Screening of a library of nanobodies towards mouse TAFI (mTAFI) revealed one nanobody (VHH-mTAFI-i49) that significantly stimulates the zymogen activity of mTAFI from undetectable (< 0.35 U/mg) to 4.4 U/mg (at a 16-fold molar ratio over mTAFI). The generated carboxypeptidase activity is unstable at 37 °C. Incubation of mTAFI with VHH-mTAFI-i49 revealed a time-dependent reduced activatability of mTAFI. Extensive *in vitro* clot lysis experiments revealed an enhanced clot lysis due to a reduced activation of mTAFI during clot formation. *In vivo* application of VHH-mTAFI-i49 in a mouse thromboembolism model dose-dependently decreased the fibrin deposition in the lungs of thromboembolism-induced mice. Epitope mapping disclosed that Arg^{227} and Lys^{212} are important for the nanobody/mTAFI interaction and suggest destabilization of mTAFI by disrupting the stabilizing interaction between the activation peptide and the dynamic flap region.

Conclusion: The novel, nanobody-induced, reduced activatability of mTAFI demonstrates to be a very potent manner to enhance clot lysis.

INTRODUCTION

Thrombin-activatable fibrinolysis inhibitor (TAFI) is a 56-kDa protein predominantly secreted by the liver [1] and present in blood at a concentration between 4 and 15 µg/mL [2, 3]. TAFI can be activated by plasmin, thrombin and the complex thrombin/thrombomodulin (T/TM) resulting in the release of the activation peptide (20 kDa) from the TAFIa moiety (36 kDa) [4-7]. The TAFIa moiety cleaves C-terminal lysine residues from partially degraded fibrin, thereby attenuating its cofactor function in the t-PA-mediated plasmin generation, this ultimately leads to an impaired fibrinolysis [8].

There are no known physiological TAFIa inhibitors to regulate its activity, however, a temperature-dependent instability of TAFIa is observed [9]. The mechanism behind this instability has been revealed by solving the crystal structure of TAFI [10]. The structure demonstrates stabilizing interactions between Val^{35} and Leu^{39}, located within the activation peptide, and Tyr^{341} in the dynamic flap region (amino acids: Phe^{296} to Trp^{350}). Upon activation of TAFI, the activation peptide is released and due to the loss of stabilizing interactions, an increased mobility of the dynamic flap region is observed. Consequently, this results in conformational changes within the catalytic cleft that lead to inactivated TAFIa [10, 11].

Besides TAFIa, also the TAFI zymogen exerts some intrinsic carboxypeptidase activity (= zymogen activity). Valnickova *et al.* [12] reported that the zymogen activity is active towards large peptide substrates and is able to attenuate fibrinolysis in an *in vitro* t-PA-induced clot lysis assay. However, Willemse *et al.* [13] suggested that Valnickovas clot lysis was compromised by *in vitro* activation of TAFI. Foley *et al.* [14] demonstrated that TAFI is effective in cleaving a small substrate but due to its inability to cleave plasmin-modified fibrin, it has no effect on the attenuation of fibrinolysis. On the other hand Mishra *et al.* [15] described two nanobodies that stimulate the zymogen activity of TAFI. Addition of these nanobodies to TAFI-depleted plasma, that was reconstituted with a non-activatable TAFI mutant, TAFI-TI-R92A, results in a significant prolongation of clot lysis time.

The previously described zymogen stimulating nanobodies [15] showed no cross-reactivity towards mouse TAFI (mTAFI) and therefore could not be tested in *in vivo* mice experiments. In this study, we aimed to generate nanobodies towards mTAFI, identify zymogen stimulating nanobodies and test their properties *in vitro* as well as *in vivo*.

MATERIALS AND METHODS

Materials

Mouse TAFI was produced as described before [16]. Oligonucleotides for cloning and sequencing were purchased from Sigma-Aldrich (St Louis, MO, USA) and Pfx50 DNA polymerase and restriction enzymes were provided by Life Technologies (Merelbeke, Belgium) and New England Biolabs (Hitchin, UK), respectively. The polymerase chain reaction (PCR) was performed with the Mastercycler Gradient from Eppendorf (Hamburg, Germany) and plasmid DNA purification was performed with the NucleobondTM AX500 kit (Machery-Nagel, Düren, Germany). The DNA was sequenced by LGC genomics (Berlin, Germany).

Human thrombin and plasmin were purchased from Sigma-Aldrich and Enzyme Research Laboratories (South Bend, UK). Rabbit thrombomodulin (TM) was obtained from American Diagnostics (Greenwich, CT, USA). H-D-phenylalanine-L-propyl-L-arginine chloromethyl ketone (PPACK), aprotinin, hippuryl-L-arginine and potato tuber carboxypeptidase inhibitor (PTCI) were obtained from Biomol Research Laboratories (Plymouth meeting, PA, USA), Fluka (Buchs, Switzerland), Bachem (Bubendorf, Switzerland) and Sigma-Aldrich, respectively. Tissue-type plasminogen activator (t-PA) and mouse plasma were kind gifts from Boehringer Ingelheim (Brussels, Belgium) and Servier (Suresnes, France), respectively. Ocriplasmin (microplasmin) was a kind gift from ThromboGenics (Leuven, Belgium).

Nanobody library construction, expression and purification

The construction of the nanobody library was performed as described before [11] using mouse TAFI (mTAFI) as antigen. Therefore, an alpaca (*Vicugna pacos*) was subcutaneously injected with 100 µg per week (7 weeks) of mTAFI mixed with Gerbu LQ#300 adjuvant (Gerbu Biotechnik GmBH, Germany). Four days after the last immunization, blood was drawn and lymphocytes were isolated. Subsequently, total RNA was isolated and transformed into cDNA by reverse transcription. The cDNA was amplified by PCR and followed by digestion with *Pst*I and *Not*I before ligation into pHEN4, a phagemid vector. By transformation of the pHEN4 vector into *E. coli*, the total VHH repertoire was displayed on phage and binders were selected via panning towards mTAFI. Binders were identified by ELISA and their respective DNA sequences were determined. The DNA, encoding VHH, was recloned in the pHEN6c production vector using *Pst*I and *Bst*EII restriction enzymes. These constructs were then transformed into *E.coli* WK6 cells and periplasmic nanobody expression was induced by IPTG (1 mM, 18 h) as described previously [17]. The periplasmic proteins were extracted, dialyzed against Tris-HCl (20 mmol/L), NaCl (0.5 mol/L;

pH 7.9) and filtered through a 0.45-µm filter prior to loading on a His-Trap HP column (GE Healthcare, Uppsala, Sweden). Bound nanobodies were eluted using an imidazole gradient (0-350 mmol/L imidazole in 20 mmol/L Tris-HCl, 0.5 mol/L NaCl; pH 7.9). Nanobody-containing fractions were selected via SDS-polyacrylamide gel electrophoresis (PAGE) (Phast-Gel^{TM} gradient 10-15% gels, GE Healthcare, Uppsala, Sweden) by coomassie staining. Finally the selected fractions were pooled and dialyzed against phosphate-buffered saline (PBS; 140 mmol/L NaCl, 2.7 mmol/L KCl, 8 mmol/L Na_2HPO_4, 1.5 mmol/L KH_2PO_4; pH 7.4).

Evaluation of the effect of VHH-mTAFI-i49 on the zymogen activity of mTAFI

The effect of VHH-mTAFI-i49 on the zymogen activity was evaluated as described before [15] with minor modifications. Therefore, mTAFI (45 nmol/L, concentration during incubation with nanobody) in HEPES buffer (25 mmol/L HEPES, 137 mmol/L NaCl, 3.5 mmol/L KCl and 0.1% BSA; pH 7.4) was incubated with nanobody (concentration varying between 0.5- and 64-fold molar ratio nanobody:mTAFI) at 25 °C for 10 min followed by addition of Hip-Arg (4 mmol/L, concentration during substrate conversion) and allowed to proceed for 15 min at 25 °C. The reaction was arrested by addition of 20 µL HCl (1 mol/L), then neutralized by 20 µL NaOH (1 mol/L) and buffered by 25 µL Na_2HPO_4 (1 mol/L; pH 7.4). Subsequently, 6% cyanuric chloride (in 1,4-dioxane) was added and the mixture was vortexed for 5 min followed by centrifugation (Eppendorf centrifuge 5415D) for 2 min at 13,200 rpm. The supernatant was then transferred into a 96-well microtiter plate and the absorbance measured at 405 nm. The generated zymogen activity (expressed as U/mg, one unit (U) carboxypeptidase activity is defined as the amount of enzyme converting 1 micromole of substrate per minute at 25°C) was calculated based on a hippuric acid standard. The limit of detection (LOD) is defined as blank plus 3 x the SD of the blank.

The stability of the VHH-mTAFI-i49-induced zymogen activity was investigated by incubation of the mTAFI with VHH-mTAFI-i49 for 10 min at 25 °C prior to incubation for different time periods (5, 10, 20, 40, 60 and 120 min) at 25 or 37 °C. The residual activity was determined by chromogenic assay as described above.

Evaluation of the effect of VHH-mTAFI-i49 on the activatability of mTAFI

Since the VHH-mTAFI-i49-induced zymogen activity appeared to be unstable, the concomitant time-dependent effect of VHH-mTAFI-i49 on the activatability of mTAFI was evaluated. Therefore, mTAFI was incubated with VHH-mTAFI-i49 for 0, 15, 30 or 60 min at 37 °C and the activity was measured as described above (zymogen activity) or after activation (25 °C, 10 min) by thrombin/thrombomodulin (20 nmol/L and 5 nmol/L, respectively) in the presence of $CaCl_2$ (5 mmol/L). The activation was arrested by PPACK (37.5 µmol/L, final concentration) and subsequently the substrate Hip-Arg (4 mmol/L, concentration during substrate conversion) was added to this activation mixture and allowed to proceed for 15 min at 25 °C. Quantification of the generated activity (activatability) was performed as described above. HEPES buffer and VHH-mTAFI-i63 (a nanobody with no functional effect on mTAFI) were included as controls.

Affinity determination

The evaluation of the binding properties of VHH-mTAFI-i49 to mTAFI was done by Surface Plasmon Resonance (SPR) using a Biacore 3000 analytical system (GE Healthcare, Uppsala, Sweden) equipped with a CM5 sensor chip as described before [11]. Briefly, nanobody was covalently coupled up to 400 RU (using a concentration of 5 µg/mL nanobody in acetate buffer 10 mmol/L; pH 4.5). Purified mTAFI was diluted in HBS-EP buffer (Biacore) to concentrations between 6.25 and 200 nM and injected at a flowrate of 30 µL/min followed by a dissociation. The chip was regenerated after each cycle with glycine (10 mmol/L; pH 1.5). Association and dissociation rate constants were calculated using the BIAcore 3000 evaluation software (Langmuir binding, local fit). Control experiments were carried out with control nanobodies VHH-mTAFI-i63 and VHH-rTAFI-i81 (a nanobody that binds mTAFI on a different epitope than VHH-mTAFI-i49).

Evaluation of the effect of VHH-mTAFI-i49 on fibrinolysis

Clot lysis experiments were performed as described before [11] with minor modifications. Plasma obtained from three mice was pooled, diluted (2-fold) with TRIS/Tween buffer (10 mmol/L Tris, 0.01% Tween 20; pH 7.5) and mixed with either TRIS/Tween buffer or VHH-mTAFI-i49 at a concentration ranging between 0.5 and 16-fold molar ratio nanobody:mTAFI (assuming a mTAFI concentration of 90 nmol/L). TM was added and the mixture was incubated at 37 °C for 1 h. After the 1 h incubation period, t-PA was added and subsequently 80 µL of this mixture was transferred into microtiter wells which contained 20 µL $CaCl_2$ (53 mmol/L) resulting in the following final concentrations: 30% pooled plasma, 700 pmol/L t-PA, 5 nmol/L TM and 10

mmol/L $CaCl_2$. The plate was then incubated at 37 °C and the absorbance measured at 405 nm every 2 min to determine the 50% clot lysis time. The 50% clot lysis time is defined as the time needed from full clot formation (i.e. maximum turbidity) to the midpoint of the maximal turbid to clear transition. Control experiments were carried out with a 16-fold molar excess of VHH-mTAFI-i63 (a nanobody with no functional effect on mTAFI)

To explore the link between nanobody-induced zymogen activity, the subsequent decreased activatability and the effect in clot lysis, mTAFI(a) activity was evaluated during the in vitro clot lysis assay. Therefore, TAFI-related activity (zymogen activity and/or TAFIa activity) was determined during the 1h incubation period prior to clot formation as well as after induction of the clot and during the subsequent lysis. Pooled plasma (30% final concentration) was mixed with either HEPES buffer or VHH-mTAFI-i49 (16-fold molar ratio over mTAFI) in the presence of TM (5 nmol/L, final concentration). Fractions (80 µl) were collected prior to clot formation (i.e. at time points -60, -55, -50, -30, -5 min) and were mixed with 20 µL HEPES buffer followed by addition of PPACK and aprotinin to inhibit thrombin and plasmin activity (final concentrations: 25 µmol/L and 0.70 µmol/L, respectively) and stored on ice until carboxypeptidase activity measurement. After 60 minutes pre-incubation with VHH-mTAFI-i49 (i.e. t = 0) t-PA (700 pmol/L, final concentration) and $CaCl_2$ (10 mmol/L, final concentration) were added. Then, clot lysis at 37°C was followed and samples were collected at different time points (0, 3, 6, 9, 15, 30 and 60 min), mixed with PPACK and aprotinin (final concentrations: 25 µmol/L and 0.70 µmol/L, respectively) and stored on ice before carboxypeptidase activity was determined.

The carboxypeptidase activity was measured in a chromogenic assay as described above with minor modifications. The samples were first diluted (1:2) in HEPES buffer (25 mmol/L HEPES, 137 mmol/L NaCl, 3.5 mmol/L KCl and 0.1% BSA; pH 7.4) either in the presence or absence of PTCI (0.15 mmol/L, final concentration). PTCI was added to distinguish between mTAFIa activity/zymogen activity and CPN activity. The mixtures were then incubated with Hip-Arg (5 mmol/L, final concentration) for 30 min at 25 °C to allow substrate conversion, the reactions were stopped and the colour development was measured as described above and hippuric acid was used as a standard to calculate the specific activity. The activity observed in the presence of PTCI (i.e. CPN activity) was subtracted from the total activity to obtain the TAFI-related activity.

Evaluation of the effect of VHH-mTAFI-i49 in a mouse thromboembolism model

To evaluate the profibrinolytic properties, the nanobody was tested in an *in vivo* thromboembolism model as described before [18] with minor modifications. Therefore, VHH-

mTAFI-i49 (2.6, 2.0, 1.3 or 0.33 mg/kg corresponding to a 24-, 18-, 12- and 2-fold molar ratio nanobody:mTAFI) were injected intravenously in overnight fasted non-anesthetized female Swiss mice (Janvier). Endotoxins were removed from nanobody preparations (administration to mice: < 5 EU/kg) using PROSEP-RemTox (Millipore). After 5 min, human tissue factor (2.5 µg/kg, Dade Innovin reagent, Siemens) was administered to induce thrombi in the lungs. Reference mice receiving saline instead of nanobody and saline instead of tissue factor were also included. After 5 min, the mice were anesthetized with pentobarbital (Nembutal; 60 mg/kg) and 5 min later 500 IU of heparin (Heparin Leo) was administered in the vena cava. Three minutes later, lungs were perfused with saline containing heparin (10 IU/mL). Then, left lung was isolated and stored at -80 °C until homogenization. Homogenization was performed by a tissue homogenizer (Ribolyzer Fast Prep 24 System, MP Biomedicals) and addition of 4 mL of PBS per gram of lung tissue. The soluble fraction was removed and the pellet, containing the insoluble fibrin, was resuspended. Subsequently ocriplasmin (2 µM, 37 °C, 4 h,), was added to convert fibrin into soluble fibrin degradation products (FbDP's). Aprotinin (4 µmol/L, final concentration) was added to stop the action of plasmin and after centrifugation, the supernatant was collected. FbDP's and thereby the corresponding fibrin deposition was determined by a mouse fibrinogen ELISA kit with reactivity for FbDP's (Immunology Consultants Laboratory, Portland). The experimental protocol was approved by the KU Leuven Ethical Committee for Animal Experiments (P112-2012).

Epitope mapping

In an initial step, different TAFI chimeras [16,19] were tested to unravel the binding region of VHH-mTAFI-i49. Desired alanine mutations to prepare single and double mutants were introduced by site-directed mutagenesis. Primers were designed to replace selected codons by GCT, GCC, GCA or GCG encoding for alanine in the template pcDNA3.1V5hisA-mTAFI. The his-tagged TAFI variants (including his-tagged 'wild-type' mTAFI) were expressed in HEK293T cells and an initial evaluation of the impact of the mutation on the effect of VHH-mTAFI-i49 was performed on the conditioned medium. Mutants for which an altered susceptibility for VHH-mTAFI-i49 was observed were purified and subjected to a more detailed analysis.

Statistical analysis

Quantitative data are presented as mean ± standard deviation (SD) unless indicated otherwise. Statistical analysis (paired t-test and one-way ANOVA with Dunnett's multiple comparison test) were performed by GraphPad Prism (GraphPad Prism 5 Software).

RESULTS

Forty-eight unique nanobodies towards mTAFI(a) were identified and based on the amino acid sequence of the CDR3 region divided into 17 clusters. Nanobodies within one cluster are expected to target the same epitope [20] and to have similar functional properties. One to three nanobodies from each cluster were selected for production and purification and subsequently evaluated for inhibitory and zymogen stimulating properties towards mTAFI. Eleven out of 17 selected nanobodies showed inhibitory or zymogen stimulating properties towards mTAFI: 5 clusters mainly inhibit the plasmin-mediated activation of TAFI, 1 cluster mainly inhibits the T/TM-mediated activation, 3 clusters revealed a combination of inhibitory properties for plasmin- and T/TM-mediated activation and 2 nanobodies stimulated the zymogen activity of mTAFI. This paper focuses on the most potent zymogen stimulating nanobody, VHH-mTAFI-i49.

Evaluation of the effect of VHH-mTAFI-i49 on the zymogen activity of mTAFI

The induced zymogen activity observed upon incubation of mTAFI for 10 min at 25 °C with a 16-fold molar excess of VHH-mTAFI-i49 over mTAFI was 4.4 ± 0.5 U/mg, while in the absence of VHH-mTAFI-i49 the zymogen activity was less than 0.35 U/mg (= LOD). A dose response curve reveals that incubation of mTAFI with nanobody increases the zymogen activity in a dose-dependent manner, however, the maximal stimulation seems not to be reached even at a 64-fold molar ratio of nanobody over mTAFI (Figure 3.1).

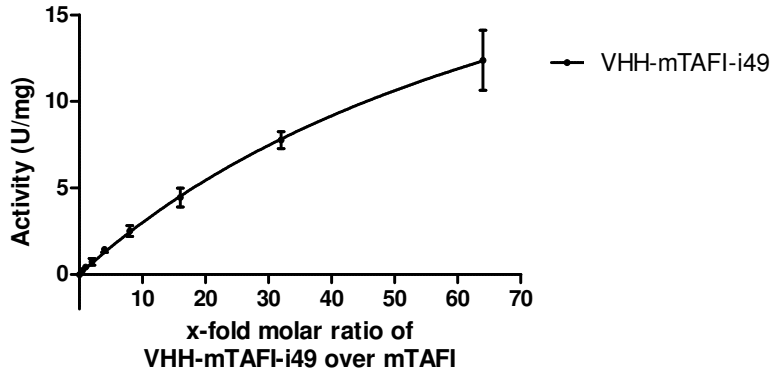

Figure 3.1: Dose-response curve of VHH-mTAFI-i49 on the zymogen activity of mTAFI (Mean ± SD; n ≥ 3).

Direct cleavage of Hip-Arg by VHH-mTAFI-i49 was excluded based upon evaluation of a chromogenic assay in the absence of mTAFI (data not shown). Generation of activated mTAFI

(mTAFIa) by VHH-mTAFI-i49 was excluded by visualization of the fragmentation pattern of mTAFI in the presence of VHH-mTAFI-i49 (i.e. mTAFI remained intact, data not shown).

Incubation of mTAFI with VHH-mTAFI-i49 and evaluation of the zymogen activity at different time points revealed that the induced zymogen activity is thermally unstable. The half-life of the induced zymogen activity at 25 °C and 37 °C was 73 ± 25 min and 8.1 ± 0.8 min, respectively.

Evaluation of the effect of VHH-mTAFI-i49 on the activatability of mTAFI

Incubation of mTAFI with a 16-fold molar excess of VHH-mTAFI-i49 over mTAFI at 37 °C resulted in an immediately induced zymogen activity of 6.5 ± 0.7 U/mg (no pre-incubation) followed by a time-dependent decrease at 37 °C resulting in 2.2 ± 0.4, 0.98 ± 0.1 and < 0.35 U/mg after 15, 30 and 60 min, respectively (Figure 3.2 A, open bars). Under these conditions, the zymogen activity in the presence of VHH-mTAFI-i63, a control nanobody with no functional effect, or in the presence of HEPES buffer was < 0.35 U/mg for all time points (Figure 3.2 A).

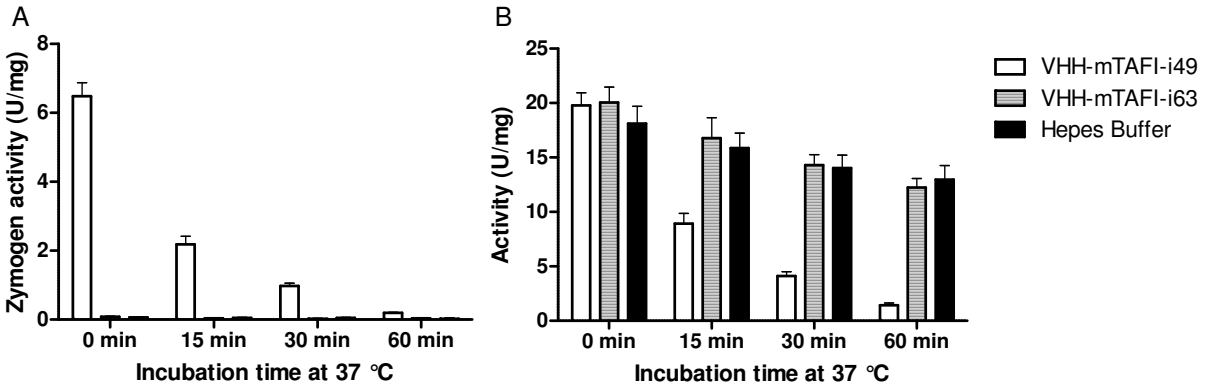

Figure 3.2: Zymogen activity (A) and activatability (B) after different incubation periods at 37 °C. (A) The generated zymogen activity of mTAFI, as determined by Hip-Arg substrate conversion, upon incubation for different time periods (0, 15, 30 and 60 min) with VHH-mTAFI-i49, VHH-mTAFI-i63 or HEPES buffer (open, hatched and black bars, respectively). (B) Residual activatability (by T/TM) of mTAFI after incubation for different time periods with VHH-mTAFI-i49, VHH-mTAFI-i63 or HEPES buffer open, hatched and black bars, respectively) (Mean ± SD; n = 3).

Strikingly, subsequent activation (by T/TM) of the mTAFI/VHH-mTAFI-i49 mixture at 0, 15, 30 and 60 min resulted in a TAFIa activity of 20 ± 2.0, 8.9 ± 1.6, 4.1 ± 0.7 and 1.4 ± 0.4 U/mg, respectively (Figure 3.2 B, open bars). In the presence of VHH-mTAFI-i63, the activation of mTAFI after 0, 15, 30 and 60 min resulted in a TAFIa activity of 20 ± 2.5, 17 ± 3.2, 14 ± 1.6 and 12 ± 1.4 U/mg, respectively, and comparable to that observed in the presence of HEPES buffer (Figure 3.2 B, hatched and black bars). These results indicate a significant reduction of the activatability of mTAFI of 1, 47, 71 and 89% after 0, 15, 30 and 60 min, respectively, in the presence of VHH-

mTAFI-i49 compared to that observed in the presence of VHH-mTAFI-i63. The reduced activatability was also confirmed for plasmin-mediated activation of mTAFI after incubation of mTAFI with VHH-mTAFI-i49 (data not shown).

Affinity determination

The association and dissociation rate constants (k_a and k_d) of VHH-mTAFI-i49 for mTAFI were 3.6 ± 1.3 x 10^4 L/mol.s and 8.5 ± 0.8 x 10^{-4} 1/s, respectively and result in an affinity constant (K_A) of 4.2 ± 1.2 x 10^7 L/mol.

Evaluation of the effect of VHH-mTAFI-i49 on fibrinolysis

To determine the effect of VHH-mTAFI-i49 on the clot lysis profile, plasma was pre-incubated with HEPES buffer with or without nanobody at 37 °C for 1 h prior to clot induction ($CaCl_2$). Under these conditions, the 50% clot lysis time in the absence of VHH-mTAFI-i49 (HEPES buffer) was 80 ± 4.2 min (Figure 3.3). In the presence of VHH-mTAFI-i49, a dose-dependent decrease in 50% clot lysis time was observed. At a 16-fold molar ratio of VHH-mTAFI-i49 over mTAFI, 50% clot lysis time shortened significantly ($p < 0.001$) to 28 ± 7.0 min (Figure 3.3). Under these conditions, VHH-mTAFI-i63 did not affect 50% clot lysis time (i.e. 81 ± 7.1 min).

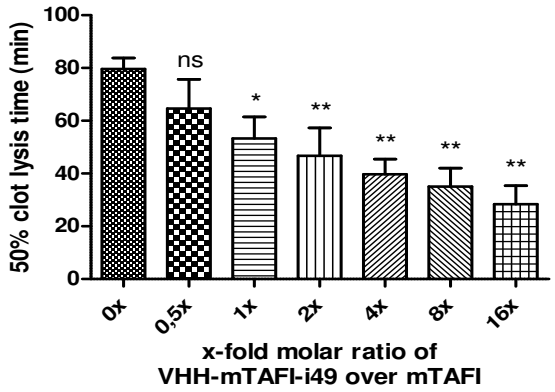

Figure 3.3: Dose-dependent reduction of the 50% clot-lysis time in the presence of different concentrations of VHH-mTAFI-i49. Plasma was incubated at 37 °C for 1 h in the absence or presence of different concentrations of VHH-mTAFI-i49 (fold molar ratio Nb:TAFI, ranging from 0 to 16) prior to clot formation ($CaCl_2$) and lysis (t-PA) and 50% clot lysis times were determined (Mean ± SD; n = 3) (* $p < 0.01$; ** $p < 0.001$; ns = not significant; one-way ANOVA; Dunnetts multiple comparison test).

To evaluate the link between the apparent profibrinolytic effect, the effect on TAFI zymogen activity and subsequent impaired activatability, TAFI related activity was quantified in this fibrinolysis experiment. In the presence of VHH-mTAFI-i49 there was an increased zymogen

activity with a maximum of 16 ± 1.1 U/L at time point -55 min. Subsequently, zymogen activity decreased to 5.4 ± 2.2 U/L at time point -5 min (Figure 3.4). In the absence of VHH-mTAFI-i49, very low TAFI-related activity was measured (0.6 ± 1.0 U/L at t = -5 min). After clot induction, there was an increased activity (zymogen + TAFIa) with a maximum of 6.9 ± 2.3 U/L and 5.5 ± 2.4 U/L observed after 15 min in the presence and absence of VHH-mTAFI-i49, respectively.

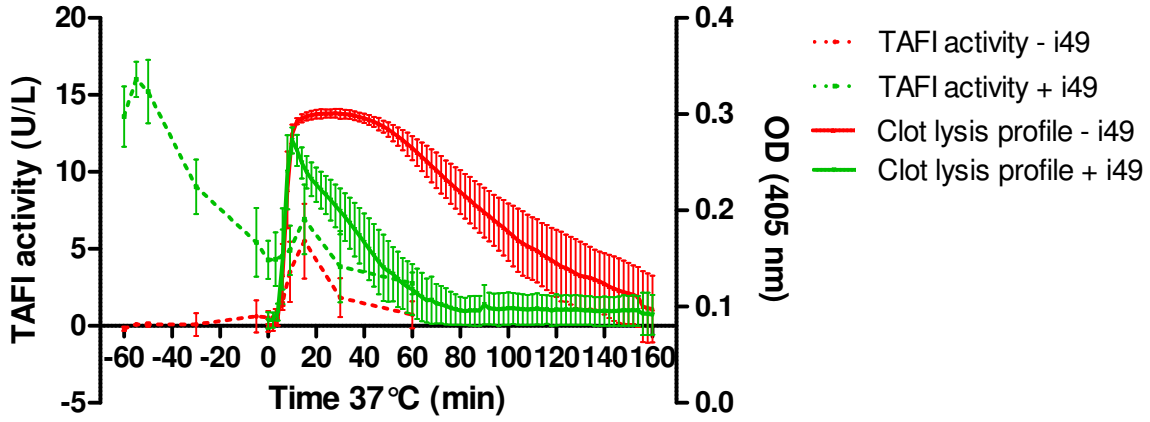

Figure 3.4: Clot lysis profile and concomitant mTAFI activity in the presence and absence of VHH-mTAFI-i49. Mouse plasma was first incubated at 37 °C for 60 min (t = -60 until t = 0) in the presence (green) or absence (red) of a 16-fold molar ratio of VHH-mTAFI-i49 over mTAFI. After 60 min (t = 0) clot formation was induced by $CaCl_2$ and measured by absorption at 405 nm (full line). Throughout the entire experiments TAFI-related activity (dashed lines) was determined (Mean ± SD; n = 3).

To calculate a comparative estimate of the total amount of TAFIa activity generated during clot formation and lysis, the area under the curve (AUC) and peak height were determined in the presence and absence of VHH-mTAFI-i49. To correct for the VHH-mTAFI-i49-induced zymogen activity (i.e. 4.3 ± 1.2 U/L at t = 0) the value of the total activity (zymogen + TAFIa) at each time point after clot formation was subtracted with the value of TAFI activity at t = 0 (= zymogen activity) before calculating the peak height and area under the curve. Both the AUC and peak height were significantly reduced in the presence of VHH-mTAFI-i49 compared to that observed in the absence of nanobody (paired t-test, $p < 0.01$ and $p < 0.05$, respectively) (Figure 3.5, panel A and B).

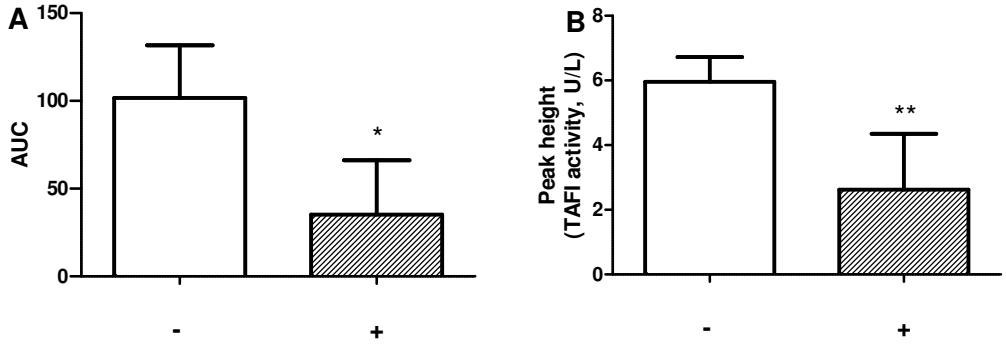

Figure 3.5: TAFIa generation during clot formation as determined by AUC (A) and peak height (B). The TAFIa AUC (panel A) and TAFIa peak height (panel B) after induction of clot formation in the presence (+) and absence (-) of VHH-mTAFI-i49 (Mean ± SD; n = 3) (* $p < 0.01$; ** $p < 0.05$; paired t-test compared to absence of VHH-mTAFI-i49).

Evaluation of the effect of VHH-mTAFI-i49 in a mouse thromboembolism model

Fibrin deposition in the lungs of thromboembolism-induced mice was significantly lower in the presence of a 24-fold molar excess of VHH-mTAFI-i49 compared to that observed in the absence of nanobody (20 ± 7 µg/mL *versus* 160 ± 37 µg/mL, mean ± SEM, n ≥ 7) ($p < 0.05$, one-way ANOVA, Dunnett's multiple comparison test) (Figure 3.6).

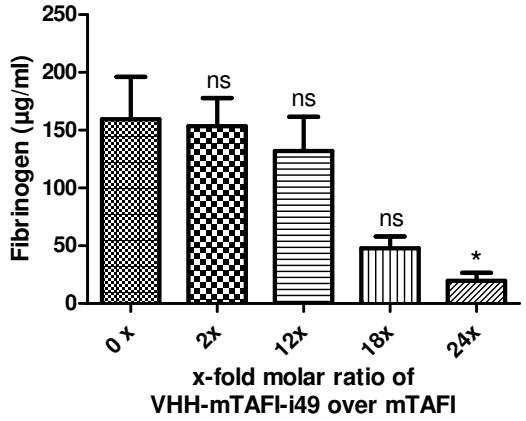

Figure 3.6: Fibrin deposition in the lungs after tissue factor (TF) treatment in the presence of saline or different concentrations of VHH-mTAFI-i49 (Mean ± SEM; n ≥ 3) (* $p < 0.01$; ns = not significant; one-way ANOVA; Dunnett's multiple comparison test, compared to saline).

Even though not statistical significant, there was a trend towards a dose-dependent decrease in fibrin deposition in the presence of an 2-,12 and 18-fold molar ratio of VHH-mTAFI-i49 over mTAFI (154 ± 24, 132 ± 30 and 48 ± 10 µg/mL, respectively, mean ± SEM, n ≥ 3). The fibrin deposition in the lungs of mice in the presence of VHH-mTAFI-i63 (16-fold molar excess over

mTAFI) was 94 ± 18 µg/mL, and was statistically not different from that in the absence of nanobody. Without thromboembolism induction, the fibrin deposition was 4.7 ± 0.7 µg/mL.

Epitope mapping

Based on the cross-reactivity of VHH-mTAFI-i49 with mouse and rat TAFI and the absence of cross-reactivity with human TAFI, available mouse/human and rat/human TAFI chimeras were used to localize the binding region of the nanobody. Evaluation of the effect of VHH-mTAFI-i49 on the zymogen activity of mouse, rat and human TAFI and the 7 chimeras allowed us to restrict the binding of the nanobody to AA 215-241 (data not shown). Within this region Ala^{222}, His^{223}, Lys^{224}, Arg^{227} and Val^{229} in mouse TAFI are different from those in human TAFI. These residues were mutated to alanine (except for Ala^{222} which was mutated to the corresponding amino acid, Phe, in human TAFI). Preliminary screening on conditioned medium revealed that only the mTAFI-R227A was less susceptible to zymogen stimulation by VHH-mTAFI-i49. Subsequently, charged amino acids within a radius of 20 ångström of Arg^{227} (based on the three-dimensional structure of human TAFI [10]) were mutated to alanine (i.e. Glu^{28}, Glu^{38}, Lys^{212}, Arg^{220} and Glu^{254}). Screening on conditioned medium revealed that only mTAFI-K212A was less susceptible to zymogen stimulation by VHH-mTAFI-i49. For unknown reasons, mTAFI-R220A was not expressed. Based on the results obtained with conditioned media, mTAFI-K212A, mTAFI-R227A and the double mutant mTAFI-K212A/R227A were produced and purified. In addition, mTAFI and mTAFI-K224A were also produced and purified as controls.

At a 16-fold molar excess of VHH-mTAFI-i49 over mTAFI variants an induced zymogen activity of 4.4 ± 0.3, 3.0 ± 0.3, 0.15 ± 0.07, 0.51 ± 0.12 and 0.05 ± 0.08 U/mg was observed for mTAFI, mTAFI-K224A, mTAFI-K212A, mTAFI-R227A and mTAFI-K212A/R227A, respectively (Table 3.1). There was only a minor difference between the mutants regarding activatability by T/TM with the exception of mTAFI-R227A which generated a 2-fold increased activity (data not shown).

Table 3.1: Affinity constant (K_A) and zymogen activity stimulation of VHH-mTAFI-i49 towards mTAFI and mTAFI mutants

	Zymogen stimulation (U/mg)	K_A (L/mol)
mTAFI	4.4 ± 0.3	$5.0 \pm 1.2 \times 10^7$
mTAFI-K212A	< 0.35 *	$0.73 \pm 0.59 \times 10^7$ †
mTAFI-K224A	3.0 ± 0.3 *	$8.5 \pm 0.4 \times 10^7$ †
mTAFI-R227A	0.51 ± 0.12 †	$1.2 \pm 0.4 \times 10^7$ †
mTAFI-K212A/R227A	<< 0.35 *	NB

Mean ± SD; n = 6; NB = no binding, * $p < 0.005$; † $p < 0.0001$
Paired t-test, compared to mTAFI.

The affinity (K_A) of VHH-mTAFI-i49 for mTAFI was $5.0 \pm 1.2 \times 10^7$ L/mol, mutation of Lys^{224} resulted in a 1.7-fold increased affinity (Table 3.1). In line with the observed decreased effect of

VHH-mTAFI-i49 on the zymogen activity, mutations at position 212 and 227 resulted in a 7- and 4-fold reduction of the affinity, respectively, which is mainly due to a strongly increased dissociation rate constant (data not shown). Combination of the mutations at position 212 and 227 resulted in a lack of binding of VHH-mTAFI-i49. VHH-rTAFI-i81 (a control nanobody that binds mTAFI) exhibits similar affinities for mTAFI and all mTAFI mutants, indicating that the observed decreased affinity of VHH-mTAFI-i49 is not caused by overall conformational changes that could have been induced by any of the mutations.

DISCUSSION

The intrinsic zymogen activity of TAFI and its function to cleave C-terminal lysine residues from partially degraded fibrin has been a matter of debate [12-14]. Recently, two nanobodies were generated that stimulate the zymogen activity of human TAFI [15]. Using TAFI depleted plasma reconstituted with a non-activatable TAFI mutant, the zymogen induction by these nanobodies resulted in a prolongation of clot lysis. This effect was explained by the translocation of the activation peptide, making the catalytic cleft accessible for larger substrates such as C-terminal lysines on partially degraded fibrin.

Nanobody, VHH-mTAFI-i49, described in the current study induces an increased zymogen activity of mTAFI, but reduces the clot lysis time in an *in vitro* clot lysis experiment. Further experiments on purified mTAFI and synthetic small substrate (Hip-Arg) demonstrate that induction of zymogen activity leads to a time-dependent reduced activatability of mTAFI. Extensive *in vitro* clot lysis experiments in the presence of VHH-mTAFI-i49 were performed to support this hypothesis. Clot lysis profiles and concomitant TAFI activity were determined and revealed reduced TAFIa generation after clot induction in the presence of VHH-mTAFI-i49 (1 h incubation of plasma with VHH-mTAFI-i49 prior to clot formation). The significantly reduced TAFIa formation in the presence of VHH-mTAFI-i49 confirms that the profibrinolytic effect of VHH-mTAFI-i49 is due to the reduced activatability of mTAFI. The absolute value of the total TAFI activity in the presence of VHH-mTAFI-i49 is higher compared to that in the absence of nanobody since this value is a combination of TAFI zymogen activity and TAFIa activity (the activity is measured by Hip-Arg and does not distinguish between the zymogen and TAFIa activity). The increased activity after clot induction can only originate from TAFIa generation during the clot formation (VHH-mTAFI-i49 has no stabilizing properties on TAFIa, data not shown) and is significantly lower (AUC and peak height) in the presence of VHH-mTAFI-i49.

The epitope studies point out that Lys^{212} and Arg^{227} are important for nanobody interaction (Figure 3.7). Even though both functional assay and SPR analysis confirm the amino acids important for VHH-mTAFI-i49/mTAFI interaction, the reduction in affinity of VHH-mTAFI-i49 to mutants mTAFI-K212A and mTAFI-R227A was only 6.5- and 4-fold, respectively, while an almost complete absence of zymogen stimulation was observed for these mutants. There was no interaction between VHH-mTAFI-i49 and the double mutant mTAFI-K212A/R227A suggesting that these two amino acids are critically involved in the interaction. It cannot be fully excluded that the lack of susceptibility to zymogen stimulation by VHH-mTAFI-i49 would be due to an

intrinsic incapability of zymogen activity because of these mutations. However, this is very unlikely since all the mTAFI mutants have similar behavior to 'wild-type' mTAFI regarding e.g. activation by T/TM and binding to a control nanobody. Both amino acids, Lys^{212} and Arg^{227}, are in close proximity of the activation peptide (Figure 3.7) and suggest that a translocation of the activation peptide by VHH-mTAFI-i49 may be responsible for the increased zymogen activity. Subsequently this translocation most likely compromises the stabilizing interactions between activation peptide and the dynamic flap region [10], thereby destabilizing TAFI prior to activation. However, allosteric changes induced by binding of VHH-mTAFI-i49 resulting in an alternative mode of inactivation cannot be fully excluded.

It is tempting to speculate that there are different magnitudes of translocating the activation peptide of TAFI (uncovering the catalytic cleft and thereby inducing zymogen activity) distinguishing between small (Hip-Arg) and larger substrates (C-terminal lysine residues on partially degraded fibrin). We hypothesize that VHH-mTAFI-i49 stimulated zymogen activity does not to play a role in removing C-terminal lysine residues from partially degraded fibrin. This hypothesis is further supported by the observations of clot lysis profiles where the clot induction was performed when the stimulated zymogen activity is high (data not shown): after incubation of nanobody with plasma at 37 °C for 10 min (see Figure 3.4, time point -50 min). Under these conditions, there was a reduction of the clot lysis time by 61% in the presence of a 16-fold molar ratio of VHH-mTAFI-i49 over mTAFI compared to no addition of nanobody (18 min *versus* 46 min, respectively), whereas one would expect a prolongation of clot lysis time if the generated zymogen activity was able to remove C-terminal lysine residues.

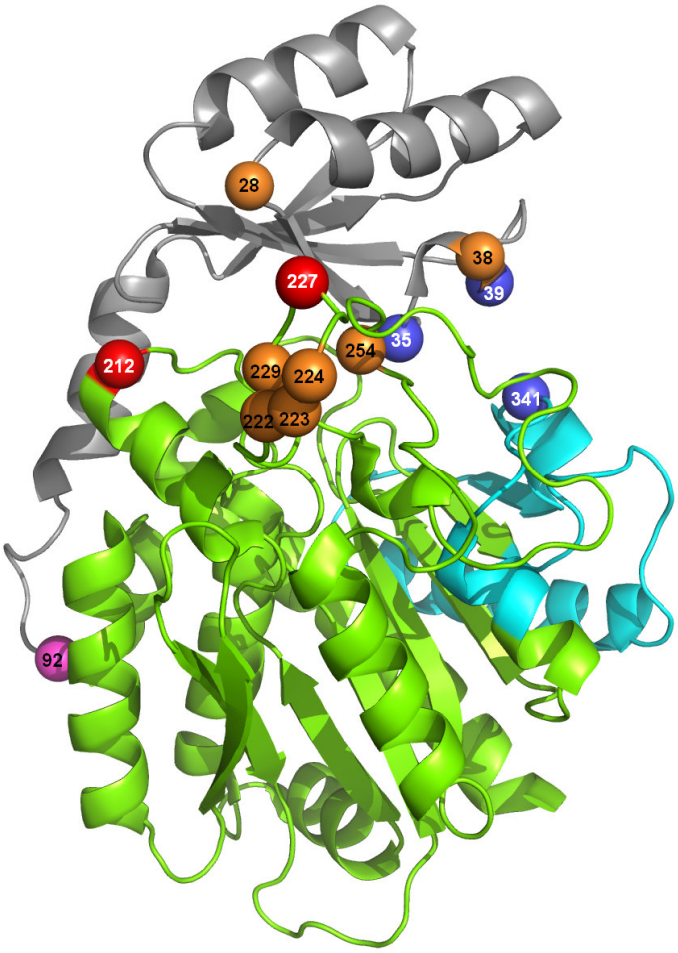

Figure 3.7: Three-dimensional structure of thrombin-activatable fibrinolysis inhibitor (TAFI) and localization of the screened amino acids. Ribbon drawing of the TAFI structure with the activation peptide colored in gray, catalytic domain in green, dynamic flap region in blue and the cleavage site, Arg^{92}, is depicted in purple (PBD ID 3D66). The screened amino acids for which mutation did not affect the zymogen stimulating properties of VHH-mTAFI-i49 are shown as orange spheres, the two amino acids for which mutation resulted in a reduced stimulation of zymogen activity by VHH-mTAFI-i49 are depicted in red. The amino acids important for the stabilizing interaction between the activation peptide (Val^{35} and Leu^{39}) and the dynamic flap region (Tyr^{341}) are shown as dark blue spheres.

It was long believed that the only way to obtain carboxypeptidase activity of TAFI was by activating TAFI to TAFIa. The activation is performed by proteolytic cleavage at Arg^{92} resulting in the release of the activation peptide [4]. It was discovered quite recently that also TAFI exerts some carboxypeptidase activity [12] and that this activity can be increased by binding of nanobodies [15]. Based upon the current observations and our previous study [15] it is tempting to speculate that it should be feasible to raise nanobodies to other proenzymes (plasminogen, protein C, factors of the coagulation cascade…) exerting similar effects, i.e. an induction of the enzymatic activity in the absence of a proteolytical activation step. Such mechanism has already been described for the interaction between streptokinase and plasminogen. Upon binding of

streptokinase to plasminogen, the active site is exposed without conversion of "single-chain" plasminogen into "double-chain" plasmin [21, 22]. In the case of TAFI, due to the instability of the generated zymogen activity, this leads to a reduced activatability and a subsequent unexpected functional effect. It is reasonable to assume that as a general concept other pro-enzymes could be 'activated' by binding of a specific nanobody which induce allosteric changes and thereby increase the affinity and/or catalytic rate constant of the substrate [23].

Besides its role in the inhibition of fibrinolysis, TAFIa also plays an important role in inflammation [24] as it is able to inactivate several inflammatory mediators such as bradykinin, anaphylatoxins C3a and C5a and osteopontin [25]. The TAFI zymogen is capable of cleaving small synthetic substrates [14] and it can be expected that the VHH-mTAFI-i49-induced zymogen activity exerts a similar or even increased activity. In view of the instability of the induced zymogen activity it is currently not clear what the applicability of VHH-mTAFI-i49 would be on the inflammatory components. Therefore, it would be interesting to test whether stimulating agents of the TAFI zymogen activity (such as VHH-mTAFI-i49) could be interesting tools to investigate anti-inflammatory properties of the VHH-mTAFI-i49-induced zymogen activity.

Multiple mechanisms have been reported inhibiting the function of TAFI by either interfering with the activation of TAFI (inhibition of thrombin-, T/TM- or plasmin-mediated activation by monoclonal antibodies or nanobodies) or by direct interference with enzymatic activity of activated TAFI (by low molecular weight compounds, antibodies or nanobodies) [26]. In this manuscript we describe a new concept for interfering with the TAFIa generation i.e. reduction of activatability through zymogen depletion. Evaluation of this mechanism in an *in vivo* mouse thromboembolism model demonstrates that this approach results in a strong profibrinolytic effect and is thereby a step forward in the development of a new profibrinolytic drug.

REFERENCES

1. Bouma BN, Marx PF, Mosnier LO, Meijers JC. Thrombin-activatable fibrinolysis inhibitor (tafi, plasma procarboxypeptidase b, procarboxypeptidase r, procarboxypeptidase u). *Thromb Res*. 2001;101:329-354
2. Mosnier LO, von dem Borne PA, Meijers JC, Bouma BN. Plasma tafi levels influence the clot lysis time in healthy individuals in the presence of an intact intrinsic pathway of coagulation. *Thromb Haemost*. 1998;80:829-835
3. Bajzar L, Nesheim ME, Tracy PB. The profibrinolytic effect of activated protein c in clots formed from plasma is tafi-dependent. *Blood*. 1996;88:2093-2100
4. Bajzar L, Manuel R, Nesheim ME. Purification and characterization of tafi, a thrombin-activable fibrinolysis inhibitor. *J Biol Chem*. 1995;270:14477-14484
5. Schatteman KA, Goossens FJ, Scharpe SS, Hendriks DF. Proteolytic activation of purified human procarboxypeptidase u. *Clin Chim Acta*. 2000;292:25-40
6. Boffa MB, Bell R, Stevens WK, Nesheim ME. Roles of thermal instability and proteolytic cleavage in regulation of activated thrombin-activable fibrinolysis inhibitor. *J Biol Chem*. 2000;275:12868-12878
7. Boffa MB, Wang W, Bajzar L, Nesheim ME. Plasma and recombinant thrombin-activable fibrinolysis inhibitor (tafi) and activated tafi compared with respect to glycosylation, thrombin/thrombomodulin-dependent activation, thermal stability, and enzymatic properties. *J Biol Chem*. 1998;273:2127-2135
8. Fleury V, Angles-Cano E. Characterization of the binding of plasminogen to fibrin surfaces: The role of carboxy-terminal lysines. *Biochemistry*. 1991;30:7630-7638
9. Marx PF, Hackeng TM, Dawson PE, Griffin JH, Meijers JC, Bouma BN. Inactivation of active thrombin-activable fibrinolysis inhibitor takes place by a process that involves conformational instability rather than proteolytic cleavage. *J Biol Chem*. 2000;275:12410-12415
10. Marx PF, Brondijk TH, Plug T, Romijn RA, Hemrika W, Meijers JC, Huizinga EG. Crystal structures of tafi elucidate the inactivation mechanism of activated tafi: A novel mechanism for enzyme autoregulation. *Blood*. 2008;112:2803-2809
11. Hendrickx ML, De Winter A, Buelens K, Compernolle G, Hassanzadeh-Ghassabeh G, Muyldermans S, Gils A, Declerck PJ. Tafia inhibiting nanobodies as profibrinolytic tools and discovery of a new tafia conformation. *J Thromb Haemost*. 2011;9:2268-2277
12. Valnickova Z, Thogersen IB, Potempa J, Enghild JJ. Thrombin-activable fibrinolysis inhibitor (TAFI) zymogen is an active carboxypeptidase. *J Biol Chem*. 2007;282:3066-3076
13. Willemse JL, Heylen E, Hendriks DF. The intrinsic enzymatic activity of procarboxypeptidase u (tafi) does not significantly influence the fibrinolysis rate: A rebuttal. *J Thromb Haemost*. 2007;5:1334-1336
14. Foley JH, Kim P, Nesheim ME. Thrombin-activable fibrinolysis inhibitor zymogen does not play a significant role in the attenuation of fibrinolysis. *J Biol Chem*. 2008;283:8863-8867
15. Mishra N, Buelens K, Theyskens S, Compernolle G, Gils A, Declerck PJ. Increased zymogen activity of thrombin-activatable fibrinolysis inhibitor prolongs clot lysis. *J Thromb Haemost*. 2012;10:1091-1099

16. Gils A, Ceresa E, Macovei AM, Marx PF, Peeters M, Compernolle G, Declerck PJ. Modulation of TAFI function through different pathways--implications for the development of tafi inhibitors. *J Thromb Haemost*. 2005;3:2745-2753

17. Conrath KE, Lauwereys M, Galleni M, Matagne A, Frere JM, Kinne J, Wyns L, Muyldermans S. Beta-lactamase inhibitors derived from single-domain antibody fragments elicited in the camelidae. *Antimicrob Agents Chemother*. 2001;45:2807-2812

18. Vercauteren E, Emmerechts J, Peeters M, Hoylaerts MF, Declerck PJ, Gils A. Evaluation of the profibrinolytic properties of an anti-TAFI monoclonal antibody in a mouse thromboembolism model. *Blood*. 2011;117:4615-4622

19. Hillmayer K, Vancraenenbroeck R, De Maeyer M, Compernolle G, Declerck PJ, Gils A. Discovery of novel mechanisms and molecular targets for the inhibition of activated thrombin activatable fibrinolysis inhibitor. *J Thromb Haemost*. 2008;6:1892-1899

20. De Genst E, Silence K, Ghahroudi MA, Decanniere K, Loris R, Kinne J, Wyns L, Muyldermans S. Strong in vivo maturation compensates for structurally restricted H3 loops in antibody repertoires. *J Biol Chem*. 2005;280:14114-14121

21. Reddy KN, Markus G. Mechanism of activation of human plasminogen by streptokinase. Presence of active center in streptokinase-plasminogen complex. *J Biol Chem*. 1972;247:1683-1691

22. Schick LA, Castellino FJ. Direct evidence for the generation of an active site in the plasminogen moiety of the streptokinase-human plasminogen activator complex. *Biochemical and biophysical research communications*. 1974;57:47-54

23. Saboury AA. Enzyme inhibition and activation: A general theory. *J Iran Chem Soc*. 2009;6:219-229

24. Bouma BN, Mosnier LO. Thrombin activatable fibrinolysis inhibitor (tafi)--how does thrombin regulate fibrinolysis? *Ann Med*. 2006;38:378-388

25. Morser J, Gabazza EC, Myles T, Leung LL. What has been learnt from the thrombin-activatable fibrinolysis inhibitor-deficient mouse? *J Thromb Haemost*. 2010;8:868-876

26. Vercauteren E, Gils A, Declerck PJ. Thrombin activatable fibrinolysis inhibitor: A putative target to enhance fibrinolysis. *Semin Thromb Hemost*. 2013

Chapter 4

In vitro and *in vivo* characterization of the profibrinolytic effect of an anti-rat TAFI nanobody

M. L. V. HENDRICKX*, M. ZATLOUKALOVA*, G. HASSANZADEH-GHASSABEH †‡, S. MUYLDERMANS †§, A. GILS* and P. J. DECLERCK*

* Laboratory for Therapeutic and Diagnostic Antibodies, Department of Pharmaceutical and Pharmacological Sciences, KU Leuven, Belgium † Laboratory of Cellular and Molecular Immunology, Faculty of Sciences, Vrije Universiteit Brussel, Brussels; ‡ Nanobody Service facility (NSF), VIB, Brussels, Belgium and §VIB Department of Structural Biology, Brussels, Belgium

Thromb Haemost , Under review

SUMMARY

Background: One of the main disadvantages of current t-PA thrombolytic treatment is the increased bleeding risk. Upon activation, thrombin activatable fibrinolysis inhibitor (TAFI) is a very powerful antifibrinolytic enzyme. Therefore, co-administration of a TAFI inhibitor during thrombolysis could reduce the required t-PA dose, thereby decreasing bleeding risks without compromising the efficacy.

Objective: In this study we generate and characterize an inhibitory nanobody towards rat TAFI and evaluate its profibrinolytic property *in vitro* and *in vivo*.

Methods and results: Nanobody VHH-rTAFI-i81 inhibits (at a 16-fold molar ratio nanobody over TAFI) the thrombin/thrombomodulin (T/TM)-mediated activation of rat TAFI (rTAFI) by 83 ± 1.8 % with an IC_{50} of 0.46 (molar ratio nanobody over TAFI). The affinity (K_A) of VHH-rTAFI-i81 for rTAFI, as determined by surface plasmon resonance (Biacore®), is 2.5 ± 0.2 x 10^{10} M^{-1} and illustrates a very strong binding. In an *in vitro* clot lysis assay, administration of VHH-rTAFI-i81 strongly enhances the profibrinolytic effect of t-PA and reduces time to reach full lysis of t-PA-mediated clot lysis. Epitope mapping discloses that Lys^{392} is of primary importance for the nanobody/rTAFI interaction besides minor contributions of Tyr^{175} and Glu^{183}. *In vivo* application of VHH-rTAFI-i81 in a tissue factor-induced mouse thromboembolism model significantly decreases fibrin deposition in the lungs in the absence of exogenous administered t-PA.

Conclusion: Nanobody VHH-rTAFI-i81 is a very potent inhibitor of T/TM-mediated TAFI activation. Co-administration of this nanobody and t-PA enhances the fibrinolytic efficacy. In an *in vivo* mouse thromboembolism model, VHH-rTAFI-i81 reduces fibrin deposition in the lungs.

INTRODUCTION

Thrombin-activatable fibrinolysis inhibitor (TAFI) is a metallocarboxypeptidase mainly produced by the liver and present in the blood at a concentration between 5 and 15 µg/ml. TAFI can be cleaved at Arg^{92} by trypsin like enzymes such as plasmin, thrombin or the complex thrombin/thrombomodulin (T/TM) resulting in the generation of activated TAFI (TAFIa) [1-4]. TAFIa exerts an anti-fibrinolytic effect by removing C-terminal lysine residues from partially degraded fibrin thereby diminishing plasmin generation resulting in attenuation of the blood clot dissolution [1]. Up to date, there are no physiological inhibitors of TAFIa reported, but its function is regulated through the intrinsic, temperature-dependent instability. This results in inactivation of TAFIa by conformational changes [3, 5, 6].

Current thrombolytic therapy, based on activation of the fibrinolytic system, consists of administration of a high dose of plasminogen activators. Even though very effective, one of the main disadvantages of this approach is an increased bleeding risk. Therefore, co-administration of a TAFI inhibitor during thrombolysis has been suggested to allow reduction of the required dose of thrombolytic agent, thereby potentionally decreasing the bleeding risk without compromising the efficacy [7, 8].

Inhibitory nanobodies towards human TAFI(a) have been reported [6, 9] and demonstrate very strong profibrinolytic effects *in vitro*, however these nanobodies lack cross reactivity with mouse and/or rat TAFI (mTAFI and rTAFI) and therefore cannot be tested in an *in vivo* model. Human, mouse and rat TAFI have a very high sequence identity (rat to mouse 96% and mouse and rat to human 86%) and are considered to be biological equivalents with regard to a) activatability by T/TM b) strong temperature-dependent instability of TAFIa and c) antifibrinolytic effect during *in vitro* clot lysis [10]. We aimed to develop and characterize inhibitory nanobodies towards rTAFI and test their application in an *in vivo* thromboembolism model.

MATERIALS AND METHODS

Materials

Wild-type recombinant rat TAFI and rat TAFI-CIYQ (rTAFI-$C^{305}I^{329}Y^{333}Q^{335}$) without his-tag were prepared as described before [11, 12]. All experiments were performed with wild-type rTAFI unless indicated otherwise. Oligonucleotides, Pfx50 DNA polymerase and restriction enzymes were purchased from Sigma-Aldrich (St Louis, MO, USA), Life Technologies (Merelbeke, Belgium) and New England Biolabs (Hitchin, UK) respectively. Polymerase chain reactions (PCR) were performed with the Mastercycler Gradient from Eppendorf (Hamburg, Germany), plasmid DNA was purified with NucleobondTM AX500 kit (Machery-Nagel, Düren, Germany) and DNA sequencing was performed by LGC genomics (Berlin, Germany). Human thrombin, rabbit thrombomodulin (TM) and plasmin were purchased from Sigma-Aldrich, American Diagnostics (Greenwich, CT, USA) and Enzyme Research Laboratories (South Bend, UK), respectively. H-D-phenylalanine-L-propyl-L-arginine chloromethyl ketone (PPACK), aprotinin and hippuryl-L-arginine were obtained from Biomol Research Laboratories (Plymouth meeting, PA, USA), Fluka (Buchs, Switzerland) and Bachem (Bubendorf, Switzerland), respectively. Tissue-type plasminogen activator (t-PA) and rat plasma were kind gifts from Boehringer Ingelheim (Brussels, Belgium) and Servier (Suresnes, France) respectively. Ocriplasmin (microplasmin) was a kind gift from ThromboGenics (Leuven, Belgium).

Nanobody library construction, expression and purification.

A nanobody library was obtained as described before [13]. Therefore, an alpaca (*Vicugna pacos*) was subcutaneously injected with 100 µg (weekly, during 7 weeks) of a mixture containing activated and intact rTAFI-CIYQ mixed with Gerbu LQ#300 (Gerbu Biotechnik GmBH, Germany). Blood was collected four days after the last immunization and lymphocytes were isolated. Total RNA was isolated from the lymphocytes and cDNA was obtained by reverse transcription. The VHH gene repertoire was amplified by PCR and PCR products were digested by *Pst*I and *Not*I and ligated into the phagemid vector pMECS. Subsequently, the VHH-repertoire was displayed on phage after transformation in *E.coli* TG1 cells and binders were selected via panning either towards intact or activated rTAFI-CIYQ. Positive clones were identified by ELISA and identical clones were detected via sequencing. The plasmids of positive clones were transformed in *E.coli* WK6 cells and nanobody production was induced by IPTG as described before [13]. The periplasmic proteins were extracted, isolated and dialyzed against 20 mmol/L Tris–HCl, 0.5 mol/L NaCl (pH 7.9) followed by filtration (0.45 µm) and loaded on a His-Trap HP column (GE Healthcare,

Uppsala, Sweden). Bound proteins were eluted by an imidazole gradient (0–350 mmol/L imidazole in 20 mmol/L Tris HCl, 0.5 mol/L NaCl; pH 7.9) and the nanobody containing fractions were selected via SDS-polyacrylamide gel electrophoresis (PAGE) (Phast-Gel^{TM} gradient 10–15% gels, GE Healthcare, Uppsala, Sweden) followed by coomassie staining. Selected fractions were dialyzed against phosphate-buffered saline (PBS; 140 mmol/L NaCl, 2.7 mmol/L KCl, 8 mmol/L Na_2HPO_4, 1.5 mmol/L KH_2PO_4; pH 7.4).

Evaluation of the overall inhibitory effect of the nanobodies on TAFI activation and TAFIa activity

The overall inhibitory effect of the nanobodies on rTAFI was determined using a chromogenic assay as described before [6] with minor modifications. Briefly, rTAFI (45 nmol/L, concentration during activation) was diluted in HEPES buffer (25 mmol/L HEPES, 137 mmol/L NaCl, 3.5 mmol/L KCl and 0.1% BSA; pH 7.4) and incubated for 10 min at 25 °C with either buffer or nanobody at concentrations ranging from 0.25- to 16-fold molar ratio of nanobody over rTAFI. Subsequently, TAFI was activated by addition of thrombin and thrombomodulin (20 nmol/L and 5 nmol/L respectively, concentration during activation) in the presence of $CaCl_2$ (5 mmol/L) at 25°C for 10 min. Addition of PPACK (37.5 µmol/L, final concentration) terminated the activation and subsequently the substrate Hip-Arg (hippuryl-arginine, 4 mmol/L, concentration during substrate conversion) was added and substrate conversion was allowed to proceed for 15 min at 25 °C. The conversion was stopped by addition of 20 µl HCl (1 mol/L) followed by neutralization with 20 µl NaOH (1 mol/L) and buffered with 25 µl Na_2HPO_4 (1 mol/L; pH 7.4) prior to addition of 30 µl 6% cyanuric chloride (in 1,4-dioxane). The solution was then vortexed (5 min) and centrifuged (Eppendorf centrifuge 5415D) at max speed for 2 min and 100 µl aliquots were transferred into a 96-well microtiterplate and the absorbance measured at 405 nm. By comparison of the enzymatic activity generated upon activation of TAFI in the absence or presence of nanobody (Nb), the inhibiting capacity was calculated and expressed as percentage of inhibition (($[OD]^{no\ Nb}$-$[OD]^{with\ Nb}$)/($[OD]^{no\ Nb}$) x 100 = % inhibition). In this assay a reduced TAFIa activity could be due to either interference with the activation process or by a direct interference with TAFIa enzymatic activity. The effect of the nanobodies on plasmin-mediated activation of rTAFI was evaluated as described above, except for the use of plasmin for activation (500 nmol/L, concentration during activation), addition of aprotinin to stop the activation (1.25 µmol/L, final concentration) and substrate conversion (Hip-Arg) for 30 min. VHH-mTAFI-i63 (a control nanobody with no functional effect on rTAFI) and HEPES buffer were included as controls.

Evaluation of the effect of VHH-rTAFI-i81 on the conversion of TAFI to TAFIa

rTAFI (857 nmol/L, concentration during activation) was diluted in Tris buffer (20 mmol/L Tris, 0.1 mol/L NaCl; pH 7.4) and incubated with either buffer or VHH-rTAFI-i81 (16-fold molar excess of nanobody over rTAFI). After an incubation period at 37 °C of 10 min, this mixture was activated by T/TM (20 nmol/L and 5 nmol/L, respectively) in the presence of $CaCl_2$ (5 mmol/L) at 37 °C for 10 min. The activation was stopped with 30 µmol/L PPACK, addition of sodium dodecyl sulfate (SDS; 1% final concentration) and heating at 100 °C for 30 seconds. The generated fragments were separated by SDS-polyacrylamide gel electrophoresis (PAGE) (Phast-Gel™ gradient 10-15% gels) and visualized by silver staining. A similar setup was designed for the evaluation of the effect of VHH-rTAFI-i81 on plasmin-mediated activation: T/TM was replaced by plasmin (333 nmol/L) and PPACK was replaced by aprotinin (960 nmol/L).

Evaluation of the direct inhibitory effect of VHH-rTAFI-i81 on TAFIa

rTAFI (45 nmol/L diluted in HEPES, concentration during activation) was activated by T/TM in the presence of $CaCl_2$ (20 nmol/L, 5 nmol/L and 5 mmol/L, respectively) at 25 °C for 10 min before terminating with PPACK (37.5 µmol/L, final concentration). Subsequently, VHH-rTAFI-i81 (resulting in a 16-fold molar ratio of nanobody over rTAFI) or buffer was added and the mixture was incubated at 25 °C for 10 min. The rTAFIa activity was determined by the chromogenic assay as described above and the percentage of inhibition of the rTAFIa activity was calculated relative to the rTAFIa activity observed in the absence of nanobody.

To evaluate the effect of VHH-rTAFI-i81 on rTAFIa stability, rTAFIa was pre-incubated for 5 min at 37°C with VHH-rTAFI-i81 followed by different incubation periods (0, 7.5, 15, 30, 75, 120 and 210 min) at 37°C. The residual activity was determined as described above. The generated activity (expressed as U/mg, one unit (U) carboxypeptidase activity is defined as the amount of enzyme converting 1 micromole of substrate per minute at 25°C) was calculated based on a hippuric acid standard. VHH-mTAFI-i63 and HEPES buffer were included as controls.

Affinity determination

The affinity of VHH-rTAFI-i81 for rTAFI was determined by Surface Plasmon Resonance (SPR) using a Biacore 3000 analytical system (GE Healthcare, Uppsala, Sweden) as described before [6]. VHH-rTAFI-i81 was covalently coupled (400 RU) to a CM5 sensor chip (using a concentration of 5 µg/mL nanobody in acetate buffer 10 mmol/L; pH 4.5). rTAFI (diluted in HBS-EP buffer to concentrations between 6.25 and 200 nM) was injected at a flowrate of 30 µl/min followed by a

dissociation. After each cycle the sensor chip was regenerated by glycine (10 mmol/L, pH 1.5). The association and dissociation rate constants were determined using the BIAcore 3000 evaluation software (Langmuir binding, local fit).

Evaluation of the effect of VHH-rTAFI-i81 on fibrinolysis

Clot lysis experiments were performed in microtiterplates as described previously [14] with minor modifications. Citrated rat plasma was mixed with either buffer or nanobody diluted in Tris/Tween buffer (10 mmol/L Tris, 0.01% Tween 20, pH 7.5). The final concentrations of VHH-rTAFI-i81 resulted in a molar ratio ranging from 0.25 to 2 over rTAFI, assuming a rTAFI concentration of 90 nmol/L in plasma. After incubation at 37 °C for 10 min, t-PA was added and aliquots of 80 µl were transferred, in duplicate, to microtiter wells each containing 20 µl 100 mmol/L $CaCl_2$ resulting in the following final concentrations: 30 % plasma, 1000 pmol/L t-PA, 20 mmol/L $CaCl_2$. The plate was incubated at 37 °C and read at 405 nm at 2 min intervals. The area under the curve (AUC) was calculated (from time point 0 to 180 min) to quantify the effect on clot lysis.

Alternatively, the efficacy of different concentrations of t-PA (0 - 900 pM) was evaluated in the presence or absence of VHH-rTAFI-i81 at a two-fold molar ratio over rTAFI.

Evaluation of the effect of VHH-rTAFI-i81 in an in vivo mouse thromboembolism model

The profibrinolytic properties of VHH-rTAFI-i81 were tested in an *in vivo* mouse thromboembolism model as described before [15] with minor modifications. VHH-rTAFI-i81 (0.22, 0.66 or 1.3 mg/kg, corresponding to a 2-, 6- and 12-fold molar ratio over rTAFI) was injected intravenously in overnight fasted non-anesthetized female Swiss mice (Janvier). The endotoxins from nanobody preparations were removed (administration to mice < 5 EU/kg) using PROSEP-RemTox (Millipore). Thromboembolism was induced after 5 min using human tissue factor (TF, 2.5 µg/kg, Dade Innovin reagent, Siemens). Reference mice receiving saline instead of nanobodies or saline instead of TF were also included. Five minutes after TF injection the mice were anesthetized with pentobarbital (Nembutal; 60 mg/kg) and 5 minutes later 500 IU of heparin (Heparin Leo) was administered in the vena cava. Three minutes after heparin injection the lungs were perfused with saline containing heparin (10 IU/ml) and the left lung was isolated and stored at -80°C. Four ml of PBS was added per gram of lung followed by homogenization by a tissue homogenizer (Ribolyzer Fast Prep 24 System, MP Biomedicals). After three wash and centrifugation steps the soluble fractions were removed and the pellet, containing the insoluble fibrin, was resuspended. The resuspended pellet was incubated with ocriplasmin (microplasmin

2 µmol/L, 37°C, 4 hours) in order to convert the fibrin into soluble fibrin degradation products (FbDP's). Aprotinin (4 µmol/L, final concentration) was added to stop fibrinolysis and after homogenization and centrifugation (max speed, 20 min) the supernatants was collected. A mouse fibrinogen ELISA kit (Immunology Consultants Laboratory, Portland) with cross-reactivity for FbDP's was used to quantify the FbDP's and thereby the corresponding fibrin deposition. The experimental protocol was approved by the KU Leuven Ethical Committee for Animal Experiments (P112-2012).

Epitope mapping of VHH-rTAFI-i81

Different TAFI mutants/chimeras were used to unravel the binding epitope of VHH-rTAFI-i81 [16]. Single mutations to alanine were introduced by site-directed mutagenesis using template pcDNA5/FRT-ratTAFI-6his. The 'wild-type' rTAFI and rTAFI variants were produced by HEK293T cells and initial evaluation of the inhibitory properties of VHH-rTAFI-i81 towards the TAFI variants was performed on the conditioned medium. Subsequently TAFI variants with altered susceptibility were purified using a His-Trap HP column and the effect of mutations on the affinity and inhibitory properties of VHH-rTAFI-i81 was determined.

Statistical analysis

Quantitative data are presented as mean ± standard deviation (SD) unless indicated otherwise. Statistical analysis (paired t-test and one-way ANOVA with Dunnett's multiple comparison test) were performed by GraphPad Prism (GraphPad Prism 5 Software).

RESULTS

After 3 rounds of panning, 227 out of 285 cherry picked clones were found to produce nanobodies towards rTAFI(a). Sequence determination revealed 82 unique nanobodies and these were divided into 15 clusters based on their CDR3 region. Nanobodies within one cluster are expected to target the same epitope [17]. Therefore, one nanobody from each cluster was selected for production, purification and subsequent evaluation of inhibitory properties towards rTAFI. Six out of 15 selected nanobodies exhibit inhibitory properties towards rTAFI: three nanobodies mainly inhibit the T/TM-mediated activation, 2 nanobodies mainly inhibit the plasmin-mediated activation of TAFI, one nanobody inhibits T/TM- as well as plasmin-mediated activation. Based on the affinity of the inhibitory nanobodies, we selected VHH-rTAFI-i81, a nanobody that mainly inhibits the T/TM-mediated activation for further characterization.

Evaluation of the effect of VHH-rTAFI-i81 on TAFI activation and TAFIa activity

Addition of VHH-rTAFI-i81 to rTAFI leads to 83.2 ± 1.8 % inhibition of the T/TM-mediated activation of rTAFI (Table 4.1). A dose-response curve of the effect of VHH-rTAFI-i81 on T/TM-mediated rTAFI activation, demonstrates 50% of the maximal inhibition at a molar ratio (VHH-rTAFI-i81:rTAFI) of 0.46 (Figure 4.1).

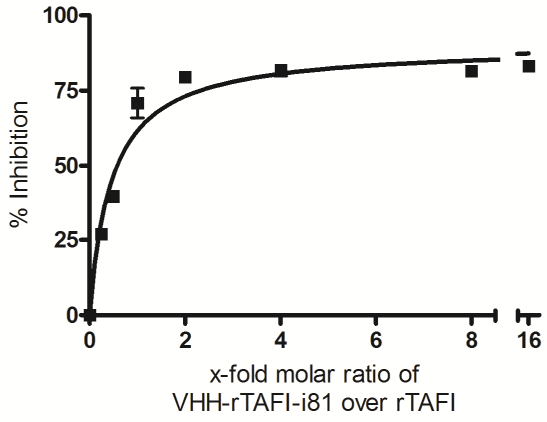

Figure 4.1: Dose-response curve for inhibition of the T/TM-mediated activation of rat TAFI by VHH-rTAFI-i81 (mean ± SD, n ≥ 3).

Surprisingly, inhibition of plasmin-mediated activation by VHH-rTAFI-i81 was -80 ± 11 % and addition of VHH-rTAFI-i81 after activation of rTAFI demonstrated an apparent inhibition of -52 ± 1.6 % (Table 4.1). The inhibition of the T/TM-mediated activation of VHH-rTAFI-i81 was confirmed by evaluation by SDS-PAGE analysis of the rTAFI fragmentation pattern after activation (i.e. reduced proteolytical cleavage from TAFI to TAFIa, data not shown).

Table 4.1: Inhibition of the T/TM- and plasmin-mediated activation of rTAFI and inhibition of rTAFIa by VHH-rTAFI-i81

	% Inhibition of the T/TM-mediated activation	% Inhibition of the plasmin-mediated activation	% Inhibition of rTAFIa
VHH-rTAFI-i81	83 ± 2	-80 ± 11	-52 ± 2

Ratio [nanobody]:[rTAFI] = 16-molar. Mean ± standard deviation, n ≥ 3

Addition of different concentrations of VHH-rTAFI-i81 to rTAFIa followed by incubation for different time periods reveals a concentration-dependent increase in the half-life of rTAFIa activity from 2.4 ± 0.3 min and 2.4 ± 0.2 min in the presence of VHH-mTAFI-i63 and HEPES buffer respectively, to 9.6 ± 0.4 min, 24.7 ± 1.8 min, 33.9 ± 6.4 min and 43.7 ± 5.9 min in the presence of a 0.125-, 1-, 4- and 64-fold molar ratio VHH-rTAFI-i81 over rTAFIa respectively (Figure 4.2).

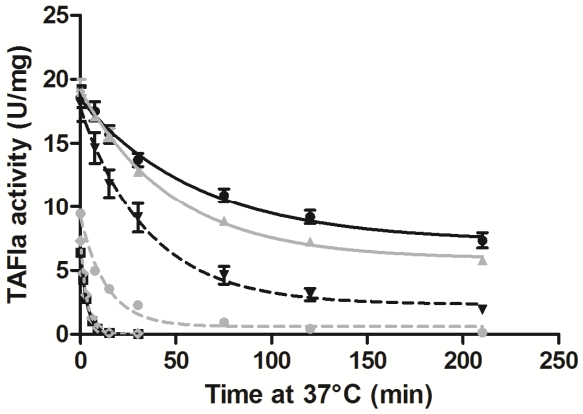

Figure 4.2: Stabilizing properties of VHH-rTAFI-i81 on rTAFIa activity. Decay of rTAFIa activity (at 37°C) in the absence of nanobody ( ), in the presence of a control nanobody VHH-mTAFI-i63 (, at a 16-fold molar ratio over rTAFI) and in the presence of varying concentrations of VHH-rTAFI-i81 (64- , 4- , 1- and 0.125-fold molar ratio over rTAFI) (mean ± SD, n ≥ 3).

Affinity determination of VHH-rTAFI-i81 to TAFI

The association and dissociation rate constants (k_a and k_d) for rTAFI were 1.8 ± 0.2 x 10^6 $M^{-1}s^{-1}$ and 7.2 ± 0,9 x 10^{-5} s^{-1}, respectively and result in an affinity constant (K_A) of 2.5 ± 0.2 x 10^{10} M^{-1}. The affinity (K_A) for mTAFI was 6.8 ± 1.2 x 10^9 M^{-1} (with k_a and k_d of 1.4 ± 0.2 x 10^6 $M^{-1}s^{-1}$ and 2.1 ± 0.1 x10^{-4} s^{-1}, respectively). There was no binding to human TAFI.

Evaluation of the effect of VHH-rTAFI-i81 on fibrinolysis

A dose-response curve of VHH-rTAFI-i81 in rat plasma in the presence of 1000 pM t-PA reveals that the maximal profibrinolytic effect is reached at an equimolar ratio of nanobody over rTAFI with a ratio AUC_{+Nb}/AUC_{-Nb} of 0.17 ± 0.03 (Figure 4.3).

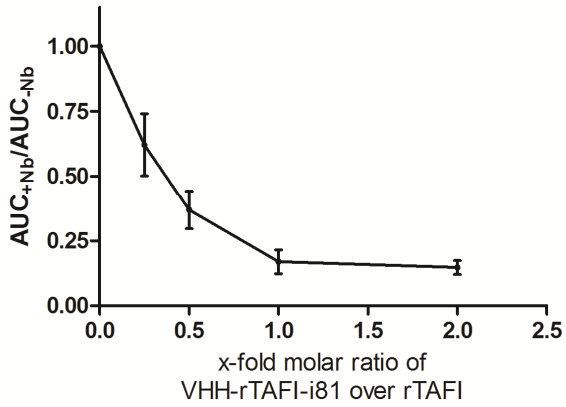

Figure 4.3: Dose-response curve of the profibrinolytic properties of VHH-rTAFI-i81 in plasma. The area under the curve (AUC) was determined for clot lysis profiles in the presence of different concentrations of VHH-rTAFI-i81 and expressed relative to the AUC in the absence of VHH-rTAFI-i81 (mean ± SD, n ≥ 3).

A dose-response curve of t-PA in the presence and absence of a two-fold molar excess of VHH-rTAFI-i81 demonstrated that (a) whereas in the absence of VHH-rTAFI-i81 lysis remains limited even at the highest concentration of t-PA (900 pM) (Figure 4.4, panel D), in the presence of a two-fold molar excess of VHH-rTAFI-i81 full lysis is achieved at t-PA concentration of 400 pM (Figure 4.4, panel C and D) and (b) the presence of VHH-rTAFI-i81 leads to a strong reduction in time to reach the maximal effect: 25 min compared to >180 min in the absence of VHH-rTAFI-i81 (Figure 4.4).

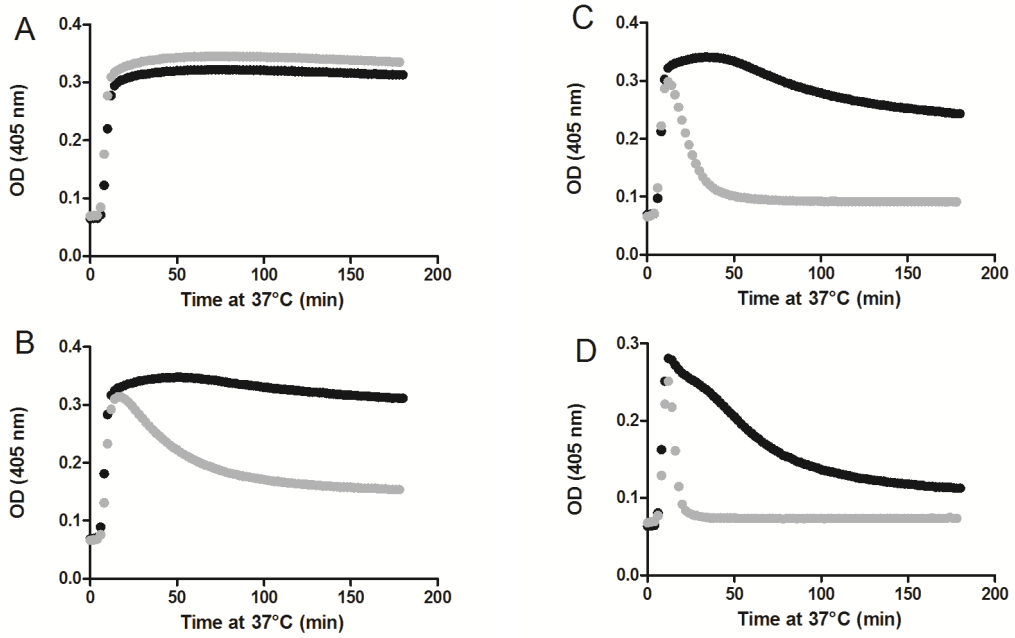

Figure 4.4: Clot lysis profiles using different concentrations of t-PA in the absence (●) or in the presence (●) of VHH-rTAFI-i81. VHH-rTAFI-i81 was used at a two-fold molar ratio over rTAFI in the presence of 0, 200, 400 and 900 pM t-PA (panel A, B, C and D, respectively). For each condition, a representative experiment out of three performed experiments is shown.

The EC_{50} of t-PA (concentration of t-PA at which 50 % of its maximal effect was observed) was 528 ± 39 pM in the absence of VHH-rTAFI-i81 and 208 ± 29 pM in the presence of a two-fold molar excess of VHH-rTAFI-i81 over rTAFI.

Evaluation of the effect of VHH-rTAFI-i81 in an in vivo mouse thromboembolism model

VHH-rTAFI-i81 cross-reacts with mTAFI and inhibits the T/TM-mediated activation of mTAFI by 78 ± 3 % at a 16-fold molar ratio over mTAFI with an IC_{50} of 0.59 (fold molar ratio VHH-rTAFI-i81 over mTAFI). Furthermore, VHH-rTAFI-i81 was also tested in an *in vitro* clot lysis experiment with mouse plasma and demonstrates a maximal effect at an equimolar ratio of VHH-rTAFI-i81 over mTAFI. Because of comparable characteristics of VHH-rTAFI-i81 towards mouse and rat TAFI and plasma, VHH-rTAFI-i81 could be evaluated in an *in vivo* mouse thromboembolism model.

Without TF injection, the fibrin deposition in the lungs is 4.4 ± 0.4 µg/ml (mean ± standard error of mean). The fibrin deposition in the lungs upon induction of thromboembolism in the absence of VHH-rTAFI-i81 (0 x) was 183 ± 18 µg/ml (expressed as fibrinogen equivalents, see methods). In the presence of a 2-, 6- and 12-fold molar ratio of VHH-rTAFI-i81, the fibrin deposition was 132 ± 28, 8 ± 2 and 14 ± 1 µg/ml respectively (Figure 4.5).

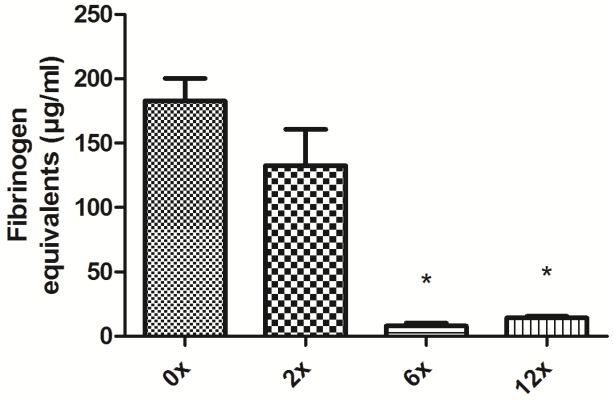

Figure 4.5: Fibrin deposition in the lung after thromboembolism induction in the presence of different concentrations of VHH-rTAFI-i81. Fibrin depositions (expressed as fibrinogen equivalents) in the left lungs upon thromboembolism induction in the presence of different concentrations of VHH-rTAFI-i81 (x-fold molar ratio of VHH-rTAFI-i81 over rTAFI) (mean ± SEM; n ≥ 3; * p < 0.001, one-way ANOVA, Dunnett's multiple comparison test compared to 0x).

Epitope mapping of VHH-rTAFI-i81 to rTAFI

Since VHH-rTAFI-i81 does not cross-react with human TAFI, rat/human TAFI-chimeras could be used to unravel the binding region of the nanobody. Evaluation of the inhibitory effect of VHH-rTAFI-i81 on rat and human TAFI and 4 chimeras (see methods) allowed us to restrict the binding region to AA 160-195. Within this region 9 AA (Tyr^{175}, Val^{176}, His^{180}; Lys^{182}, Glu^{183}, Asn^{184}, Thr^{185}, Arg^{188} and His^{192}) differ between human and rat TAFI and their alanine counterparts were produced in rTAFI. Only alanine mutations at position Tyr^{175} and Glu^{183} resulted in a reduced inhibition by VHH-rTAFI-i81, with a more pronounced effect for the mutation to alanine at position 175. Therefore charged AA within a radius of 20 ångström from Tyr^{175} were also mutated to alanine (Glu^{99}, Glu^{323}, Lys^{327}, Lys^{380} and Lys^{392}). From the latter mutants only rTAFI-K392A was less susceptible for inhibition by VHH-rTAFI-i81. Based on these results using conditioned media, rTAFI-Y175A, rTAFI-E183A, and rTAFI-K392A were selected for purification. In addition rTAFI- H180A was included as a control.

At a 16-fold molar ratio of VHH-rTAFI-i81 over rTAFI-variants, approximately 80% inhibition of the T/TM-mediated activation was observed for rTAFI and rTAFI-H180A (Table 4.2). Under these conditions the T/TM-mediated activation of rTAFI-Y175A, rTAFI-E183A and rTAFI-K392A was inhibited up to 20 ± 4 %, 36 ± 3 % and -3 ± 5 %, respectively. In line with these functional effects the affinity (K_A) of VHH-rTAFI-i81 for rTAFI-Y175A, rTAFI-E183A, and rTAFI-K392A was reduced 60-, 40- and 500-fold, respectively, compared to that for rTAFI (Table 4.2).

Table 4.2: Inhibition of the T/TM-mediated activation by VHH-rTAFI-i81 and affinity constants of VHH-rTAFI-i81 for rTAFI and rTAFI mutants

	% Inhibition of the T/TM mediated activation by VHH-rTAFI-i81	K_A (M^{-1}) VHH-rTAFI-i81
rTAFI	79 ± 1	126 ± 15 x 10^8
rTAFI-Y175A	20 ± 4 **	2.10 ± 0.25 x 10^8 ***
rTAFI-H180A	81 ± 2 ^{ns}	81.6 ± 14.7 x 10^8 ***
rTAFI-E183A	36 ± 3 *	3.10 ± 0.27 x 10^8 ***
rTAFI-K392A	-3 ± 5 **	0.26 ± 0.06 x 10^8 ***

Mean ± SD; n = 6; paired t-test compared to rTAFI; *** $p < 0.0001$; ** $p < 0.001$; * $p < 0.005$; ns = not significant

The affinity for rTAFI-H180A was virtually unchanged (1.4-fold reduction) compared to rTAFI. The affinity of a control nanobody, VHH-mTAFI-i49 which binds to another epitope on rTAFI, exhibited similar binding affinities (K_A values between 0.74 ± 0.07 x 10^8 and 2.00 ± 0.20 x 10^8 M^{-1}) for all rTAFI variants tested.

DISCUSSION

TAFIa plays an important role in the attenuation of fibrinolysis by removing C-terminal lysine residues from partially degraded fibrin. These lysine residues are an important cofactor in the t-PA mediated plasminogen activation [18]. Elevated TAFI levels have been associated with an increased risk of angina pectoris [19], venous thrombosis [20], coronary artery disease[21], ischemic stroke [22] and myocardial infarction [23]. A reduced bleeding tendency might be observed upon co-administration of t-PA and a TAFI inhibitor since it could allow a reduction of the dose of t-PA without hampering the efficacy of the treatment [24]. Nanobodies interfering with the activation of human TAFI to TAFIa [9] and nanobodies directly inhibiting human TAFIa [6] have been developed and under certain circumstances demonstrate strong profibrinolytic effects *in vitro.* Unfortunately these nanobodies lack cross-reactivity with mouse and rat TAFI and therefore could not be evaluated *in vivo.* Therefore we developed inhibitory nanobodies towards rat TAFI and evaluate their effects in an *in vivo* mouse thromboembolism model.

VHH-rTAFI-i81 revealed, in the chromogenic assay, a strong inhibition of the T/TM-mediated rTAFI activation. However, the inhibition of the plasmin-mediated activation and the inhibition of the TAFIa activity revealed a negative percentage, consistent with increased TAFIa activity in the presence of VHH-rTAFI-i81 under these conditions. There are multiple plausible explanations for the increased activity. Firstly, it is known that plasmin is a weaker activator of TAFI, therefore after 10 min of activation with plasmin a mixture of intact and activated rTAFI is present. Stimulation of the TAFI zymogen activity by nanobodies has been described before [25] and could lead to an increased activity (activity generated by plasmin activation ànd induced zymogen activity). However, no increased zymogen activity was observed after incubation of rTAFI with VHH-rTAFI-i81 (data not shown). Secondly, it has been described [26] that plasmin proteolyses TAFI at several sites, i.e. cleavage may not only occur at Arg^{92} but also cleavage at Lys^{327} and Arg^{330}. Cleavage at Lys^{327} and Arg^{330} leads to a non-active TAFI form since the cleavage product lacks the substrate binding site and residues involved in substrate specificity and hydrolysis. Epitope mapping (by chromogenic assay and affinity analysis of different rTAFI mutants) indicates that the key amino acid for VHH-rTAFI-i81 binding (Lys^{392}) is almost 20 ångström away from Lys^{327} and Arg^{330}. Furthermore, evaluation of the plasmin-induced fragmentation pattern of rTAFI in the presence of VHH-rTAFI-i81 does not indicate any changes in fragmentation pattern. It can therefore be concluded that the observed increase in TAFIa activity, upon plasmin-mediated

activation in the presence of VHH-rTAFI-i81 is not due to an impaired cleavage at positions 327 or 330. Thirdly, rTAFIa is very thermally unstable with a half-life of around 2.5 min at 37°C. Therefore, an increased activity, observed upon plasmin-mediated activation in the presence of VHH-rTAFI-i81 could be due to a stabilizing effect of VHH-rTAFI-i81 on rTAFIa. Indeed, the half-life of rTAFIa activity was strongly increased (10-fold in the presence of an equimolar concentration of VHH-rTAFI-i81) by VHH-rTAFI-i81. The TAFIa stabilizing properties of VHH-rTAFI-i81 explain the apparent negative percentage of inhibition in the chromogenic assays (Table 4.1). The key amino acid for binding, Lys^{392}, is in close proximity of the dynamic flap region (AA 296-350) (Figure 4.6) and the mobility of this region is important for the instability of TAFIa [27]. It is therefore tempting to speculate that the observed increased TAFIa stability induced by VHH-rTAFI-i81 is attributed to stabilization of the dynamic flap region. Of note, an active-site inhibitor, GEMSA, has also been shown to stabilize TAFIa through stabilization of the dynamic flap region. In the latter case, interaction with the dynamic flap region occurs through residues within the active-site pocket [27].

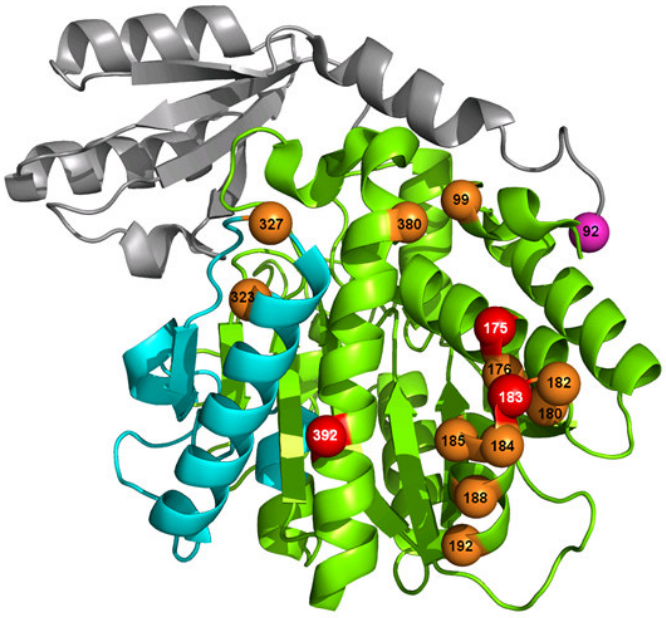

Figure 4.6: Three-dimensional structure of thrombin-activatable fibrinolysis inhibitor and localization of the screened amino acids. Ribbon drawing of the structure of TAFI with the catalytic domain in green, activation peptide in grey and the dynamic flap region (AA 296-350) in blue. Screened amino acids for which mutation had no effect on the VHH-rTAFI-i81 induced inhibition of T/TM-mediated activation of rTAFI are depicted as orange spheres, amino acids for which mutation resulted in an impaired VHH-rTAFI-i81 induced inhibition of the T/TM-mediated activation and resulted in a reduced affinity for VHH-rTAFI-i81 are shown as red spheres. The Arg^{92}, cleavage site for the release of the activation peptide is depicted in purple.

It should be noted that the molecular mechanism of inhibition of the T/TM-mediated activation of rTAFI by VHH-rTAFI-i81 is difficult to explain since the binding region is not in very close proximity of the Arg^{92} cleavage site. However, a study by Marx *et al.* already described that the region were VHH-rTAFI-i81 is binding (Tyr^{175}, Glu^{183} and Lys^{392}) is important in the activation of TAFI [28]. They demonstrated that mutations at position 182 and 183 in human TAFI decreased the rate of activation by thrombin and the complex thrombin/thrombomodulin 2-3 fold. Accordingly, these mutations led to a six-fold reduced antifibrinolytic potential, demonstrating that these residues may somehow be involved in the TAFI-activating process. Possibly, binding of VHH-rTAFI-i81 induces steric hindrance or allosteric changes resulting in a non-optimal positioning of TAFI for T/TM-mediated activation.

The characterization and identification of the various effects of VHH-rTAFI-i81 on TAFI adds to previous observations that the development of TAFI(a) inhibitors should take into considerations many possible effects on TAFI(a). Indeed, reversible active-site inhibitors [6, 29] have been shown to stabilize TAFIa under certain conditions. Even though inhibition of the activation of TAFI was not expected to affect the stability of TAFIa, our current study demonstrates the opposite. Therefore caution should be taken into consideration in the development of TAFI inhibitors and a wide screening on new compounds through different TAFI assays is recommended.

Whether the partially stabilizing effect of VHH-rTAFI-i81 on the TAFIa activity may compromise its profibrinolytic activity under certain conditions cannot be fully excluded. However previous studies using stabilized TAFIa variants have demonstrated that, even though stabilization has an effect on clot lysis, this effect (prolongation of clot lysis) is relatively small [30]. According to our current experiments, the potent inhibitory activity appears to outweigh a possible stabilizing effect and overall result in a strong profibrinolytic effect in *in vitro* clot lysis as well as in the *in vivo* thromboembolism model. It is also important to note that in the *in vivo* model, VHH-rTAFI-i81 exerts a profibrinolytic effect in the absence of a thrombolytic agent. This indicates that VHH-rTAFI-i81 strongly enhances the endogenous fibrinolytic potential. A monoclonal anti-TAFI antibody, MA-TCK26D6, previously tested in the thromboembolism model in the presence of exogenous t-PA only showed a 55% reduction of fibrin deposition in the lungs [15] while VHH-rTAF-i81 reduced the fibrin deposition by 96%. The strong effect might be related to the strong affinity of VHH-rTAFI-i81 for mTAFI ($K_A = 6.8 \pm 1.2 * 10^9$) which is 10-fold higher than the affinity of MA-TCK26D6.

In conclusion, VHH-rTAFI-i81 is a very potent inhibitor of the T/TM-mediated activation of rTAFI. Even though under certain circumstances we observed TAFIa stabilizing properties of VHH-rTAFI-i81, co-administration with t-PA in an *in vitro* clot lysis assay leads to a strong enhanced profibrinolytic effect. In an *in vivo* mouse thromboembolism model VHH-rTAFI-i81 strongly reduces fibrin deposition in the absence of exogenously added t-PA.

REFERENCES

1. Bajzar L, Manuel R, Nesheim ME. Purification and characterization of tafi, a thrombin-activable fibrinolysis inhibitor. *J Biol Chem*. 1995;270:14477-14484
2. Schatteman KA, Goossens FJ, Scharpe SS, Hendriks DF. Proteolytic activation of purified human procarboxypeptidase u. *Clin Chim Acta*. 2000;292:25-40
3. Boffa MB, Bell R, Stevens WK, Nesheim ME. Roles of thermal instability and proteolytic cleavage in regulation of activated thrombin-activable fibrinolysis inhibitor. *J Biol Chem*. 2000;275:12868-12878
4. Boffa MB, Wang W, Bajzar L, Nesheim ME. Plasma and recombinant thrombin-activable fibrinolysis inhibitor (tafi) and activated tafi compared with respect to glycosylation, thrombin/thrombomodulin-dependent activation, thermal stability, and enzymatic properties. *J Biol Chem*. 1998;273:2127-2135
5. Marx PF, Hackeng TM, Dawson PE, Griffin JH, Meijers JC, Bouma BN. Inactivation of active thrombin-activable fibrinolysis inhibitor takes place by a process that involves conformational instability rather than proteolytic cleavage. *J Biol Chem*. 2000;275:12410-12415
6. Hendrickx ML, De Winter A, Buelens K, Compernolle G, Hassanzadeh-Ghassabeh G, Muyldermans S, Gils A, Declerck PJ. Tafia inhibiting nanobodies as profibrinolytic tools and discovery of a new tafia conformation. *J Thromb Haemost*. 2011;9:2268-2277
7. Zirlik A. Tafi: A promising drug target? *Thromb Haemost*. 2004;91:420-422
8. Wang YX, da Cunha V, Vincelette J, Zhao L, Nagashima M, Kawai K, Yuan S, Emayan K, Islam I, Hosoya J, Sullivan ME, Dole WP, Morser J, Buckman BO, Vergona R. A novel inhibitor of activated thrombin activatable fibrinolysis inhibitor (tafia) - part ii: Enhancement of both exogenous and endogenous fibrinolysis in animal models of thrombosis. *Thromb Haemost*. 2007;97:54-61
9. Buelens K, Hassanzadeh-Ghassabeh G, Muyldermans S, Gils A, Declerck PJ. Generation and characterization of inhibitory nanobodies towards thrombin activatable fibrinolysis inhibitor. *J Thromb Haemost*. 2010;8:1302-1312
10. Hillmayer K, Macovei A, Pauwels D, Compernolle G, Declerck PJ, Gils A. Characterization of rat thrombin-activatable fibrinolysis inhibitor (tafi)--a comparative study assessing the biological equivalence of rat, murine and human tafi. *J Thromb Haemost*. 2006;4:2470-2477
11. Hillmayer K, Brouwers E, Leon-Tamariz F, Meijers JC, Marx PF, Declerck PJ, Gils A. Development of sandwich-type elisas for the quantification of rat and murine thrombin activatable fibrinolysis inhibitor in plasma. *J Thromb Haemost*. 2008;6:132-138
12. Hillmayer K, Ceresa E, Vancraenenbroeck R, Declerck PJ, Gils A. Conformational (in)stability of rat vs. Human activated thrombin activatable fibrinolysis inhibitor. *J Thromb Haemost*. 2008;6:1426-1428
13. Vincke C. GC, Wernery U., Devoogdt N., Hassanzadeh-Ghassabeh G. and Muyldermans S. Generation of single domain antibody fragments derived from camelids and generation of manifold constructs. *Antibody engineering: Methods and protocols*. 2012:145-176.

14. Develter J, Booth NA, Declerck PJ, Gils A. Bispecific targeting of thrombin activatable fibrinolysis inhibitor and plasminogen activator inhibitor-1 by a heterodimer diabody. *J Thromb Haemost*. 2008;6:1884-1891

15. Vercauteren E, Emmerechts J, Peeters M, Hoylaerts MF, Declerck PJ, Gils A. Evaluation of the profibrinolytic properties of an anti-tafi monoclonal antibody in a mouse thromboembolism model. *Blood*. 2011;117:4615-4622

16. Hillmayer K, Vancraenenbroeck R, De Maeyer M, Compernolle G, Declerck PJ, Gils A. Discovery of novel mechanisms and molecular targets for the inhibition of activated thrombin activatable fibrinolysis inhibitor. *J Thromb Haemost*. 2008;6:1892-1899

17. De Genst E, Silence K, Ghahroudi MA, Decanniere K, Loris R, Kinne J, Wyns L, Muyldermans S. Strong in vivo maturation compensates for structurally restricted h3 loops in antibody repertoires. *J Biol Chem*. 2005;280:14114-14121

18. Declerck PJ. Thrombin activatable fibrinolysis inhibitor. *Hamostaseologie*. 2011;31:165-166, 168-173

19. Morange PE, Juhan-Vague I, Scarabin PY, Alessi MC, Luc G, Arveiler D, Ferrieres J, Amouyel P, Evans A, Ducimetiere P. Association between tafi antigen and ala147thr polymorphism of the tafi gene and the angina pectoris incidence. The prime study (prospective epidemiological study of mi). *Thromb Haemost*. 2003;89:554-560

20. van Tilburg NH, Rosendaal FR, Bertina RM. Thrombin activatable fibrinolysis inhibitor and the risk for deep vein thrombosis. *Blood*. 2000;95:2855-2859

21. Silveira A, Schatteman K, Goossens F, Moor E, Scharpe S, Stromqvist M, Hendriks D, Hamsten A. Plasma procarboxypeptidase u in men with symptomatic coronary artery disease. *Thromb Haemost*. 2000;84:364-368

22. Montaner J, Ribo M, Monasterio J, Molina CA, Alvarez-Sabin J. Thrombin-activable fibrinolysis inhibitor levels in the acute phase of ischemic stroke. *Stroke*. 2003;34:1038-1040

23. Juhan-Vague I, Morange PE, Aubert H, Henry M, Aillaud MF, Alessi MC, Samnegard A, Hawe E, Yudkin J, Margaglione M, Di Minno G, Hamsten A, Humphries SE. Plasma thrombin-activatable fibrinolysis inhibitor antigen concentration and genotype in relation to myocardial infarction in the north and south of europe. *Arterioscler Thromb Vasc Biol*. 2002;22:867-873

24. Willemse JL, Heylen E, Nesheim ME, Hendriks DF. Carboxypeptidase u (tafia): A new drug target for fibrinolytic therapy? *J Thromb Haemost*. 2009;7:1962-1971

25. Mishra N, Buelens K, Theyskens S, Compernolle G, Gils A, Declerck PJ. Increased zymogen activity of thrombin-activatable fibrinolysis inhibitor prolongs clot lysis. *J Thromb Haemost*. 2012;10:1091-1099

26. Marx PF, Dawson PE, Bouma BN, Meijers JC. Plasmin-mediated activation and inactivation of thrombin-activatable fibrinolysis inhibitor. *Biochemistry*. 2002;41:6688-6696

27. Marx PF, Brondijk TH, Plug T, Romijn RA, Hemrika W, Meijers JC, Huizinga EG. Crystal structures of tafi elucidate the inactivation mechanism of activated tafi: A novel mechanism for enzyme autoregulation. *Blood*. 2008;112:2803-2809

28. Marx PF, Havik SR, Bouma BN, Meijers JC. Role of isoleucine residues 182 and 183 in thrombin-activatable fibrinolysis inhibitor. *J Thromb Haemost*. 2005;3:1293-1300

29. Walker JB, Hughes B, James I, Haddock P, Kluft C, Bajzar L. Stabilization versus inhibition of tafia by competitive inhibitors in vitro. *J Biol Chem*. 2003;278:8913-8921

30. Ceresa E, De Maeyer M, Jonckheer A, Peeters M, Engelborghs Y, Declerck PJ, Gils A. Comparative evaluation of stable tafia variants: Importance of alpha-helix 9 and beta-sheet 11 for tafia (in)stability. *J Thromb Haemost*. 2007;5:2105-2112

Chapter 5

Development of a nanobody-based assay for activated thrombin-activatable fibrinolysis inhibitor (TAFIa)

M. L. V. HENDRICKX*, N. MOLLEKENS*, P. VERHAMME†, A. GILS* and P. J. DECLERCK*

* Laboratory for Therapeutic and Diagnostic Antibodies, Department of Pharmaceutical and Pharmacological Sciences, KU Leuven, † Molecular and Vascular Biology, Department of Vascular Medicine, University Hospitals Leuven, Belgium

Arterioscler Thromb Vasc Biol., submitted

SUMMARY

Background: Many ELISAs have been developed to measure TAFI antigen levels. However, not the total antigen levels but the amount of activated TAFI (TAFIa) represents the enzymatic activity essential for its biological function. Previously reported ELISAs to quantify TAFIa demonstrate cross-reactivity with $TAFIa_i$, an inactivated TAFIa form.

Objective: Development of a human TAFIa specific ELISA and quantitation of TAFIa levels in plasma from patients who suffered from venous thromboembolism.

Methods and results: A sandwich-type ELISA was developed based on a highly selective TAFIa nanobody for capture and a HRP-conjugated monoclonal antibody directed against TAFI for detection. The assay demonstrated equal response to all four naturally occurring TAFIa isoforms and did not react with $TAFIa_i$. An excellent correlation between the response in ELISA and the generated TAFIa activity, as determined by chromogenic assay, is observed with purified recombinant TAFI as well as during *in vitro* clot lysis. Analyzing plasma samples revealed that patients with a history of a venous thrombotic event have significantly higher TAFIa levels compared to healthy controls.

Conclusion: An ELISA specifically detecting TAFIa was developed. The ELISA is a useful tool to quantify TAFIa in different settings.

INTRODUCTION

TAFIa, encoded by the *CPB2* gene, is a metallocarboxypeptidase which is generated upon activation of the TAFI zymogen (56 kDa) by trypsin-like enzymes such as thrombin, plasmin or the thrombin/thrombomodulin complex. The activation consists of proteolytical cleavage of the Arg^{92}-Ala^{93} bond resulting in the release of the activation peptide (20 kDa; Phe^{1}-Arg^{92}) from the active protease moiety, TAFIa (36 kDa; Ala^{93}-Val^{401})[1-4]. Four naturally occurring isoforms exist with on position 147 either Ala or Thr and on position 325 Ile or Thr. The polymorphism at position 325 influences the half-life of TAFIa, the Thr^{325}-isoform is characterized with a half-life of 8 min at 37°C whereas the Ile^{325}-isoform has a half-life of 15 min at 37°C [5]. This temperature-dependent instability is the consequence of a conformational change resulting in the formation of an inactive TAFIa form, TAFIai [4, 6].

Clinical studies have demonstrated elevated levels of TAFI in cardiovascular diseases such as angina pectoris [7], venous thrombosis [8], coronary artery disease [9] and ischemic stroke [10]. However, all of the studies were based on total TAFI antigen levels. Two monoclonal antibody-based ELISAs to determine the released activation peptide and to determine TAFIa/TAFIai were developed by Ceresa *et al.* [11] and demonstrated higher plasma levels of both the activation peptide and TAFIa/TAFIai in patients with hyperlipidemia compared to healthy individuals. There was no difference in total TAFI antigen levels between the two groups. Using another ELISA, based on capture by potato tuber carboxypeptidase inhibitor (PTCI) and detecting both TAFIa and TAFIai [12] elevated levels of TAFIa/TAFIai were observed in sepsis patients [13]. Alternatively, TAFIa can be determined through its activity, e.g. by its capacity to convert hippuryl-arginine to hippuric acid, which can subsequently be detected by a colorimetric reaction [14]. A TAFIa assay based on the fact that TAFIa decreases the cofactor activity of high-molecular-weight fibrin degradation products in the stimulation of plasminogen cleavage was also developed [15]. These functional assays however lack sufficient sensitivity and specificity [14] or require the use of reagents that are not generally available [15] thereby excluding implementation in a routine clinical setting.

Besides conventional antibodies, the serum of *Camelidae* contains considerable amounts of unique antibodies, naturally devoid of the light chain and lacking the CH1-domain [16]. These functional antibodies, termed heavy chain antibodies, bind their targets by a single domain, i.e. the variable domain of the heavy-chain antibodies (VHH) or Nanobody [17]. Many VHHs show longer CDR3s (complementarity determining regions 3), often forming an extended loop which is

stabilized by a disulfide bridge. The potent enzyme binding properties of VHHs are ascribed to this protruding paratope [18]. TAFIa binding nanobodies that specifically bind in the catalytic cleft of active TAFIa have been characterized [19]. In the current study we exploited their high selectivity for TAFIa for the development of a sandwich-type ELISA in which such a nanobody is used as capture.

MATERIAL AND METHODS

Materials

Recombinant TAFI-T^{147}-I^{325} (TAFI-TI), TAFI-A^{147}-I^{325} (TAFI-AI), TAFI-T^{147}-T^{325} (TAFI-TT), TAFI-A^{147}-T^{325} (TAFI-AT) were produced as described before [20]. All the experiments were performed with TAFI-TI unless indicated otherwise. Five nanobodies towards TAFIa and 29 HRP-conjugated monoclonal antibodies towards TAFI were produced as described [19, 21-23]. Human thrombin was purchased from Sigma-Aldrich. Rabbit thrombomodulin (TM) was obtained from American Diagnostics (Greenwich, CT, USA). H-D-phenylalanine-L-propyl-L-arginine chloromethyl ketone (PPACK), hippuryl-L-arginine and potato tuber carboxypeptidase inhibitor (PTCI) were obtained from Biomol Research labs (Plymouth PA, USA), Bachem (Bubendorf, Switzerland) and Sigma-Aldrich respectively. Tissue-type plasminogen activator (t-PA) was a kind gift from Boehringer Ingelheim (Brussels, Belgium). A citrated human plasma pool (26 healthy volunteers), collected with their written consent, was prepared in-house and stored at -80°C. TAFI-depleted plasma (TDP) was prepared from the human plasma pool as described before [20].

Construction of a sandwich type ELISA for the detection of TAFIa.

Nanobodies were diluted to 4 µg/mL in PBS (140 mM NaCl, 2.7 mM KCl, 8 mM Na_2HPO_4 and 1.5 mM KH_2PO_4, pH 7.4). Two hundred µL of this solution was transferred in each well of a polystyrene microtiter plate (Costar) and incubated for 72 h at 4°C. Subsequently, the plates were emptied and incubated with PBS containing albumin (1%) for 2 hours at room temperature. Then, the plates were washed with PBS containing 0.002% Tween 80 (PBS-Tween) and incubated with 200 µL/well storage solution (100 g/L mannitol and 20 g/L saccharose in water). After 4 min the wells are emptied and the plates stored at -20 °C. Immediately before use, the plates are washed with PBS-Tween. Samples were diluted in PBS containing 0.002% Tween 80 and 1 g/L BSA (PTA) by serial two-fold dilutions and applied on the plate (180 µL) at 4 °C for approximately 18 h. Subsequently the plate was washed with PBS-Tween. Then, the wells were filled with 170 µL of a HRP-conjugated monoclonal antibody (diluted 1:2000) in PTA, and incubated for 2 h at room temperature. The plates were washed with PBS-Tween and 160 µL of a citrate buffer buffer (0.1 M sodiumcitrate and 0.2 M sodiumphosphate, pH 5.0) containing 400 µg/mL o-phenylenediamine and 0.003% hydrogen peroxide was added. After 1 h at room temperature the reaction was stopped by addition of 50 µl of 4 M H_2SO_4. The absorbance was measured at 492 nm with an EL808 Ultra Microplate Reader (Bio-Tek instruments Inc).

Calibration was performed based on an in-house TAFIa standard which was prepared by activation of TAFI-TI (concentration during activation 90 nM) by thrombin and thrombomodulin (T/TM, 20 and 5 nM respectively) in the presence of $CaCl_2$ (5 mM) at 25 °C for 10 min. The activation was arrested by PPACK (37.5 µM) and fractions were frozen at -80 °C. The TAFIa standard is diluted in PTA to 360 pM followed by serial two-fold dilutions.

The activity of the TAFIa standard was determined in a chromogenic assay using hippuryl-arginine 4 mM (at 25 °C for 15 min). The substrate reaction was arrested by HCl (1 M), neutralized by NaOH (1 M) and buffered with Na_2HPO_4 (1 M, pH 7.4). After addition of 6% cyanuric chloride (in 1,4-dioxane), the mixture was vortexed (5 min) and centrifuged (Eppendorf centrifuge 5415D) at maximal speed for 2 min. Then, aliquots of 100 µL were transferred into a 96-well microtiterplate and the absorbance was measured at 405 nm. The TAFIa activity was determined based on a hippuric acid standard curve. One unit (U) carboxypeptidase activity is defined as the amount of enzyme converting 1 micromole of substrate per minute at 25°C.

Reactivity of different TAFIa isoforms and TAFI(a) variants in the TAFIa ELISA

Recombinant TAFI isoforms (TAFI-TI, TAFI-TT, TAFI-AT and TAFI-AI) were activated as described for the TAFIa standard. Subsequently one fraction was used to quantitate TAFIa antigen by the ELISA, another fraction was used to quantitate the TAFIa activity by the chromogenic assay. Cross-reactivity of the ELISA with intact TAFI was evaluated using TAFI-TI prior to activation as well as using a non-activatable TAFI mutant (TAFI-R92A) [24]. In addition, reactivity with human carboxypeptidase N (30 nM) was also tested.

Evaluation of the effect of conformational inactivation of TAFIa to TAFIai on the reactivity in the TAFIa ELISA

TAFI (428.5 nM, concentration during activation) was diluted in Tris buffer (20 mM Tris, 0.1 M NaCl; pH 7.4) and activated at 37 °C for 10 min by T/TM (20 nM and 5 nM, respectively) in the presence of $CaCl_2$ (5 mM). The activation was stopped by addition of 30 µM PPACK and the mixture was incubated at 37°C. Fractions were taken after different incubation periods (0, 5, 10, 20, 30 and 60 min) and placed on ice. Subsequently, fractions were analyzed in the TAFIa ELISA and in the chromogenic TAFIa activity assay as described above.

Comparison of the reactivity of plasma, before and after activation of TAFI by T/TM, in the TAFIa ELISA

Pooled human plasma was diluted (1/50) in HEPES buffer (25 mM HEPES, 137 mM NaCl, 3.5 mM KCl, pH 7.4 in the presence of 0.1% BSA). Fifty microliters of this dilution was incubated (25 °C for 10 min) with T/TM (both 8 nM) in the presence of $CaCl_2$ (concentrations during activation 6.8 mM). The activation was arrested by addition of PPACK (38 μM). The samples were tested in the ELISA at a final plasma dilution of 1/500 followed by a two-fold dilution series in PTAE buffer (PTA buffer containing 5 mM of EDTA). Also "non-activated" plasma, subjected to an identical final dilution was tested in the ELISA.

Recovery experiments

TAFI (10 μg/ml or 2 μg/ml) was added to TAFI depleted plasma (TDP) or HEPES buffer, samples were diluted (1/50) and activated by T/TM (both 8 nM) in the presence of 6.8 mM $CaCl_2$. The activation (at 25°C for 10 min) was arrested by PPACK (38 μM). The samples were then added to the plate (final plasma dilution 1/500) followed by serial two-fold dilutions in PTAE buffer. Recovery was calculated based upon a comparison of the response in plasma and HEPES buffer.

To evaluate the recoveries of low amounts of activated TAFI, 75 pM TAFIa or TAFIa-CIIYQ (a stable TAFIa mutant with a 180-fold increased stability [25]) was added to diluted plasma (1/8 to 1/512 dilution, 2-fold dilution series) or to buffer. The response observed in spiked plasma was corrected for the base-line response of plasma at the corresponding dilution. This corrected response was then compared to the response in buffer to calculate recoveries.

TAFIa during *in vitro* clot lysis

Clot lysis experiments were performed in microtiterplates as described before [11] with minor modifications. Turbidity, TAFIa antigen levels and TAFIa activity were measured during clot lysis. Therefore, pooled plasma (final concentration 30 %) was diluted in buffer (20 mM HEPES, 0.01% Tween 20; pH; 7.4), TM (0.5 nM) and t-PA (final concentration 480 pM) were added. Clot formation was induced by addition of $CaCl_2$ (final concentration 10.6 mM). This reaction mixture was made in duplicate: one was used to determine the change in turbidity every 2 min at 405 nm (EL808 Ultra Microplate Reader (Bio-Tek instruments Inc)). The other was used to aliquot samples at different time points and to stop the reaction by addition of PPACK (final concentration 46 μM) and aprotinin (1.28 μM). Then, the samples were placed on ice and TAFIa antigen was quantitated by the ELISA and TAFIa activity was quantitated by the chromogenic

assay (substrate conversion was allowed for 30 min at 25°C). To correct for the enzymatic activity of carboxypeptidase N in plasma, substrate conversion was also performed in the presence of PTCI (final concentration: 3 mM) and values obtained in the presence of PTCI were subtracted from the values obtained in the absence of PTCI in order to obtain the specific TAFIa activity.

TAFIa, activation peptide and intact TAFI levels in plasma of healthy individuals

Blood of 20 healthy individuals (10 female, 10 male; age between 22 and 55 years, average 35), was collected with their written consent. Blood was placed on ice until further processing. Plasma was prepared by centrifugation at 3500 rpm (Jouan CR412) for 20 min at 4°C and stored at -80°C. The plasma samples were analyzed on three different ELISAs: MA-T12D11/MA-T18A8-HRP for the quantitation of the activation peptide, MA-T12D11/MA-T30E5A2-HRP for the quantitation of intact TAFI and VHH-TAFI-i391/MA-TCK26D6-HRP for the quantitation of TAFIa. Samples were appropriately diluted: ¼ in PTAE for quantification of TAFIa and the activation peptide and 1/160 in PTAE for intact TAFI. The activation peptide ELISA was calibrated based on the TAFIa standard, described above, assuming the presence of 360 pM of activation peptide.

To evaluate potential *ex vivo* TAFI activation upon blood collection, blood was collected on citrate (BD Vacutainer 0.109 M sodium citrate) in the presence or absence of PPACK (7 µM, thrombin inhibitor) and aprotinin (8 µM, plasmin inhibitor).

Evaluation of TAFIa in venous thromboembolism patients

Eighty-eight patients diagnosed with a venous thrombotic event were included (average age 49 years, average days between diagnosis and blood sample: 253 days). A control group comprised 86 healthy individuals with no history of thrombosis (average age 35 years). Blood samples were collected in BD Vacutainer tubes (3.2% buffered sodium citrate) and plasma was prepared by centrifugation at 2000 rpm at 4°C for 20 min and stored at -20 °C until analysis. TAFIa levels were quantitated as described above and expressed relative to a plasma pool of healthy controls, prepared from blood obtained from 29 healthy individuals and processed and stored under conditions identical to those of the study samples. All patients gave written consent to participate in the IRB-approved “Vlaamse Erfelijkheidsstudie Crohn en Colitis ulcerosa” (VLECC), registry (B322201213950S53684).

Statistical analysis

Quantitative data are presented as mean ± standard deviation (SD). Statistical analysis (paired/unpaired t-test and Mann Whitney test) were performed by GraphPad Prism (GraphPad Prism 5 Software).

RESULTS

Five nanobodies, used as capture, were pair-wise tested with 29 HRP-conjugated monoclonal antibodies for detection. Based on the high affinity of VHH-TAFI-i391 for TAFIa [19] and the good sensitivity and linear response to TAFIa when used in combination with the well characterized MA-TCK26D6 [23], this pair was selected for the development of an ELISA for the detection of TAFIa.

Reactivity of different TAFIa isoforms and TAFI(a) variants in the ELISA

A linear dose-response between 11 and 180 pM was observed for all TAFIa isoforms (TAFIa-TI, TAFIa-AT, TAFIa-AI and TAFIa-TT). To evaluate the relationship between TAFIa antigen determined by the ELISA and TAFIa activity determined by chromogenic assay, both values obtained for the various isoforms were compared (Figure 5.1).

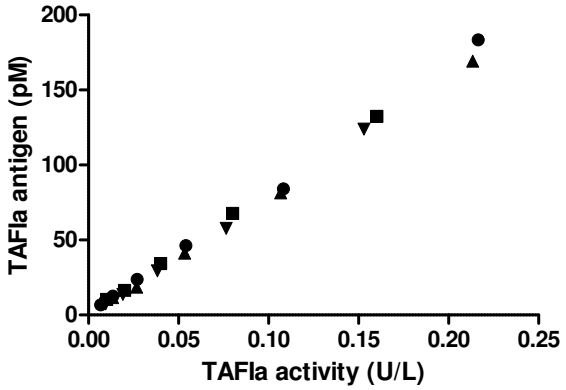

Figure 5.1: Correlation between TAFIa antigen levels and TAFIa activity. For the different TAFIa isoforms (TAFIa-TI ●, TAFIa-AT ■, TAFIa-AI ▲ and TAFIa-TT ▼) TAFIa antigen levels are determined by the TAFIa ELISA and TAFIa activity by a chromogenic assay. A representative experiment out of three performed experiments is shown.

The slopes for TAFIa-TI, TAFIa-AT, TAFIa-AI and TAFIa-TT were 0.83 ± 0.02, 0.82 ± 0.01, 0.79 ± 0.01 and 0.81 ± 0.02 nmol/U , respectively and demonstrate a similar response for all TAFIa isoforms. The coefficients of determination exceed 0.99. The limit of detection (LOD) is 22.5 pM.

Recombinant intact TAFI revealed a response of 0.54 ± 0.05 % compared to that of TAFIa (Figure 5.2, panel A). To determine whether this small response was due to an intrinsic cross-reactivity of intact TAFI or due to the presence of small amounts of activated TAFI, a TAFI mutant (TAFI-R92A), which cannot be activated to TAFIa, was also included. The response of TAFI-R92A was 30-fold higher compared to that of intact 'wild-type' TAFI but did not change upon treatment of TAFI-R92A with T/TM. No reactivity was observed for CPN up to 30 nM.

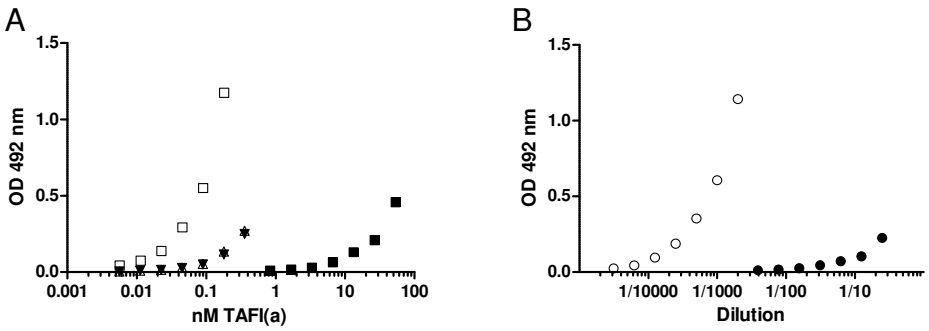

Figure 5.2: Response of different TAFI variants (panel A) and response of activated and non-activated plasma (panel B) in the ELISA. Difference in response between non-activated TAFI (■), activated TAFI (□) and TAFI-R92A before (▼) and after activation (△) in the ELISA (panel A). Reactivity of plasma (panel B) before (●) and after (○) TAFI activation. A representative experiment out of three performed experiments is shown.

Activation of TAFI in plasma resulted in TAFIa levels of 274 ± 15 nM. Non-activated plasma revealed a response of 0.13 ± 0.04 % versus activated plasma (Figure 5.2, panel B).

Evaluation of the effect of conformational inactivation of TAFIa to TAFIai on the reactivity in the ELISA

Incubation of TAFIa at 37°C results in loss of response in the TAFIa ELISA (Figure 5.3, panel A, full line). This loss in antigenic response coincides with the loss of activity (Figure 5.3, panel A, dashed line) indicating that the ELISA only reacts with TAFIa and not with TAFIai. The half-life for the loss of binding in the ELISA was 8.9 ± 3.3 min. The half-life of TAFIa activity, as determined by the chromogenic assay, was 8.5 ± 0.6 min.

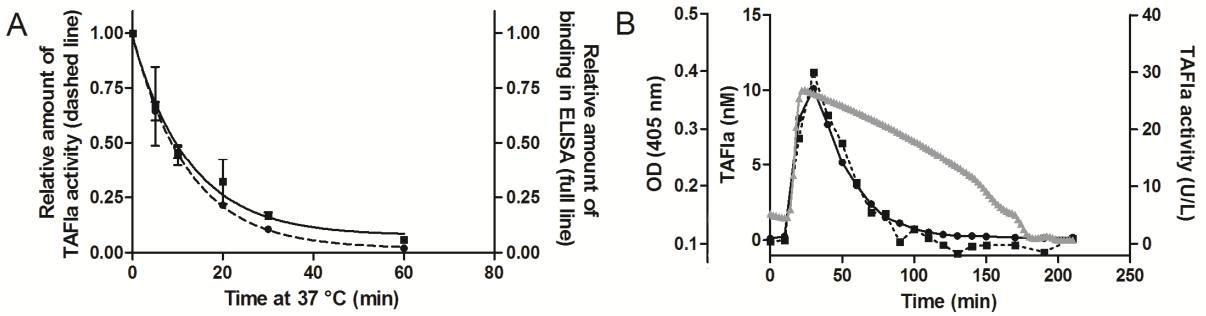

Figure 5.3: Effect of inactivation of TAFIa on reactivity in the ELISA and TAFIa activity (panel A) and generation of TAFIa activity during clot formation and lysis (panel B). Residual binding of TAFIa in the ELISA (full square, full line) and concomitant TAFIa activity (full circle, dashed line) after incubation of TAFIa for different time periods at 37°C (mean ± SD, n = 3) (panel A). A representative clot lysis profile (OD (405 nm); grey triangles) and concomitant TAFIa values determined by the TAFIa ELISA (TAFIa (nM); full circle, full line) and chromogenic assay (TAFIa (U/L); full square, dashed line) is shown (panel B).

Recovery experiments

Addition of TAFI to TAFI-depleted plasma followed by activation revealed a recovery of 104.7 ± 9.2 % and 97.4 ± 12.1 % for 10 µg/ml and 2 µg/ml TAFI respectively. Experiments with 10 µg/ml TAFI showed an intra-assay coefficient of variation of 7.4 % and an inter-assay variability of 8.8 %. Experiments with 2 µg/ml TAFI showed an intra-assay coefficient of variation of 10.6 % and an inter-assay variability of 12.5 %. The interdilution coefficients of variation were 7.5 % (n = 5; serial 2-fold dilutions) and 11.7 % (n = 3; serial 2-fold dilutions) for 10 µg/ml and 2 µg/ml TAFI, respectively.

Addition of 75 pM TAFIa to 1/8 diluted plasma resulted in a recovery of 20 ± 5 % for TAFIa-TI and 31 ± 5 % for TAFIa-CIIYQ. Recoveries increased gradually when using plasma at a higher dilution, reaching a plateau (59 % and 97 % for TAFIa-TI and TAFIa-CIIYQ, respectively) at a 1/128 dilution.

TAFIa during *in vitro* clot lysis

Generation of TAFIa antigen and activity was monitored during *in vitro* clot lysis. A good correlation (r = 0.98) was observed between TAFIa antigen as determined by the TAFIa ELISA and TAFIa activity as determined with the chromogenic assay (Figure 5.3, panel B). The maximal response in the ELISA as well as maximal TAFIa activity was observed 30 min after clot formation and corresponds to a TAFIa antigen concentration around 10 nM and a TAFIa activity of 30 U/L.

TAFIa, activation peptide and intact TAFI levels in healthy individuals

In plasma from 20 healthy individuals, levels of TAFIa, activation peptide and intact TAFI were 457 pM (median; interquartile range = 332 pM to 708 pM), 335 pM (median; interquartile range

= 225 pM to 720 pM) and 106 nM (median; interquartile range = 97 nM to 129 nM), respectively. There was no correlation between the amount of TAFIa and activation peptide (Pearson r = 0.19, p = ns), TAFI and TAFIa (Pearson r = 0.09, p = ns) and TAFI and activation peptide (Pearson r = -0.03, p = ns) in plasma (Figure 5.4, panels A, B and C, repsectively).

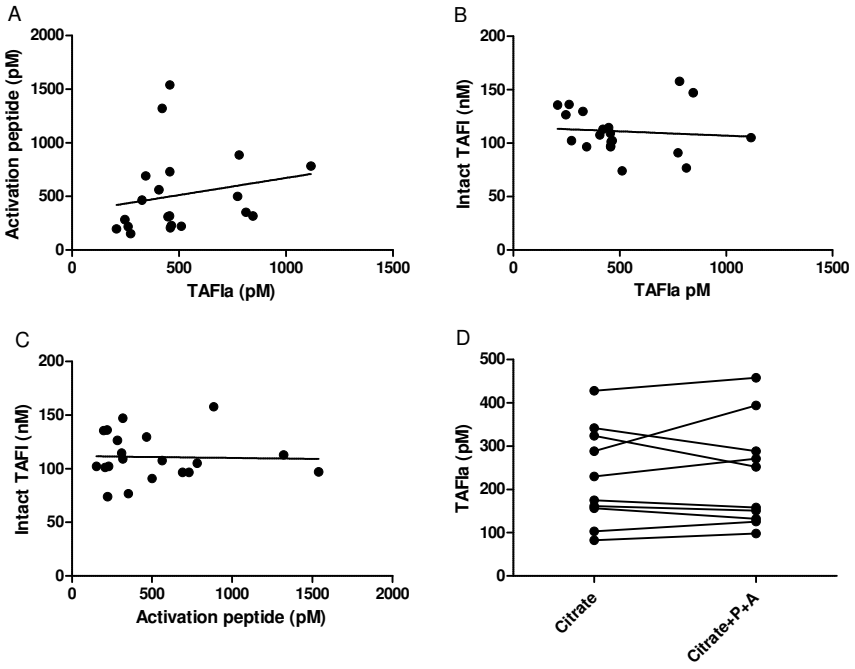

Figure 5.4: Correlations between different TAFI derivatives in plasma (A, B, C) and impact of different blood collections on plasma TAFIa levels (D). Correlation between levels of activation peptide and TAFIa (panel A), intact TAFI and TAFIa (panel B) and intact TAFI and activation peptide (panel C) in plasma of 20 healthy volunteers. Full lines represent linear regressions (panel A, B and C). Plasma TAFIa levels upon blood collection on citrate either in the absence or in the presence of PPACK (P) and aprotinin (A) (panel D).

Furthermore no correlation was observed between TAFIa levels and age and no significant difference was observed in TAFIa levels between male and female (unpaired t-test). There was no significant difference (paired t-test) in TAFIa levels in plasma prepared from blood collected in the presence or absence of PPACK and aprotinin, thereby excluding *ex vivo* activation of TAFI upon blood collection (Figure 5.4, panel D).

Evaluation of TAFIa in venous thromboembolism patients

TAFIa levels in plasma from HC were 93.3 % (median; interquartiles: 59.3 % to 146.7 %) whereas TAFIa levels in plasma from patients with a history of VTE were significantly higher 171.7 % (median; interquartiles: 104.9 % to 279.8 %) (Mann Whitney $p < 0.0001$) (Figure 5.5).

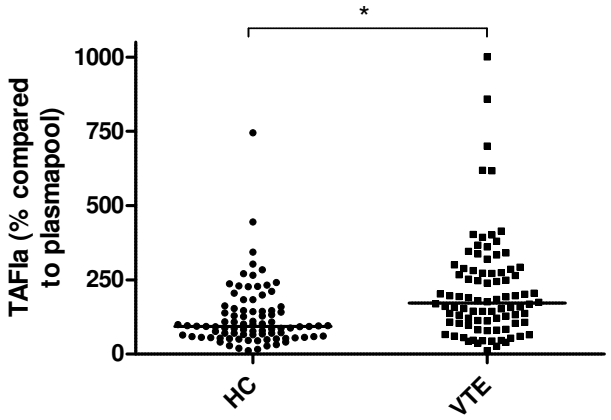

Figure 5.5: TAFIa levels in venous thromboembolism. TAFIa levels in healthy controls (HC) and venous thromboembolism patients (VTE) (* Mann Whitney: $p < 0.0001$).

There was no correlation between TAFIa levels and age in the HC and the VTE group. A significant difference in TAFIa levels was observed between male and female in the HC group (126 % and 92 %, respectively; $p < 0.05$, unpaired t-test), but not in the VTE group (160 % and 176 % for male and female, respectively).

DISCUSSION

TAFIa is formed upon proteolytical cleavage of TAFI by T, T/TM or plasmin and exerts an antifibrinolytic effect. However, TAFIa is thermally unstable and undergoes conformational changes to TAFIai. All reported TAFIa ELISAs cross-react with inactive TAFIai. Since TAFIa is responsible for the enzymatic activity, measurement of TAFIa levels instead of intact TAFI is believed to be more relevant for studies on the association between TAFI(a) and cardiovascular diseases. Further evidence suggesting that measuring TAFIa instead of TAFI is more relevant is provided by the threshold dependent mechanism of TAFI. The principle of this mechanism implies that not the total amount of TAFI but the amount of TAFIa is critical in fibrinolysis [26].

Therefore, we have developed a highly selective TAFIa ELISA without cross-reactivity with TAFIai. Indeed, simultaneous TAFIa activity determination by hippuryl-arginine and TAFIa antigen quantification in the ELISA, after incubation of TAFIa for different time periods at 37°C, demonstrate an excellent correlation between the loss of activity and the loss of TAFIa antigen detection (Figure 5.3, panel A). ELISAs for TAFI often exhibit different reactivities towards different TAFI isoforms [20]. The currently described TAFIa ELISA shows an equal response to all four naturally occurring TAFIa isoforms. A 0.5 % response was found for intact TAFI suggesting a small degree of cross-reactivity of intact TAFI in the TAFIa ELISA. However, the apparent cross-reactivity is in contradiction with the observation that VHH-TAFI-i391 only binds to TAFIa and not to TAFI in a Biacore setup [19]. The cross-reactivity might be related to the reported zymogen activity of TAFI [27] since the TAFI-R92A mutant with a 5-fold increased zymogen activity [24] also demonstrated and increased response in the ELISA. However, comparison between “activated” and “non-activated” plasma demonstrate a reactivity in the TAFIa ELISA of only 0.13 % (before versus after activation). This apparent reactivity of “non-activated” plasma in the TAFIa ELISA can be due to either a cross-reactivity with intact TAFI or the presence of baseline levels of TAFIa or a combination of both. Indeed, it has been reported that besides intact TAFI also baseline levels of TAFIa are present in plasma [15], therefore the apparent cross-reactivity between TAFI and TAFIa is most likely an over estimation and the real cross-reactivity is most likely very low. Since no correlation is observed between intact TAFI and TAFIa in plasma of healthy volunteers, a significant contribution of “cross-reactive” intact TAFI from plasma in the TAFIa ELISA can be excluded. The cross-reactivity of 0.5% as observed between intact and activated TAFI might indeed be an *in vitro* artifact observed for recombinantly produced and purified TAFI.

The LOD (limit of detection) of the TAFIa ELISA described in this manuscript (22.5 pM) is comparable to the other antigen-based assays (LOD around 27 pM [28]) and only slightly higher compared to the TAFIa activity-based assays (LOD around 10 pM [15, 29]). Using our TAFIa ELISA, an average of 500 pM TAFIa was found in plasma of 20 healthy volunteers. Other studies using different assays report a broad range of average TAFIa levels in plasma: from no TAFIa [29] and very low TAFIa levels (20 pM) [15] in TAFIa activity-based assays, up to 450 pM [12] and 2300 pM [28] in TAFIa/TAFIai antigen-based assays. The reason for the discrepancy in TAFIa levels determined by either functional assays or antigen-based assays can only be partially explained by the cross-reactivity of the antigen-based assays with TAFIai.

The recovery experiments in which intact TAFI was added to TAFI-depleted plasma at "physiological" concentration and subsequently activated yielded good recoveries. However, spiking of TAFI-depleted plasma with low concentrations (75 pM) of TAFIa gave very poor recoveries. Plasma proteins interacting with TAFIa have been described (plasminogen and fibrinogen) [30], however they only had a minor influence on the poor recovery (data not shown). Even though the reason for the poor recovery is still unknown, experiments with an activated stable TAFIa mutant (TAFIa-CIIYQ) [25] yielded better recoveries suggesting that the intrinsic instability of TAFIa might be involved. To avoid reporting ambiguous absolute TAFIa antigen levels, TAFIa levels of the VTE study are therefore expressed relatively compared to the response of a plasma pool.

Analysis of plasma samples from VTE patients demonstrate significantly increased levels of TAFIa compared to a control group (HC). This might suggest that individuals with higher TAFIa levels might have an increased risk for a venous thrombotic event but should be confirmed by prospective studies. It should be noted that the blood samples were collected on average 253 days after the incidence of the thrombotic event, thereby excluding that the high TAFIa levels would merely be the consequence of TAFI activation during the thrombotic event. Even though the mean age of the patients in the VTE group is more than 10 years higher compared to the HC group, we anticipate that this is not the reason for the elevated TAFIa levels since no correlation between TAFIa levels and age was observed in neither of the two groups.

In conclusion, to the best of our knowledge this is the first report on a TAFIa ELISA without cross-reactivity with TAFIai. Application of the ELISA in different settings (purified TAFIa, clot lysis assay and plasma samples) allowed reliable quantitation of TAFIa levels. In addition, elevated levels of

TAFIa were detected in VTE patients. The simplicity of the use of this ELISA can facilitate further research on the role of TAFIa in different pathophysiological conditions.

REFERENCES

1. Bajzar L, Manuel R, Nesheim ME. Purification and characterization of tafi, a thrombin-activable fibrinolysis inhibitor. *J Biol Chem*. 1995;270:14477-14484
2. Schatteman KA, Goossens FJ, Scharpe SS, Hendriks DF. Proteolytic activation of purified human procarboxypeptidase u. *Clin Chim Acta*. 2000;292:25-40
3. Boffa MB, Bell R, Stevens WK, Nesheim ME. Roles of thermal instability and proteolytic cleavage in regulation of activated thrombin-activable fibrinolysis inhibitor. *J Biol Chem*. 2000;275:12868-12878
4. Boffa MB, Wang W, Bajzar L, Nesheim ME. Plasma and recombinant thrombin-activable fibrinolysis inhibitor (tafi) and activated tafi compared with respect to glycosylation, thrombin/thrombomodulin-dependent activation, thermal stability, and enzymatic properties. *J Biol Chem*. 1998;273:2127-2135
5. Schneider M, Boffa M, Stewart R, Rahman M, Koschinsky M, Nesheim M. Two naturally occurring variants of tafi (thr-325 and ile-325) differ substantially with respect to thermal stability and antifibrinolytic activity of the enzyme. *J Biol Chem*. 2002;277:1021-1030
6. Marx PF, Hackeng TM, Dawson PE, Griffin JH, Meijers JC, Bouma BN. Inactivation of active thrombin-activable fibrinolysis inhibitor takes place by a process that involves conformational instability rather than proteolytic cleavage. *J Biol Chem*. 2000;275:12410-12415
7. Morange PE, Juhan-Vague I, Scarabin PY, Alessi MC, Luc G, Arveiler D, Ferrieres J, Amouyel P, Evans A, Ducimetiere P. Association between tafi antigen and ala147thr polymorphism of the tafi gene and the angina pectoris incidence. The prime study (prospective epidemiological study of mi). *Thromb Haemost*. 2003;89:554-560
8. van Tilburg NH, Rosendaal FR, Bertina RM. Thrombin activatable fibrinolysis inhibitor and the risk for deep vein thrombosis. *Blood*. 2000;95:2855-2859
9. Silveira A, Schatteman K, Goossens F, Moor E, Scharpe S, Stromqvist M, Hendriks D, Hamsten A. Plasma procarboxypeptidase u in men with symptomatic coronary artery disease. *Thromb Haemost*. 2000;84:364-368
10. Juhan-Vague I, Morange PE, Aubert H, Henry M, Aillaud MF, Alessi MC, Samnegard A, Hawe E, Yudkin J, Margaglione M, Di Minno G, Hamsten A, Humphries SE. Plasma thrombin-activatable fibrinolysis inhibitor antigen concentration and genotype in relation to myocardial infarction in the north and south of europe. *Arterioscler Thromb Vasc Biol*. 2002;22:867-873
11. Ceresa E, Brouwers E, Peeters M, Jern C, Declerck PJ, Gils A. Development of elisas measuring the extent of tafi activation. *Arterioscler Thromb Vasc Biol*. 2006;26:423-428
12. Hulme John P. ASSA. Detecting activated thrombin activatable fibrinolysis inhibitor (tafia) and inactivated tafia (tafiai) in normal and hemophilia a plasmas *Bull Korean Chem Soc*. 2009;30:77-82
13. Park R SJ, An SS. Elevated levels of thrombin-activatable fibrinolysis inhibitor in patients with sepsis. *Korean J Hematol*. 2010;45:264-268
14. Mosnier LO, von dem Borne PA, Meijers JC, Bouma BN. Plasma tafi levels influence the clot lysis time in healthy individuals in the presence of an intact intrinsic pathway of coagulation. *Thromb Haemost*. 1998;80:829-835

15. Neill EK, Stewart RJ, Schneider MM, Nesheim ME. A functional assay for measuring activated thrombin-activatable fibrinolysis inhibitor in plasma. *Anal Biochem*. 2004;330:332-341

16. Hamers-Casterman C, Atarhouch T, Muyldermans S, Robinson G, Hamers C, Songa EB, Bendahman N, Hamers R. Naturally occurring antibodies devoid of light chains. *Nature*. 1993;363:446-448

17. Muyldermans S, Atarhouch T, Saldanha J, Barbosa JA, Hamers R. Sequence and structure of vh domain from naturally occurring camel heavy chain immunoglobulins lacking light chains. *Protein Eng*. 1994;7:1129-1135

18. Lauwereys M, Arbabi Ghahroudi M, Desmyter A, Kinne J, Holzer W, De Genst E, Wyns L, Muyldermans S. Potent enzyme inhibitors derived from dromedary heavy-chain antibodies. *EMBO J*. 1998;17:3512-3520

19. Hendrickx ML, A DEW, Buelens K, Compernolle G, Hassanzadeh-Ghassabeh G, Muyldermans S, Gils A, Declerck PJ. Tafia inhibiting nanobodies as profibrinolytic tools and discovery of a new tafia conformation. *J Thromb Haemost*. 2011;9:2268-2277

20. Gils A, Alessi MC, Brouwers E, Peeters M, Marx P, Leurs J, Bouma B, Hendriks D, Juhan-Vague I, Declerck PJ. Development of a genotype 325-specific procpu/tafi elisa. *Arterioscler Thromb Vasc Biol*. 2003;23:1122-1127

21. Gils A, Ceresa E, Macovei AM, Marx PF, Peeters M, Compernolle G, Declerck PJ. Modulation of tafi function through different pathways--implications for the development of tafi inhibitors. *J Thromb Haemost*. 2005;3:2745-2753

22. Mishra N, Vercauteren E, Develter J, Bammens R, Declerck PJ, Gils A. Identification and characterisation of monoclonal antibodies that impair the activation of human thrombin activatable fibrinolysis inhibitor through different mechanisms. *Thromb Haemost*. 2011;106:90-101

23. Vercauteren E, Emmerechts J, Peeters M, Hoylaerts MF, Declerck PJ, Gils A. Evaluation of the profibrinolytic properties of an anti-tafi monoclonal antibody in a mouse thromboembolism model. *Blood*. 2011;117:4615-4622

24. Mishra N, Buelens K, Theyskens S, Compernolle G, Gils A, Declerck PJ. Increased zymogen activity of thrombin-activatable fibrinolysis inhibitor prolongs clot lysis. *J Thromb Haemost*. 2012;10:1091-1099

25. Ceresa E, Peeters M, Declerck PJ, Gils A. Announcing a tafia mutant with a 180-fold increased half-life and concomitantly a strongly increased antifibrinolytic potential. *J Thromb Haemost*. 2007;5:418-420

26. Leurs J, Nerme V, Sim Y, Hendriks D. Carboxypeptidase u (tafia) prevents lysis from proceeding into the propagation phase through a threshold-dependent mechanism. *J Thromb Haemost*. 2004;2:416-423

27. Willemse JL, Polla M, Hendriks DF. The intrinsic enzymatic activity of plasma procarboxypeptidase u (tafi) can interfere with plasma carboxypeptidase n assays. *Anal Biochem*. 2006;356:157-159

28. Raza I, Davenport R, Rourke C, Platton S, Manson J, Spoors C, Khan S, De'ath HD, Allard S, Hart DP, Pasi KJ, Hunt BJ, Stanworth S, MacCallum PK, Brohi K. The incidence and magnitude of fibrinolytic activation in trauma patients. *J Thromb Haemost*. 2013;11:307-314

29. Heylen E, Van Goethem S, Augustyns K, Hendriks D. Measurement of carboxypeptidase u (active thrombin-activatable fibrinolysis inhibitor) in plasma: Challenges overcome by a novel selective assay. *Anal Biochem*. 2010;403:114-116

30. Marx PF, Havik SR, Marquart JA, Bouma BN, Meijers JC. Generation and characterization of a highly stable form of activated thrombin-activable fibrinolysis inhibitor. *J Biol Chem*. 2004;279:6620-6628

Chapter 6

Concluding discussion

Activated TAFI (TAFIa) exerts an antifibrinolytic effect by removing C-terminal lysine residues from partially degraded fibrin. The C-terminal lysine residues are an important co-factor for t-PA-mediated plasminogen activation. The development of TAFI(a) inhibitors as profibrinolytic agents is therefore an attractive concept [29]. Several naturally occurring and small synthetic TAFI inhibitors have been tested in different animal models and show an enhancement of endogenous fibrinolysis. However the most promising approach is the use of TAFI inhibitors in combination with t-PA, this would allow lowering the dose of t-PA thereby decreasing its side effects without compromising the efficacy of the treatment [29]. The synthetic and naturally occurring TAFI inhibitors lack specificity. Generation of monoclonal antibodies resolved the specificity problem but in general, due to their mouse origin they induce immunogenicity and the production costs are quite high. Chimeric and humanized antibodies or smaller antibody fragments such as Fabs and scFvs could circumvent these immunogenicity problems, but antibody fragments have other problems such as low production yields and a tendency to aggregate. Nanobodies (single-domain fragments derived from heavy-chain-only antibodies) are one of the smallest antigen binding fragments with high specificity, good production yields and low immunogenicity [109].

Therefore, the aim of this PhD project was to generate inhibitory nanobodies towards TAFI. Three immunizations with human TAFIa, mouse TAFI and rat TAFI were performed and resulted in the discovery of unique nanobodies. During the characterization of these inhibitory nanobodies serendipity comes into play: inhibitory nanobodies towards human TAFIa were able to identify a novel conformational transition in TAFIa (**chapter 2**), a nanobody towards mouse TAFI revealed a novel way to impair TAFI activation (**chapter 3**), a nanobody towards rat TAFI demonstrated a strong profibrinolytic effect but has TAFIa stabilizing properties (**chapter 4**) and the use of a nanobody in the development of a nanobody-based ELISA resulted in the first TAFIa ELISA without cross-reactivity with an inactive conformation of TAFIa ($TAFIa_i$) (**chapter 5**).

Nanobodies towards human TAFIa

Buelens et al. reported inhibitory nanobodies towards human TAFI [41] but no specific TAFIa inhibitory nanobodies were found. We aimed to generate TAFIa inhibitory nanobodies, however the development of nanobodies towards human TAFIa is hampered by the intrinsic instability of TAFIa (half-life at 37°C of approximately 10 min) [22]. Therefore a TAFIa mutant [23], with a 180-fold increased stability was used for the immunization. Screening of the generated library of

nanobodies resulted in a diverse panel of inhibitory nanobodies. We focused on the specific TAFIa inhibitory nanobodies.

Profibrinolytic effects were observed in the presence of these nanobodies in an *in vitro* clot lysis assay. Unexpectedly, the nanobodies demonstrate an antifibrinolytic effect in the presence of exogenous TM: transient (depending on concentration) for VHH-TAFI-i391 but occurring at all tested concentrations for VHH-TAFI-a428. Transient antifibrinolytic effects have been described for other reversible TAFIa inhibitors such as GEMSA and PTCI [34]. Therefore, development of irreversible TAFIa inhibitors could possibly overcome this antifibrinolytic effect. However, the concentration window at which a slight antifibrinolytic effect is observed is rather small for VHH-TAFI-i391 (see Figure 2.2 B, chapter 2). Furthermore, VHH-TAFI-i391 has the highest affinity of the nanobodies, suggesting that the concentration window at which the antifibrinolytic effect is observed is depending on the affinity.

Due to their long CDR3 region, nanobodies are often found to bind in cavities of enzymes [89] and 'hidden' epitopes, inaccessible for conventional antibodies [119]. Therefore, it comes as no surprise that the TAFIa nanobodies were found to bind in the active-site region of TAFIa and their time-dependent differential binding behavior, during TAFIa inactivation, revealed the occurrence of a yet unknown intermediate conformational transition. However, the generally accepted statement that nanobodies have a longer CDR3 region (13-27 AA) compared to VHH (9-17 AA) [84] was not confirmed in this study.

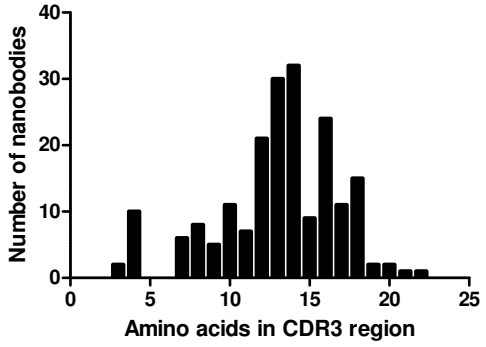

Figure 6.1: Distribution of the nanobodies based on their CDR3 length.

Determination of the length of the CDR3 region in the almost 200 generated nanobodies (towards human, mouse and rat TAFI) revealed an average CDR3 length of 13 AA, furthermore it should be noted that CDR3 regions with more than 20 AA are rather exceptional (Figure 6.1).

It has been proposed that the affinity of *in vivo* matured nanobodies is comparable to conventional antibodies (K_D's in nanomolar to subnanomolar range) [89]. Nanobodies with nanomolar K_D's were frequently observed among all our characterized nanobodies from the three immunizations however, nanobodies with a higher affinity are rather exceptional (we only found two in the panel generated with rTAFI). It is rather unlikely that a different panning procedure (e.g. more panning rounds) would have generated stronger binders since a rather harsh elution procedure is used. Performing more panning rounds would decrease the diversity of nanobodies.

Unfortunately, the human TAFIa nanobodies did not show any cross-reactivity with mouse or rat TAFI. The absence of cross-reactivity is striking because a high sequence identity is observed between human and mouse or rat TAFI (86 %). Furthermore, in the TAFIa catalytic cleft, all amino acids essential for substrate binding, substrate specificity and zinc binding are conserved between these species [120]. Even though a high sequence similarity is observed in TAFI of these different species, the absence of cross-reactivity confirms the very high specificity of the nanobodies. Unfortunately this means that the human TAFIa nanobodies could not be evaluated in mouse or rat models for thrombosis. Therefore, new immunizations with mouse and rat TAFI were performed to obtain TAFI-inhibitory nanobodies that could be evaluated *in vivo*.

Nanobodies towards mTAFI and rTAFI

Screening of the library, obtained after immunization of an alpaca with mouse TAFI, resulted in the identification of nanobody, VHH-mTAFI-i49, with a strong profibrinolytic effect in the *in vitro* clot lysis experiment (**chapter 3**). The mechanism of action of this nanobody was puzzling since it enhanced the zymogen activity of mTAFI. The zymogen activity of TAFI is a rather new observation and the relevance has been a point of discussion [62, 63]. Foley *et al.* [64] suggested that the intrinsic zymogen activity cannot attenuate fibrinolysis. VHH-mTAFI-i49 enhances the zymogen activity, but paradoxically it has a profibrinolytic effect in clot lysis experiments.

By inducing the zymogen activity of TAFI, VHH-mTAFI-i49 most likely disrupts the stabilizing interactions between the activation peptide and the dynamic flap region in TAFI [24]. Disruption of these stabilizing interactions in intact TAFI lead to a TAFI conformation which cannot be activated anymore. Therefore, this novel way of interfering with the activation might have a place in fibrinolytic therapy. Indeed, further proof of concept was given by application of VHH-

mTAFI-i49 in the tissue factor-induced mouse thromboembolism model and clearly demonstrates enhanced lysis.

Immunization of an alpaca with rTAFI resulted in a diverse panel of nanobodies, we focused on VHH-rTAFI-i81, an inhibitory nanobody with a high affinity (**chapter 4**). Full characterization of the effect of VHH-rTAFI-i81 revealed inhibitory effects on the T/TM-mediated activation of rTAFI however, also TAFIa stabilizing properties were observed. Even though the stabilizing effects of VHH-rTAFI-i81 might interfere with the inhibitory properties on the T/TM-mediated activation, strong profibrinolytic effects were observed in the *in vitro* clot lysis assay. Furthermore co-administration of VHH-rTAFI-i81 and t-PA strongly enhances the degree of lysis and reduces time to reach full lysis in a t-PA-mediated clot lysis assay. Therefore it was no surprise that VHH-rTAFI-i81 exerts a strong profibrinolytic effect in the mouse thromboembolism model.

As observed with the human TAFIa nanobodies, VHH-mTAFI-i49 and VHH-rTAFI-i81 demonstrate a very high specificity and do not cross-react with human TAFI. However, mouse and rat TAFI have a sequence identity of 96 % [120]. VHH-mTAFI-i49 cross-reacts with rat TAFI but the induced zymogen activity was lower in the latter. More importantly, VHH-rTAFI-81 cross-reacts with mouse TAFI with similar inhibitory capacities. This allowed the use of this nanobody in the mouse thromboembolism model.

Different mouse models of venous thrombosis have been developed based on Virchow's triad, the models induce changes in a) vessel wall b) pattern of blood flow or c) constituents of the blood an in this way cause thrombus formation. The tissue factor-induced mouse thromboembolism model [38] in which the nanobodies were tested is a very acute model with a high concentration of tissue factor and falls under category c). Therefore it might be interesting to evaluate the profibrinolytic effects of the nanobodies in other models. Models studying the role of the vessel wall in venous thrombosis introduce damage to walls by extravascular $FeCl_3$ application [121] or electrolytic activation [122] and give a reproducible, local thrombus formation. Models that alter the blood flow pattern have been performed by ligation induced flow restriction and results in a 'damage free' model [123]. Furthermore it would be interesting to test the effect of the nanobodies in different mouse models, deficient for anticoagulation proteins, since TAFI inhibition might interfere with their spontaneous thrombotic phenotypes [124].

Development of a specific TAFIa ELISA

The ambiguous results in different studies [68, 69, 125, 126] regarding the role of TAFI in cardiovascular diseases are most likely due to different populations, risk factors and also by the different quantitative methods used. The quantification of "total" antigen level is partially hampered by the different reactivities of different assays for the different TAFI isoforms [71]. Furthermore, the threshold-dependent mechanism [44] points out that not the amount of intact TAFI but the amount of TAFIa is critical in the interference of fibrinolysis. Even though TAFIa ELISAs have been developed, they detect, besides TAFIa, also $TAFIa_i$ which has no enzymatic activity. Therefore the development of an assay for the detection of TAFIa with no cross-reactivity for $TAFIa_i$ is a critical step forward in further research on the pathofysiological role of TAFIa.

Based on the nanobodies targeting TAFIa (**chapter 2**) we have developed a TAFIa ELISA with equal response for all TAFIa isoforms (**chapter 5**). The ELISA was used to evaluate the role of TAFIa in venous thrombosis and was able to demonstrate increased levels of TAFIa in patients with a venous thromboembolism.

In a Biacore setting VHH-TAFI-i391 was able to detect conformational changes in TAFIa by interaction with three TAFIa conformations (**chapter 2**)**.** However, in the ELISA setup, VHH-TAFI-i391 in combination with MA-TCK26D6-HRP only detects the TAFIa forms with enzymatic activities (**chapter 5**). Even though this might sound as a contradiction, both methods are drastically different: in the Biacore experiments the reaction mixture (containing TAFIa/$TAFIa_i$) flows over a sensorchip (at 25°C) coated with VHH-TAFI-i391. In the ELISA setting, the reaction mixture is incubated overnight (at 4°C) and is only detected upon interaction with MA-TCK26D6-HRP.

The major advantage of this ELISA, compared to other TAFIa ELISAs, is that it does not cross-reacts with $TAFIa_i$. Furthermore, in the TAFIa ELISA there is no interference of CPN, a major interfering factor in many TAFIa assays [127] and there is an equal response for all 4 TAFI isoforms. There is currently no standard activation protocol for TAFI. The standard used in our ELISA is an in-house activated TAFI standard, stored at -80°C. Activation of TAFI has been performed at different temperatures, incubation times and by different activators and concentration of these activators [21, 73, 128]. However, since the different activators can also cleave TAFIa [26] and the TAFIa activity is thermally unstable, different extents of activation and deactivation can occur. We decided to activate TAFI at 25°C for 10 minutes, thereby minimizing the fast thermal decay of TAFIa. Furthermore we used T/TM as activator since a full activation is observed after 10 min.

For comparison between different assays it might be interesting that a standard protocol is put forward.

Further perspectives

Besides its role in the inhibition of fibrinolysis, TAFIa also plays an important role in inflammation [129] as it is able to inactivate several inflammatory mediators such as bradykinin, anaphylatoxins C3a and C5a and osteopontin [130]. The relationship between C5a and TAFI is most studied compared to other inflammatory mediators. C5a can both recruit and activate neutrophils [131, 132], increase the vascular permeability [133, 134] and cause lysosomal degranulation resulting in histamine and TNF-α release [135, 136]. *In vivo* studies demonstrated that wild-type mice showed significantly less inflammation compared to TAFI-deficient mice in a C5a-induced alveolitis model [55]. Furthermore, wild-type mice were partially protected (compared to TAFI-deficient mice) against arthritis, induced by an anti-collagen antibody [136]. Due to the TAFIa stabilizing properties of VHH-TAFI-a428 (**chapter 2**) this nanobody could have a potential anti-inflammatory effect since it would allow a prolonged TAFIa activity. On the other hand the TAFI zymogen is also capable of cleaving small synthetic substrates [64] and it can be expected that the VHH-mTAFI-i49-induced zymogen activity (**chapter 3**) exerts an increased activity to inactivate the inflammatory mediators. Although in view of the instability of the induced zymogen activity it is currently not clear what the applicability of VHH-mTAFI-i49 would be on the inflammatory components. Therefore, it would be interesting to test whether stimulating agents of the TAFI zymogen activity (such as VHH-mTAFI-i49) could be interesting tools to investigate anti-inflammatory properties.

Furthermore TAFI has also been associated with bleeding complications in hemophilia. These bleeding complications are not only due to an impaired coagulation but are also exacerbated by the inability of the coagulation system to protect the clot from rapid break down by the fibrinolytic system. This results in prolonged bleeding and recurrent re-bleeding typically observed in hemophilia patients [46]. The enhanced fibrinolytic breakdown of the hemophilia clot is partially a result of reduced activation of TAFI [50] and treatment of hemophilia A patients with FVIII increases TAFI activation and normalizes protection of the clot against premature lysis [51]. Since TAFIa is very thermally unstable, stabilization of TAFIa might be a novel, promising approach for the treatment of hemophilia. Therefore, VHH-TAFI-a428 (**chapter 2**) might be good

candidate to stabilize the blood clot and thereby reduce the bleeding tendency in hemophilia patients.

Enhancement of the zymogen activity could also stabilize the blood clot if the induced zymogen activity is not only active for small substrates but also for partially degraded fibrin. Whether the induced zymogen activity is able to remove C-terminal lysine residues is most likely dependent on the degree of translocation of the activation peptide. Induction of a blood clot when the VHH-mTAFI-i49-induced zymogen activity is at its maximum did not result in a stabilization of the clot (reflected by the absence of a prolongation of clot lysis time). Therefore it is unlikely that VHH-mTAFI-i49 (**chapter 3**) would have an effect on stabilization of the blood clot in hemophilia patients. However, other agents inducing the zymogen activity in such a way that also larger substrates could be cleaved (by an increased extent of translocation of the activation peptide) might improve the clot stability.

Even though the small size of nanobodies has some advantages (e.g. better clot penetration [41]) the *in vivo* half-life is rather short (ca 35 min [94]) due to the rather low molecular weight. This results in a fast renal clearance. The effect of the nanobodies in the acute *in vivo* thromboembolism model (**chapter 3 and 4**) was not hampered by their short half-life. However in studies where a prolonged half-life is required, different solutions to overcome this problem have been proposed such as PEGylation or the construction of bi/multivalent nanobody constructs [94, 100]. Such bi/multivalent constructs could target both TAFI and other risk factors for thrombosis (e.g. PAI-1) and could lead to an enhanced treatment and a prolonged half-life.

ENGLISH SUMMARY

Upon activation, thrombin-activatable fibrinolysis inhibitor (TAFI) delays lysis of blood clots. TAFI is activated by trypsin-like enzymes such as thrombin and plasmin to active TAFI (TAFIa). TAFIa removes C-terminal lysine residues on the surface of the blood clot, thereby hampering plasmin generation and lysis of clots. Therefore, TAFI(a) is considered to be a risk factor for cardiovascular diseases. Current thrombolytic therapy, mainly based on plasminogen activators (such as t-PA), is very effective but leads to severe side effects such as increased bleeding risks and neurotoxicity. Co-administration of TAFI(a) inhibiting agents and t-PA could decrease these side effects by reducing the required dose of t-PA without compromising the efficacy of the treatment.

Nanobodies (derived from a unique subtype of camel antibodies) are one of the smallest antigen binding fragments. They are often very potent enzyme inhibitors and less immunogenic compared to conventional antibodies. We aimed to generate inhibitory nanobodies towards human, mouse and rat TAFI and to characterize their inhibitory properties *in vitro* and *in vivo.* During the characterization of these inhibitory nanobodies serendipity comes into play: inhibitory nanobodies towards human TAFIa were able to identify a novel conformational transition in TAFIa (**chapter 2**), a nanobody towards mouse TAFI revealed a novel way to impair TAFI activation (**chapter 3**), a nanobody towards rat TAFI demonstrated a strong profibrinolytic effect but has TAFIa stabilizing properties (**chapter 4**) and the use of a nanobody in the development of a nanobody-based ELISA resulted in the first TAFIa ELISA without cross-reactivity with an inactive conformation of TAFIa ($TAFIa_i$) (**chapter 5**).

In the first part of this study (**chapter 2**) inhibitory nanobodies towards human TAFIa were identified and characterized. *In vitro* clot lysis experiments in the absence of thrombomodulin (TM) demonstrated that the nanobodies accelerate clot lysis. However, in the presence of TM, one nanobody delays clot lysis at all concentrations tested, whereas the other nanobodies exert a slight delay at low concentrations and a pronounced acceleration of clot lysis at higher concentrations. This biphasic pattern was highly dependent on the concentration of TM and t-PA. Furthermore, the nanobodies were found to bind in the active-site region of TAFIa and their time-dependent differential binding behavior during TAFIa inactivation revealed the occurrence of a yet unknown intermediate conformational transition.

Screening of a library of nanobodies towards mouse TAFI (mTAFI) revealed one nanobody (VHH-mTAFI-i49) that significantly stimulates the zymogen activity of mTAFI (**chapter 3**). The generated zymogen activity is unstable at 37 °C and incubation of mTAFI with VHH-mTAFI-i49 revealed a time-dependent reduced activatability of mTAFI. *In vitro* clot lysis experiments in the presence of VHH-mTAFI-i49 revealed a strongly enhanced clot lysis due to a reduced activation of mTAFI during clot formation. *In vivo* application of VHH-mTAFI-i49 in a mouse thromboembolism model dose-dependently decreased the fibrin deposition in the lungs. Furthermore, epitope mapping suggested that this novel way of interfering with TAFI activation is a result of destabilization of mTAFI by disrupting stabilizing interactions between the activation peptide and the catalytic moiety.

Chapter 4 focused on the most potent nanobody towards rat TAFI, VHH-rTAFI-i81, which mainly inhibits the thrombin/thrombomodulin (T/TM)-mediated activation of rat TAFI. In an *in vitro* clot lysis assay, co-administration of t-PA and VHH-rTAFI-i81 strongly enhanced the degree of lysis and reduced time to reach full lysis of t-PA-mediated clot lysis. *In vivo* application of VHH-rTAFI-i81 in a mouse thromboembolism model significantly decreased fibrin deposition in the lungs.

In **chapter 5**, the development of a specific TAFIa ELISA based on a TAFIa capturing nanobody (VHH-TAFI-i391) is described. The assay reacts equally well with all four naturally occurring TAFIa isoforms and does not cross-react with inactivated TAFIa. In an *in vitro* clot lysis assay, an excellent correlation is observed between the TAFIa activity determined by a functional assay and the TAFIa antigen determined by the ELISA. Analysis of plasma samples obtained from patients with a history of a venous thrombotic event demonstrated significantly higher TAFIa levels compared to healthy controls.

In conclusion, this study demonstrates that nanobodies targeting TAFI(a) are useful as conformational probes, as tools for the development of diagnostic assays and as potent inhibitors of TAFI(a). The latter properties of these nanobodies make them well suited as putative lead compounds in the development of strategies to increase the endogenous fibrinolytic capacity in blood and to improve thrombolytic therapy.

NEDERLANDSTALIGE SAMENVATTING

'Thrombin-activatable fibrinolysis inhibitor' (TAFI) vertraagt na activatie de bloedklonterafbraak. TAFI kan door trypsine-achtige enzymes zoals trombine en plasmine geactiveerd worden tot het actief enzyme TAFIa. TAFIa verwijdert C-terminale lysine residues aan het oppervlak van een bloedklonter, remt zo de plasmine productie en bijgevolg de afbraak van bloedklonters. Daarom wordt TAFI(a) beschouwd als een risicofactor voor cardiovasculaire aandoeningen. Trombolytische therapie, gebaseerd op plasminogeen activatoren (zoals t-PA) is zeer efficiënt maar kan leiden tot ernstige neveneffecten zoals een verhoogde bloedingneiging en neurotoxiciteit. Simultane toediening van TAFI(a) inhiberende agentia en t-PA zou deze neveneffecten kunnen verminderen doordat de hoeveelheid toe te dienen t-PA kan verlaagd worden zonder de efficaciteit van de therapie te verminderen.

Nanobodies (afgeleid van een bijzondere soort van kameel antilichamen) zijn één van de kleinste antigen bindende fragmenten. Ze zijn dikwijls zeer potente enzyme inhibitoren en minder immunogeen in vergelijking met conventionele antilichamen. Het doel van deze studie was de aanmaak van inhibitorische nanobodies tegen humaan, muis en rat TAFI en de karakterisering van hun eigenschappen *in vitro* en *in vivo*. Tijdens de karakterisering werden enkele interessante ontdekkingen gedaan zoals de identificatie van een, tot nog toe onbekende, conformationele transitie van TAFIa (**hoofdstuk 2**), de identificatie van een unieke wijze om met behulp van een nanobody TAFI te destabiliseren zodat activatie onmogelijk wordt (**hoofdstuk 3**), een rat TAFI inhiberend nanobody heeft een sterk profibrinolytisch effect maar contradictorisch ook TAFIa stabiliserende eigenschappen (**hoofdstuk 4**) en het gebruik van een nanobody in de ontwikkeling van een ELISA dat heel selectief TAFIa herkent, maar niet $TAFIa_i$ (**hoofdstuk 5**).

In het eerste deel van deze studie (**hoofdstuk 2**) werden inhibitorische nanobodies tegen humaan TAFIa geïdentificeerd en gekarakteriseerd. *In vitro* clot lysis experimenten in de afwezigheid van trombomoduline (TM) toonden aan dat deze nanobodies de afbraak van de bloedklonter versnelden. Echter, in aanwezigheid van TM vertraagt één van de nanobodies de bloedklonter afbraak bij alle geteste concentraties terwijl een ander nanobody een lichte vertraging vertoonde bij lage concentraties maar een uitgesproken versnelling bij hogere concentraties. Het bifasisch patroon was zowel TM als t-PA afhankelijk. Er werd tevens aangetoond dat de nanobodies in de 'active-site' van TAFIa binden. Verder vertoonden de nanobodies een veranderend bindingspatroon voor TAFIa gedurende inactivatie van deze laatste. Op deze manier werd een nieuwe conformationele transitie in TAFIa aangetoond.

Screening van een panel van nanobodies tegen muis TAFI (mTAFI) leverde één nanobody (VHH-mTAFI-i49) dat de zymogene activiteit van TAFI stimuleert **(hoofdstuk 3)**. De gegenereerde zymogene activiteit is instabiel bij 37°C en incubatie van mTAFI met VHH-mTAFI-i49 resulteerde in een verminderde activeerbaarheid van mTAFI. *In vitro* clot lysis experimenten toonden een versnelde klonterafbraak aan in aanwezigheid van VHH-mTAFI-i49 door de verminderde activeerbaarheid van mTAFI. De toepassing van dit nanobody in een *in vivo* muis trombo-embolisme model toonde een significant verminderde fibrine depositie in de longen aan. Verder suggereert de bindingsplaats van VHH-mTAFI-i49 een nanobody-geïnduceerd destabiliserend effect in mTAFI door interferentie met de stabiliserende interacties tussen het activatiepeptide en de dynamische flap regio.

In **hoofdstuk 4** werd gefocust op het meest potente nanobody tegen rat TAFI, VHH-rTAFI-i81, dat vooral de trombine/trombomoduline gemedieerde activatie van rTAFI inhibeert. In een *in vitro* clot lysis assay werd aangetoond dat simultane toediening van t-PA en VHH-rTAFI-i81 de totale lysis en snelheid van de lysis verbeterde. *In vivo* toepassing van VHH-rTAFI-i81 in een muis trombo-embolisme model toont een significante vermindering van de fibrine depositie in de longen aan.

In **hoofstuk 5** werd een TAFIa specifieke ELISA ontwikkeld met behulp van een TAFIa bindend nanobody (VHH-TAFI-i391). De vier natuurlijk voorkomende isovormen reageerden op identieke wijze in de ELISA terwijl geïnactiveerd TAFIa niet herkend werd. In een *in vitro* clot lysis experiment werd een excellente correlatie vastgesteld tussen de response in ELISA en de TAFIa activiteit. Analyse van plasma stalen toonde verhoogde TAFIa waarden aan in patiënten met een geschiedenis van een veneuze trombotische aandoening ten opzichte van gezonde controles.

In conclusie, deze studie toont aan dat nanobodies tegen TAFI(a) ook diagnostische toepassingen hebben naast hun uitstekende inhibitorische eigenschappen. De beschikbaarheid van TAFI(a) inhiberende nanobodies opent nieuwe perspectieven voor de optimalisatie van trombolytische therapie.

Curriculum Vitae:

Personalia

Name: Maarten Louis Veronique Hendrickx
Date of birth: March 29, 1986
Place of birth: Leuven, Belgium
@: Maarten.Hendrickx@outlook.com

Education

2009 - 2013	**PhD in Pharmaceutical Sciences**: Laboratory for Therapeutic and Diagnostic Antibodies, **KU Leuven** Thesis: "Generation and characterization of nanobodies towards thrombin-activatable fibrinolysis inhibitor" Supervisor and co-supervisor: Prof. Paul Declerck and Prof. Ann Gils.
2007-2009	**Master of Science** Pharmacy, Drug Design and Development, KU Leuven Master thesis: "Characterization of RNA aptamer binding to PAI-1" Supervisors: Prof. Peter Andreasen, Department of Molecular Biology and Genetics, **Aarhus University**, Denmark and Prof. Paul Declerck, Laboratory for Therapeutic and Diagnostic Antibodies, **KU Leuven**.
2004-2007	**Bachelor of Science**, Pharmaceutical Sciences, **KU Leuven**
1998-2004	**High school:** Science-Mathematics, Sint-Albertuscollege, Haasrode

Scientific honors, awards and fellowships

2013

Award for outstanding oral presentation at the XIVth International Workshop – Molecular and Cellular Biology of Plasminogen Activation *"Identification of a novel, nanobody-induced, mechanism of TAFI inactivation and its in vivo application"* Notre Dame, IN, USA

FWO fellowship for a long stay abroad to the Scripps Research Institute, La Jolla, CA, USA. "*TAFIa stabilization and its applicability in the treatment of hemophilia A"*

Control of Anticoagulation Award, Scientific and Standardization Committee (SSC) at the XXIVth Conference of International Society on Thrombosis and Haemostasis (ISTH) *"Enhanced t-PA-mediated fibrinolysis through co-administration of a TAFI-inhibiting nanobody"* Amsterdam, The Netherlands

Fellowship award to attend the XIVth International Workshop – Molecular and Cellular Biology of Plasminogen Activation for oral presentation *"Identification of a novel, nanobody-induced, mechanism of TAFI inactivation and its in vivo application"* Notre Dame, IN, USA

Broaden your horizon call KU Leuven travel funding for oral presentation *"Identification of a novel, nanobody-induced, mechanism of TAFI inactivation and its in vivo application"* at the XIVth International Workshop - Molecular and Cellular Biology of Plasminogen Activation, Notre Dame, IN, USA

2012 **Pier M Mannucci Award** for Best Article in 2011 by a Young Investigator, "*TAFIa inhibiting nanobodies as profibrinolytic tools and discovery of a new TAFIa conformation*" Journal of Thrombosis and Haemostasis (Impact factor: 5.731)

Travel grant BGFW (Belgian Society for Pharmaceutical Sciences) for presentation "*Identification of a new conformation of activated thrombin-activatable fibrinolysis inhibitor (TAFIa) by a TAFIa specific nanobody"* at the Gordon Research Conference, Ventura, CA, USA

2011 **Young Investigators Award**, XXIIIth Conference of the International Society on Thrombosis and Haemostasis (ISTH), *"Specific TAFIa inhibiting nanobodies as profibrinolytic tools and discovery of a new TAFIa conformation"* (Kyoto)

Travel grant BSTH (Belgian Society on Thrombosis and Haemostasis) for oral presentation *"Specific TAFIa inhibiting nanobodies as profibrinolytic tools and discovery of a new TAFIa conformation"* at the ISTH conference Kyoto, Japan

2010 Exploitation of research – Technology and knowledge transfer (KU Leuven LRD): Winner of the **Award for the Best Exploitation Plan**, "*Lysozyme inhibitors as novel drug targets*" (Leuven)

PhD fellowship; Strategic Basic Research: **IWT doctoral funding** (2010-2014): *Production and characterization of nanobodies towards mouse 'thrombin activatable fibrinolysis inhibitor' (mTAFI).* Agency for Innovation by Science and Technology (IWT) (Brussels)

Conference participations

2013 Hendrickx MLV *et al*. *Enhanced t-PA-mediated fibrinolysis through co-administration of a TAFI-inhibiting nanobody*. **Congress of the International Society on Thrombosis and Haemostasis (ISTH),** Amsterdam, The Netherlands, e-poster oral presentation.

Hendrickx MLV *et al*. *Identification of a novel, nanobody-induced, mechanism of TAFI inactivation and its in vivo application*. **Congress of the International Society on Thrombosis and Haemostasis (ISTH),** Amsterdam, The Netherlands, e-poster oral presentation.

Hendrickx MLV *et al*. *Identification of a novel, nanobody-induced, mechanism of TAFI inactivation and its in vivo application*. **XIVth International Workshop - Molecular and Cellular Biology of Plasminogen Activation**, Notre Dame, IN, USA oral presentation.

2012 Hendrickx MLV *et al*. *Profibrinolytic properties of a destabilizing anti-TAFI nanobody.* **Belgian Society on Thrombosis and Haemostasis (BSTH) conference.** Antwerp**,** poster presentation.

Hendrickx MLV *et al*. *Development of a sandwich-type ELISA for the detection of human active thrombin activatable fibrinolysis inhibitor (TAFIa)*, **International Society for Proteolysis and Fibrinolysis (ISFP) conference**, Brighton, UK, poster presentation.

Hendrickx MLV *et al*. *Development of a sandwich-type ELISA for the detection of human active thrombin activatable fibrinolysis inhibitor (TAFIa),* **Belgian Society for Pharmaceutical Sciences (BGFW) conference.** Blankenberge, oral presentation.

Hendrickx MLV *et al*. *Identification of a new conformation of activated thrombin activatable fibrinolysis inhibitor (TAFIa) by a TAFIa specific nanobody,* **Gordon Research Conference**, Ventura, USA, poster presentation.

2011 Hendrickx MLV *et al*. *Specific TAFIa inhibiting nanobodies as profibrinolytic tools and discovery of a new TAFIa conformation*, **Congress of the International Society on Thrombosis and Haemostasis (ISTH),** Kyoto, Japan, oral presentation.

Hendrickx MLV *et al*. *Nanobodies as probes to monitor conformational changes in activated thrombin activatable fibrinolysis inhibitor (TAFIa),* **ULLA summer school,** Parma, Italy, oral presentation.

Hendrickx MLV *et al*. *Nanobodies as probes to monitor conformational changes in activated thrombin activatable fibrinolysis inhibitor (TAFIa),* **Belgian Society for Pharmaceutical Sciences (BGFW) conference.** Spa, 2011, oral presentation

2010 Hendrickx MLV *et al*. *Biphasic effect of nanobodies encountering TAFIa activity,* **Belgian Society on Thrombosis and Haemostasis (BSTH) conference.** Gent**,** poster presentation.

Hendrickx MLV *et al*. *Biphasic effect of VHH's encountering TAFIa activity,* **Single domain antibodies come of age conference**. Gent, poster presentation.

REFERENCES (INTRODUCTION AND CONCLUDING DISCUSSION)

1. Adams RL, Bird RJ. Review article: Coagulation cascade and therapeutics update: Relevance to nephrology. Part 1: Overview of coagulation, thrombophilias and history of anticoagulants. *Nephrology*. 2009;14:462-470
2. Cesarman-Maus G, Hajjar KA. Molecular mechanisms of fibrinolysis. *Br J Haematol*. 2005;129:307-321
3. Rijken DC, Lijnen HR. New insights into the molecular mechanisms of the fibrinolytic system. *J Thromb Haemost*. 2009;7:4-13
4. Hendriks D, Scharpe S, van Sande M, Lommaert MP. Characterisation of a carboxypeptidase in human serum distinct from carboxypeptidase n. *J Clin Chem Clin Biochem*. 1989;27:277-285
5. Campbell W, Okada H. An arginine specific carboxypeptidase generated in blood during coagulation or inflammation which is unrelated to carboxypeptidase n or its subunits. *Biochemical and biophysical research communications*. 1989;162:933-939
6. Eaton DL, Malloy BE, Tsai SP, Henzel W, Drayna D. Isolation, molecular cloning, and partial characterization of a novel carboxypeptidase b from human plasma. *J Biol Chem*. 1991;266:21833-21838
7. Bajzar L, Manuel R, Nesheim ME. Purification and characterization of tafi, a thrombin-activable fibrinolysis inhibitor. *J Biol Chem*. 1995;270:14477-14484
8. Vanhoof G, Wauters J, Schatteman K, Hendriks D, Goossens F, Bossuyt P, Scharpe S. The gene for human carboxypeptidase u (cpu)--a proposed novel regulator of plasminogen activation--maps to 13q14.11. *Genomics*. 1996;38:454-455
9. Boffa MB, Reid TS, Joo E, Nesheim ME, Koschinsky ML. Characterization of the gene encoding human tafi (thrombin-activable fibrinolysis inhibitor; plasma procarboxypeptidase b). *Biochemistry*. 1999;38:6547-6558
10. Boffa MB, Koschinsky ML. Curiouser and curiouser: Recent advances in measurement of thrombin-activatable fibrinolysis inhibitor (tafi) and in understanding its molecular genetics, gene regulation, and biological roles. *Clinical biochemistry*. 2007;40:431-442
11. Brouwers GJ, Vos HL, Leebeek FW, Bulk S, Schneider M, Boffa M, Koschinsky M, van Tilburg NH, Nesheim ME, Bertina RM, Gomez Garcia EB. A novel, possibly functional, single nucleotide polymorphism in the coding region of the thrombin-activatable fibrinolysis inhibitor (tafi) gene is also associated with tafi levels. *Blood*. 2001;98:1992-1993
12. Bajzar L, Nesheim ME, Tracy PB. The profibrinolytic effect of activated protein c in clots formed from plasma is tafi-dependent. *Blood*. 1996;88:2093-2100
13. Mosnier LO, von dem Borne PA, Meijers JC, Bouma BN. Plasma tafi levels influence the clot lysis time in healthy individuals in the presence of an intact intrinsic pathway of coagulation. *Thromb Haemost*. 1998;80:829-835
14. Mosnier LO, Buijtenhuijs P, Marx PF, Meijers JC, Bouma BN. Identification of thrombin activatable fibrinolysis inhibitor (tafi) in human platelets. *Blood*. 2003;101:4844-4846

15. Guimaraes AH, Barrett-Bergshoeff MM, Gils A, Declerck PJ, Rijken DC. Migration of the activation peptide of thrombin-activatable fibrinolysis inhibitor (tafi) during sds-polyacrylamide gel electrophoresis. *J Thromb Haemost*. 2004;2:780-784

16. Declerck PJ. Thrombin activatable fibrinolysis inhibitor. *Hamostaseologie*. 2011;31:165-166, 168-173

17. Bajzar L, Morser J, Nesheim M. Tafi, or plasma procarboxypeptidase b, couples the coagulation and fibrinolytic cascades through the thrombin-thrombomodulin complex. *J Biol Chem*. 1996;271:16603-16608

18. Esmon CT. The protein c pathway. *Chest*. 2003;124:26S-32S

19. Mao SS, Cooper CM, Wood T, Shafer JA, Gardell SJ. Characterization of plasmin-mediated activation of plasma procarboxypeptidase b. Modulation by glycosaminoglycans. *J Biol Chem*. 1999;274:35046-35052

20. Leurs J, Wissing BM, Nerme V, Schatteman K, Bjorquist P, Hendriks D. Different mechanisms contribute to the biphasic pattern of carboxypeptidase u (tafia) generation during in vitro clot lysis in human plasma. *Thromb Haemost*. 2003;89:264-271

21. Boffa MB, Wang W, Bajzar L, Nesheim ME. Plasma and recombinant thrombin-activable fibrinolysis inhibitor (tafi) and activated tafi compared with respect to glycosylation, thrombin/thrombomodulin-dependent activation, thermal stability, and enzymatic properties. *J Biol Chem*. 1998;273:2127-2135

22. Schneider M, Boffa M, Stewart R, Rahman M, Koschinsky M, Nesheim M. Two naturally occurring variants of tafi (thr-325 and ile-325) differ substantially with respect to thermal stability and antifibrinolytic activity of the enzyme. *J Biol Chem*. 2002;277:1021-1030

23. Ceresa E, Peeters M, Declerck PJ, Gils A. Announcing a tafia mutant with a 180-fold increased half-life and concomitantly a strongly increased antifibrinolytic potential. *J Thromb Haemost*. 2007;5:418-420

24. Marx PF, Brondijk TH, Plug T, Romijn RA, Hemrika W, Meijers JC, Huizinga EG. Crystal structures of tafi elucidate the inactivation mechanism of activated tafi: A novel mechanism for enzyme autoregulation. *Blood*. 2008;112:2803-2809

25. Boffa MB, Bell R, Stevens WK, Nesheim ME. Roles of thermal instability and proteolytic cleavage in regulation of activated thrombin-activable fibrinolysis inhibitor. *J Biol Chem*. 2000;275:12868-12878

26. Marx PF, Dawson PE, Bouma BN, Meijers JC. Plasmin-mediated activation and inactivation of thrombin-activatable fibrinolysis inhibitor. *Biochemistry*. 2002;41:6688-6696

27. Wang W, Hendriks DF, Scharpe SS. Carboxypeptidase u, a plasma carboxypeptidase with high affinity for plasminogen. *J Biol Chem*. 1994;269:15937-15944

28. Leurs J, Hendriks D. Carboxypeptidase u (tafia): A metallocarboxypeptidase with a distinct role in haemostasis and a possible risk factor for thrombotic disease. *Thromb Haemost*. 2005;94:471-487

29. Willemse JL, Heylen E, Nesheim ME, Hendriks DF. Carboxypeptidase u (tafia): A new drug target for fibrinolytic therapy? *J Thromb Haemost*. 2009;7:1962-1971

30. Redlitz A, Tan AK, Eaton DL, Plow EF. Plasma carboxypeptidases as regulators of the plasminogen system. *J Clin Invest*. 1995;96:2534-2538

31. Reverter D, Vendrell J, Canals F, Horstmann J, Aviles FX, Fritz H, Sommerhoff CP. A carboxypeptidase inhibitor from the medical leech hirudo medicinalis. Isolation, sequence analysis, cdna cloning, recombinant expression, and characterization. *J Biol Chem*. 1998;273:32927-32933

32. Arolas JL, Lorenzo J, Rovira A, Castella J, Aviles FX, Sommerhoff CP. A carboxypeptidase inhibitor from the tick rhipicephalus bursa: Isolation, cdna cloning, recombinant expression, and characterization. *J Biol Chem*. 2005;280:3441-3448

33. Schneider M, Nesheim M. Reversible inhibitors of tafia can both promote and inhibit fibrinolysis. *J Thromb Haemost*. 2003;1:147-154

34. Walker JB, Hughes B, James I, Haddock P, Kluft C, Bajzar L. Stabilization versus inhibition of tafia by competitive inhibitors in vitro. *J Biol Chem*. 2003;278:8913-8921

35. Gils A, Ceresa E, Macovei AM, Marx PF, Peeters M, Compernolle G, Declerck PJ. Modulation of tafi function through different pathways--implications for the development of tafi inhibitors. *J Thromb Haemost*. 2005;3:2745-2753

36. Binette TM, Taylor FB, Jr., Peer G, Bajzar L. Thrombin-thrombomodulin connects coagulation and fibrinolysis: More than an in vitro phenomenon. *Blood*. 2007;110:3168-3175

37. Mishra N, Vercauteren E, Develter J, Bammens R, Declerck PJ, Gils A. Identification and characterisation of monoclonal antibodies that impair the activation of human thrombin activatable fibrinolysis inhibitor through different mechanisms. *Thromb Haemost*. 2011;106:90-101

38. Vercauteren E, Emmerechts J, Peeters M, Hoylaerts MF, Declerck PJ, Gils A. Evaluation of the profibrinolytic properties of an anti-tafi monoclonal antibody in a mouse thromboembolism model. *Blood*. 2011;117:4615-4622

39. Hillmayer K, Vancraenenbroeck R, De Maeyer M, Compernolle G, Declerck PJ, Gils A. Discovery of novel mechanisms and molecular targets for the inhibition of activated thrombin activatable fibrinolysis inhibitor. *J Thromb Haemost*. 2008;6:1892-1899

40. Develter J, Dewilde M, Gils A, Declerck PJ. Comparative study of inhibitory antibody derivatives towards thrombin activatable fibrinolysis inhibitor. *Thromb Haemost*. 2009;102:69-75

41. Buelens K, Hassanzadeh-Ghassabeh G, Muyldermans S, Gils A, Declerck PJ. Generation and characterization of inhibitory nanobodies towards thrombin activatable fibrinolysis inhibitor. *J Thromb Haemost*. 2010;8:1302-1312

42. Fleury V, Angles-Cano E. Characterization of the binding of plasminogen to fibrin surfaces: The role of carboxy-terminal lysines. *Biochemistry*. 1991;30:7630-7638

43. Hoylaerts M, Rijken DC, Lijnen HR, Collen D. Kinetics of the activation of plasminogen by human tissue plasminogen activator. Role of fibrin. *J Biol Chem*. 1982;257:2912-2919

44. Leurs J, Nerme V, Sim Y, Hendriks D. Carboxypeptidase u (tafia) prevents lysis from proceeding into the propagation phase through a threshold-dependent mechanism. *J Thromb Haemost*. 2004;2:416-423

45. Walker JB, Bajzar L. The intrinsic threshold of the fibrinolytic system is modulated by basic carboxypeptidases, but the magnitude of the antifibrinolytic effect of activated

thrombin-activable fibrinolysis inhibitor is masked by its instability. *J Biol Chem*. 2004;279:27896-27904

46. Broze GJ, Jr., Higuchi DA. Coagulation-dependent inhibition of fibrinolysis: Role of carboxypeptidase-u and the premature lysis of clots from hemophilic plasma. *Blood*. 1996;88:3815-3823

47. Mosnier LO, Lisman T, van den Berg HM, Nieuwenhuis HK, Meijers JC, Bouma BN. The defective down regulation of fibrinolysis in haemophilia a can be restored by increasing the tafi plasma concentration. *Thromb Haemost*. 2001;86:1035-1039

48. Lisman T, Mosnier LO, Lambert T, Mauser-Bunschoten EP, Meijers JC, Nieuwenhuis HK, de Groot PG. Inhibition of fibrinolysis by recombinant factor viia in plasma from patients with severe hemophilia a. *Blood*. 2002;99:175-179

49. Mosnier LO, Bouma BN. Regulation of fibrinolysis by thrombin activatable fibrinolysis inhibitor, an unstable carboxypeptidase b that unites the pathways of coagulation and fibrinolysis. *Arterioscler Thromb Vasc Biol*. 2006;26:2445-2453

50. Foley JH, Nesheim ME, Rivard GE, Brummel-Ziedins KE. Thrombin activatable fibrinolysis inhibitor activation and bleeding in haemophilia a. *Haemophilia : the official journal of the World Federation of Hemophilia*. 2012;18:e316-322

51. Mikovic D, Woodhams BJ, Holmstrom M, Elezovic I, Antovic A, Mobarrez F, Elfvinge P, Antovic JP. On-demand but not prophylactic treatment with fviii concentrate increase thrombin activatable fibrinolysis inhibitor activation in severe haemophilia a patients. *Int J Lab Hematol*. 2012;34:35-40

52. Foley JH, Nesheim ME. Soluble thrombomodulin partially corrects the premature lysis defect in fviii-deficient plasma by stimulating the activation of thrombin activatable fibrinolysis inhibitor. *J Thromb Haemost*. 2009;7:453-459

53. Myles T, Nishimura T, Yun TH, Nagashima M, Morser J, Patterson AJ, Pearl RG, Leung LL. Thrombin activatable fibrinolysis inhibitor, a potential regulator of vascular inflammation. *J Biol Chem*. 2003;278:51059-51067

54. Shinohara T, Sakurada C, Suzuki T, Takeuchi O, Campbell W, Ikeda S, Okada N, Okada H. Pro-carboxypeptidase r cleaves bradykinin following activation. *International archives of allergy and immunology*. 1994;103:400-404

55. Nishimura T, Myles T, Piliponsky AM, Kao PN, Berry GJ, Leung LL. Thrombin-activatable procarboxypeptidase b regulates activated complement c5a in vivo. *Blood*. 2007;109:1992-1997

56. Song JJ, Hwang I, Cho KH, Garcia MA, Kim AJ, Wang TH, Lindstrom TM, Lee AT, Nishimura T, Zhao L, Morser J, Nesheim M, Goodman SB, Lee DM, Bridges SL, Jr., Consortium for the Longitudinal Evaluation of African Americans with Early Rheumatoid Arthritis R, Gregersen PK, Leung LL, Robinson WH. Plasma carboxypeptidase b downregulates inflammatory responses in autoimmune arthritis. *J Clin Invest*. 2011;121:3517-3527

57. Renckens R, Roelofs JJ, ter Horst SA, van 't Veer C, Havik SR, Florquin S, Wagenaar GT, Meijers JC, van der Poll T. Absence of thrombin-activatable fibrinolysis inhibitor protects against sepsis-induced liver injury in mice. *J Immunol*. 2005;175:6764-6771

58. te Velde EA, Wagenaar GT, Reijerkerk A, Roose-Girma M, Borel Rinkes IH, Voest EE, Bouma BN, Gebbink MF, Meijers JC. Impaired healing of cutaneous wounds and colonic

anastomoses in mice lacking thrombin-activatable fibrinolysis inhibitor. *J Thromb Haemost*. 2003;1:2087-2096

59. Willemse JL, Polla M, Hendriks DF. The intrinsic enzymatic activity of plasma procarboxypeptidase u (tafi) can interfere with plasma carboxypeptidase n assays. *Anal Biochem*. 2006;356:157-159

60. Valnickova Z, Thogersen IB, Potempa J, Enghild JJ. Thrombin-activable fibrinolysis inhibitor (tafi) zymogen is an active carboxypeptidase. *J Biol Chem*. 2007;282:3066-3076

61. Wu C, Dong N, da Cunha V, Martin-McNulty B, Tran K, Nagashima M, Wu Q, Morser J, Wang YX. Activated thrombin-activatable fibrinolysis inhibitor attenuates spontaneous fibrinolysis of batroxobin-induced fibrin deposition in rat lungs. *Thromb Haemost*. 2003;90:414-421

62. Willemse JL, Heylen E, Hendriks DF. The intrinsic enzymatic activity of procarboxypeptidase u (tafi) does not significantly influence the fibrinolysis rate: A rebuttal. *J Thromb Haemost*. 2007;5:1334-1336

63. Valnickova Z, Thogersen IB, Potempa J, Enghild JJ. The intrinsic enzymatic activity of procarboxypeptidase u (tafi) does not significantly influence the fibrinolytic rate: Reply to a rebuttal. *J Thromb Haemost*. 2007;5:1336-1337

64. Foley JH, Kim P, Nesheim ME. Thrombin-activable fibrinolysis inhibitor zymogen does not play a significant role in the attenuation of fibrinolysis. *J Biol Chem*. 2008;283:8863-8867

65. Mishra N, Buelens K, Theyskens S, Compernolle G, Gils A, Declerck PJ. Increased zymogen activity of thrombin-activatable fibrinolysis inhibitor prolongs clot lysis. *J Thromb Haemost*. 2012;10:1091-1099

66. Morange PE, Juhan-Vague I, Scarabin PY, Alessi MC, Luc G, Arveiler D, Ferrieres J, Amouyel P, Evans A, Ducimetiere P. Association between tafi antigen and ala147thr polymorphism of the tafi gene and the angina pectoris incidence. The prime study (prospective epidemiological study of mi). *Thromb Haemost*. 2003;89:554-560

67. van Tilburg NH, Rosendaal FR, Bertina RM. Thrombin activatable fibrinolysis inhibitor and the risk for deep vein thrombosis. *Blood*. 2000;95:2855-2859

68. Silveira A, Schatteman K, Goossens F, Moor E, Scharpe S, Stromqvist M, Hendriks D, Hamsten A. Plasma procarboxypeptidase u in men with symptomatic coronary artery disease. *Thromb Haemost*. 2000;84:364-368

69. Montaner J, Ribo M, Monasterio J, Molina CA, Alvarez-Sabin J. Thrombin-activable fibrinolysis inhibitor levels in the acute phase of ischemic stroke. *Stroke*. 2003;34:1038-1040

70. Juhan-Vague I, Morange PE, Aubert H, Henry M, Aillaud MF, Alessi MC, Samnegard A, Hawe E, Yudkin J, Margaglione M, Di Minno G, Hamsten A, Humphries SE. Plasma thrombin-activatable fibrinolysis inhibitor antigen concentration and genotype in relation to myocardial infarction in the north and south of europe. *Arterioscler Thromb Vasc Biol*. 2002;22:867-873

71. Gils A, Alessi MC, Brouwers E, Peeters M, Marx P, Leurs J, Bouma B, Hendriks D, Juhan-Vague I, Declerck PJ. Development of a genotype 325-specific procpu/tafi elisa. *Arterioscler Thromb Vasc Biol*. 2003;23:1122-1127

72. Ceresa E, Brouwers E, Peeters M, Jern C, Declerck PJ, Gils A. Development of elisas measuring the extent of tafi activation. *Arterioscler Thromb Vasc Biol*. 2006;26:423-428

73. Hulme John P. ASSA. Detecting activated thrombin activatable fibrinolysis inhibitor (tafia) and inactivated tafia (tafiai) in normal and hemophilia a plasmas *Bull Korean Chem Soc*. 2009;30:77-82

74. Park R SJ, An SS. Elevated levels of thrombin-activatable fibrinolysis inhibitor in patients with sepsis. *Korean J Hematol*. 2010;45:264-268

75. Raza I, Davenport R, Rourke C, Platton S, Manson J, Spoors C, Khan S, De'ath HD, Allard S, Hart DP, Pasi KJ, Hunt BJ, Stanworth S, MacCallum PK, Brohi K. The incidence and magnitude of fibrinolytic activation in trauma patients. *J Thromb Haemost*. 2013;11:307-314

76. Schatteman KA, Goossens FJ, Scharpe SS, Neels HM, Hendriks DF. Assay of procarboxypeptidase u, a novel determinant of the fibrinolytic cascade, in human plasma. *Clin Chem*. 1999;45:807-813

77. Hendriks D, van Sande M, Scharpe S. Colorimetric assay for carboxypeptidase n in serum. *Clin Chim Acta*. 1986;157:103-108

78. Mock WL, Stanford DJ. Anisylazoformylarginine: A superior assay substrate for carboxypeptidase b type enzymes. *Bioorg Med Chem Lett*. 2002;12:1193-1194

79. Heylen E, Van Goethem S, Augustyns K, Hendriks D. Measurement of carboxypeptidase u (active thrombin-activatable fibrinolysis inhibitor) in plasma: Challenges overcome by a novel selective assay. *Anal Biochem*. 2010;403:114-116

80. Neill EK, Stewart RJ, Schneider MM, Nesheim ME. A functional assay for measuring activated thrombin-activatable fibrinolysis inhibitor in plasma. *Anal Biochem*. 2004;330:332-341

81. Hamers-Casterman C, Atarhouch T, Muyldermans S, Robinson G, Hamers C, Songa EB, Bendahman N, Hamers R. Naturally occurring antibodies devoid of light chains. *Nature*. 1993;363:446-448

82. Whitlow M, Bell BA, Feng SL, Filpula D, Hardman KD, Hubert SL, Rollence ML, Wood JF, Schott ME, Milenic DE, et al. An improved linker for single-chain fv with reduced aggregation and enhanced proteolytic stability. *Protein Eng*. 1993;6:989-995

83. Muyldermans S. Single domain camel antibodies: Current status. *J Biotechnol*. 2001;74:277-302

84. Vu KB, Ghahroudi MA, Wyns L, Muyldermans S. Comparison of llama vh sequences from conventional and heavy chain antibodies. *Mol Immunol*. 1997;34:1121-1131

85. Conrath KE, Lauwereys M, Galleni M, Matagne A, Frere JM, Kinne J, Wyns L, Muyldermans S. Beta-lactamase inhibitors derived from single-domain antibody fragments elicited in the camelidae. *Antimicrob Agents Chemother*. 2001;45:2807-2812

86. Arbabi Ghahroudi M, Desmyter A, Wyns L, Hamers R, Muyldermans S. Selection and identification of single domain antibody fragments from camel heavy-chain antibodies. *FEBS Lett*. 1997;414:521-526

87. van der Linden RH, Frenken LG, de Geus B, Harmsen MM, Ruuls RC, Stok W, de Ron L, Wilson S, Davis P, Verrips CT. Comparison of physical chemical properties of llama vhh

antibody fragments and mouse monoclonal antibodies. *Biochim Biophys Acta*. 1999;1431:37-46

88. Dolk E, van der Vaart M, Lutje Hulsik D, Vriend G, de Haard H, Spinelli S, Cambillau C, Frenken L, Verrips T. Isolation of llama antibody fragments for prevention of dandruff by phage display in shampoo. *Applied and environmental microbiology*. 2005;71:442-450

89. De Genst E, Silence K, Decanniere K, Conrath K, Loris R, Kinne J, Muyldermans S, Wyns L. Molecular basis for the preferential cleft recognition by dromedary heavy-chain antibodies. *Proc Natl Acad Sci U S A*. 2006;103:4586-4591

90. Lauwereys M, Arbabi Ghahroudi M, Desmyter A, Kinne J, Holzer W, De Genst E, Wyns L, Muyldermans S. Potent enzyme inhibitors derived from dromedary heavy-chain antibodies. *EMBO J*. 1998;17:3512-3520

91. Decanniere K, Desmyter A, Lauwereys M, Ghahroudi MA, Muyldermans S, Wyns L. A single-domain antibody fragment in complex with rnase a: Non-canonical loop structures and nanomolar affinity using two cdr loops. *Structure*. 1999;7:361-370

92. Yau KY, Dubuc G, Li S, Hirama T, Mackenzie CR, Jermutus L, Hall JC, Tanha J. Affinity maturation of a v(h)h by mutational hotspot randomization. *J Immunol Methods*. 2005;297:213-224

93. Baral TN, Magez S, Stijlemans B, Conrath K, Vanhollebeke B, Pays E, Muyldermans S, De Baetselier P. Experimental therapy of african trypanosomiasis with a nanobody-conjugated human trypanolytic factor. *Nature medicine*. 2006;12:580-584

94. Coppieters K, Dreier T, Silence K, de Haard H, Lauwereys M, Casteels P, Beirnaert E, Jonckheere H, Van de Wiele C, Staelens L, Hostens J, Revets H, Remaut E, Elewaut D, Rottiers P. Formatted anti-tumor necrosis factor alpha vhh proteins derived from camelids show superior potency and targeting to inflamed joints in a murine model of collagen-induced arthritis. *Arthritis Rheum*. 2006;54:1856-1866

95. Vincke C, Loris R, Saerens D, Martinez-Rodriguez S, Muyldermans S, Conrath K. General strategy to humanize a camelid single-domain antibody and identification of a universal humanized nanobody scaffold. *J Biol Chem*. 2009;284:3273-3284

96. Saerens D, Ghassabeh GH, Muyldermans S. Single-domain antibodies as building blocks for novel therapeutics. *Current opinion in pharmacology*. 2008;8:600-608

97. Hmila I, Abdallah RB, Saerens D, Benlasfar Z, Conrath K, Ayeb ME, Muyldermans S, Bouhaouala-Zahar B. Vhh, bivalent domains and chimeric heavy chain-only antibodies with high neutralizing efficacy for scorpion toxin aahi'. *Mol Immunol*. 2008;45:3847-3856

98. Emmerson CD, van der Vlist EJ, Braam MR, Vanlandschoot P, Merchiers P, de Haard HJ, Verrips CT, van Bergen en Henegouwen PM, Dolk E. Enhancement of polymeric immunoglobulin receptor transcytosis by biparatopic vhh. *PloS one*. 2011;6:e26299

99. Els Conrath K, Lauwereys M, Wyns L, Muyldermans S. Camel single-domain antibodies as modular building units in bispecific and bivalent antibody constructs. *J Biol Chem*. 2001;276:7346-7350

100. Wesolowski J, Alzogaray V, Reyelt J, Unger M, Juarez K, Urrutia M, Cauerhff A, Danquah W, Rissiek B, Scheuplein F, Schwarz N, Adriouch S, Boyer O, Seman M, Licea A, Serreze DV, Goldbaum FA, Haag F, Koch-Nolte F. Single domain antibodies: Promising experimental and therapeutic tools in infection and immunity. *Medical microbiology and immunology*. 2009;198:157-174

101. Koide S. Engineering of recombinant crystallization chaperones. *Current opinion in structural biology*. 2009;19:449-457

102. Korotkov KV, Pardon E, Steyaert J, Hol WG. Crystal structure of the n-terminal domain of the secretin gspd from etec determined with the assistance of a nanobody. *Structure*. 2009;17:255-265

103. Steyaert J, Kobilka BK. Nanobody stabilization of g protein-coupled receptor conformational states. *Current opinion in structural biology*. 2011;21:567-572

104. Rasmussen SG, Choi HJ, Fung JJ, Pardon E, Casarosa P, Chae PS, Devree BT, Rosenbaum DM, Thian FS, Kobilka TS, Schnapp A, Konetzki I, Sunahara RK, Gellman SH, Pautsch A, Steyaert J, Weis WI, Kobilka BK. Structure of a nanobody-stabilized active state of the beta(2) adrenoceptor. *Nature*. 2011;469:175-180

105. Rothbauer U, Zolghadr K, Tillib S, Nowak D, Schermelleh L, Gahl A, Backmann N, Conrath K, Muyldermans S, Cardoso MC, Leonhardt H. Targeting and tracing antigens in live cells with fluorescent nanobodies. *Nature methods*. 2006;3:887-889

106. Olichon A, Surrey T. Selection of genetically encoded fluorescent single domain antibodies engineered for efficient expression in escherichia coli. *J Biol Chem*. 2007;282:36314-36320

107. Deckers N, Saerens D, Kanobana K, Conrath K, Victor B, Wernery U, Vercruysse J, Muyldermans S, Dorny P. Nanobodies, a promising tool for species-specific diagnosis of taenia solium cysticercosis. *International journal for parasitology*. 2009;39:625-633

108. Minaeian S, Rahbarizadeh F, Zarkesh Esfahani SH, Ahmadvand D. Characterization and enzyme-conjugation of a specific anti-l1 nanobody. *Journal of immunoassay & immunochemistry*. 2012;33:422-434

109. Muyldermans S. Nanobodies: Natural single-domain antibodies. *Annual review of biochemistry*. 2013

110. Vaneycken I, Devoogdt N, Van Gassen N, Vincke C, Xavier C, Wernery U, Muyldermans S, Lahoutte T, Caveliers V. Preclinical screening of anti-her2 nanobodies for molecular imaging of breast cancer. *FASEB journal : official publication of the Federation of American Societies for Experimental Biology*. 2011;25:2433-2446

111. Broisat A, Hernot S, Toczek J, De Vos J, Riou LM, Martin S, Ahmadi M, Thielens N, Wernery U, Caveliers V, Muyldermans S, Lahoutte T, Fagret D, Ghezzi C, Devoogdt N. Nanobodies targeting mouse/human vcam1 for the nuclear imaging of atherosclerotic lesions. *Circ Res*. 2012;110:927-937

112. Hussack G, Arbabi-Ghahroudi M, van Faassen H, Songer JG, Ng KK, MacKenzie R, Tanha J. Neutralization of clostridium difficile toxin a with single-domain antibodies targeting the cell receptor binding domain. *J Biol Chem*. 2011;286:8961-8976

113. Cook DA, Samarasekara CL, Wagstaff SC, Kinne J, Wernery U, Harrison RA. Analysis of camelid igg for antivenom development: Immunoreactivity and preclinical neutralisation of venom-induced pathology by igg subclasses, and the effect of heat treatment. *Toxicon : official journal of the International Society on Toxinology*. 2010;56:596-603

114. Harrison RA, Hasson SS, Harmsen M, Laing GD, Conrath K, Theakston RD. Neutralisation of venom-induced haemorrhage by igg from camels and llamas immunised with viper venom and also by endogenous, non-igg components in camelid sera. *Toxicon : official journal of the International Society on Toxinology*. 2006;47:364-368

115. Hmila I, Saerens D, Ben Abderrazek R, Vincke C, Abidi N, Benlasfar Z, Govaert J, El Ayeb M, Bouhaouala-Zahar B, Muyldermans S. A bispecific nanobody to provide full protection against lethal scorpion envenoming. *FASEB journal : official publication of the Federation of American Societies for Experimental Biology*. 2010;24:3479-3489

116. Pant N, Marcotte H, Hermans P, Bezemer S, Frenken L, Johansen K, Hammarstrom L. Lactobacilli producing bispecific llama-derived anti-rotavirus proteins in vivo for rotavirus-induced diarrhea. *Future microbiology*. 2011;6:583-593

117. Strokappe N, Szynol A, Aasa-Chapman M, Gorlani A, Forsman Quigley A, Hulsik DL, Chen L, Weiss R, de Haard H, Verrips T. Llama antibody fragments recognizing various epitopes of the cd4bs neutralize a broad range of hiv-1 subtypes a, b and c. *PloS one*. 2012;7:e33298

118. Kontermann RE. Strategies for extended serum half-life of protein therapeutics. *Current opinion in biotechnology*. 2011;22:868-876

119. Revets H, De Baetselier P, Muyldermans S. Nanobodies as novel agents for cancer therapy. *Expert opinion on biological therapy*. 2005;5:111-124

120. Hillmayer K, Macovei A, Pauwels D, Compernolle G, Declerck PJ, Gils A. Characterization of rat thrombin-activatable fibrinolysis inhibitor (tafi)--a comparative study assessing the biological equivalence of rat, murine and human tafi. *J Thromb Haemost*. 2006;4:2470-2477

121. Eckly A, Hechler B, Freund M, Zerr M, Cazenave JP, Lanza F, Mangin PH, Gachet C. Mechanisms underlying fecl3-induced arterial thrombosis. *J Thromb Haemost*. 2011;9:779-789

122. Diaz JA, Alvarado CM, Wrobleski SK, Slack DW, Hawley AE, Farris DM, Henke PK, Wakefield TW, Myers DD, Jr. The electrolytic inferior vena cava model (eim) to study thrombogenesis and thrombus resolution with continuous blood flow in the mouse. *Thromb Haemost*. 2013;109:1158-1169

123. Cleuren AC, van Hoef B, Hoylaerts MF, van Vlijmen BJ, Lijnen HR. Short-term ethinyl estradiol treatment suppresses inferior caval vein thrombosis in obese mice. *Thromb Haemost*. 2009;102:993-1000

124. Cui J, Eitzman DT, Westrick RJ, Christie PD, Xu ZJ, Yang AY, Purkayastha AA, Yang TL, Metz AL, Gallagher KP, Tyson JA, Rosenberg RD, Ginsburg D. Spontaneous thrombosis in mice carrying the factor v leiden mutation. *Blood*. 2000;96:4222-4226

125. Schroeder V, Kucher N, Kohler HP. Role of thrombin activatable fibrinolysis inhibitor (tafi) in patients with acute pulmonary embolism. *J Thromb Haemost*. 2003;1:492-493

126. Juhan-Vague I, Morange PE, Group PS. Very high tafi antigen levels are associated with a lower risk of hard coronary events: The prime study. *J Thromb Haemost*. 2003;1:2243-2244

127. Heylen E, Van Goethem S, Willemse J, Olsson T, Augustyns K, Hendriks D. Development of a sensitive and selective assay for the determination of procarboxypeptidase u (thrombin-activatable fibrinolysis inhibitor) in plasma. *Anal Biochem*. 2010;396:152-154

128. Hendrickx ML, De Winter A, Buelens K, Compernolle G, Hassanzadeh-Ghassabeh G, Muyldermans S, Gils A, Declerck PJ. Tafia inhibiting nanobodies as profibrinolytic tools and discovery of a new tafia conformation. *J Thromb Haemost*. 2011;9:2268-2277

129. Bouma BN, Mosnier LO. Thrombin activatable fibrinolysis inhibitor (tafi)--how does thrombin regulate fibrinolysis? *Ann Med*. 2006;38:378-388

130. Morser J, Gabazza EC, Myles T, Leung LL. What has been learnt from the thrombin-activatable fibrinolysis inhibitor-deficient mouse? *J Thromb Haemost*. 2010;8:868-876

131. Marder SR, Chenoweth DE, Goldstein IM, Perez HD. Chemotactic responses of human peripheral blood monocytes to the complement-derived peptides c5a and c5a des arg. *J Immunol*. 1985;134:3325-3331

132. Mollnes TE, Brekke OL, Fung M, Fure H, Christiansen D, Bergseth G, Videm V, Lappegard KT, Kohl J, Lambris JD. Essential role of the c5a receptor in e coli-induced oxidative burst and phagocytosis revealed by a novel lepirudin-based human whole blood model of inflammation. *Blood*. 2002;100:1869-1877

133. Mulligan MS, Schmid E, Beck-Schimmer B, Till GO, Friedl HP, Brauer RB, Hugli TE, Miyasaka M, Warner RL, Johnson KJ, Ward PA. Requirement and role of c5a in acute lung inflammatory injury in rats. *J Clin Invest*. 1996;98:503-512

134. Liu ZM, Zhu SM, Qin XJ, Cheng ZD, Liu MY, Zhang HM, Liu DX. Silencing of c5a receptor gene with sirna for protection from gram-negative bacterial lipopolysaccharide-induced vascular permeability. *Mol Immunol*. 2010;47:1325-1333

135. Kikuchi Y, Kaplan AP. A role for c5a in augmenting igg-dependent histamine release from basophils in chronic urticaria. *J Allergy Clin Immunol*. 2002;109:114-118

136. el-Lati SG, Dahinden CA, Church MK. Complement peptides c3a- and c5a-induced mediator release from dissociated human skin mast cells. *The Journal of investigative dermatology*. 1994;102:803-806